University of Alberta
Printing Department

THE UNIVERSITY OF ALBERTA

FRACTURE ANALYSIS IN THE CANADIAN ROCKY MOUNTAINS

A THESIS

SUBMITTED TO THE FACULTY OF GRADUATE STUDIES

IN PARTIAL FULFILMENT OF THE REQUIREMENTS FOR THE DEGREE

OF MASTER OF SCIENCE

DEPARTMENT OF GEOLOGY

by

GUNTER KURT MUECKE, B.Sc.

EDMONTON, ALBERTA

September, 1964

UNIVERSITY OF ALBERTA

FACULTY OF GRADUATE STUDIES

The undersigned certify that they have read, and recommend to the Faculty of Graduate Studies for acceptance, a thesis entitled "Fracture Analysis in the Canadian Rocky Mountains", submitted by Gunter Kurt Muecke, B.Sc., in partial fulfilment of the requirements for the degree of Master of Science.

ABSTRACT

The geometric analysis of macroscopic fractures in the Foothills, Eastern Ranges, and Main Ranges of the Canadian Rocky Mountains reveals a systematic fracure pattern. Most observed joints are found to fall into either, two conjugate hkl sets, a 0kl set replacing the hkl sets, or an h0l set.

New methods of fracture analysis are introduced which utilize an IBM 1620 computer system. The counting out and plotting of orientation diagrams, the evaluation of individual maxima, β -axis determinations, and the determination of individual planar intersections, are all accomplished using computer programs.

Principal stress trajectories are postulated to have been subparallel to bedding at the time of joint formation. Changes in the dihedral angle between conjugate shear fractures reveal that areas presently at equal elevations were at one time subject to different overburden pressures. The joints are postulated to have formed in response to unloading by erosion. Three changes in the principal stress directions during unloading account for the orientation of the observed joint sets and their directions of movement.

ACKNOWLEDGMENTS

The writer wishes to express his gratitude to Dr. H.A.K. Charlesworth for his invaluable guidance and assistance both in the field and during the preparation of this thesis. The suggestions, stimulation, and criticism of members of the Department of Geology and the Department of Computing Sciences, Dr. M.H. Dodson, and Dr. J. Hospers are also gratefully acknowledged. A special thanks is extended to Mr. V. Yanda for many tedious hours of assistance in computer programming.

Financial assistance making this thesis feasible was provided by the Consolidated Mining and Smelting Company of Canada Limited in the form of a graduate research fellowship, by the University of Alberta in the form of a teaching assistantship, and by Shell Oil of Canada Limited who underwrote the field expenses. The writer extends his deepest gratitude to all these organizations.

TABLE OF CONTENTS

LIST OF FIGURES

INTRODUCTION

Jointing has received only a limited amount of attention in structural investigations of the Canadian Rocky Mountains. The analysis of mesoscopic fractures has shed new light onto the tectonic history of many areas, and a study of the joints in the Canadian Rocky Mountains promised to be a profitable project. During the summer of 1963, a total of 10,250 joints were measured at localities in the Foothills, Eastern Ranges, and Main Ranges of the Canadian Rocky Mountains.

The purpose of the study may be summarized as follows:

a) to describe the different types of mesoscopic fractures found in the area, to separate these into groups of apparently common origin, and to attempt to determine the relative ages of the groups;

b) to determine the regional preferred orientation of the most important mesoscopic fractures;

c) to correlate the mesoscopic geometry with the macroscopic geometry;

d) to suggest a kinematic and dynamic interpretation of the observed fracture pattern.

JOINTING IN SEDIMENTARY ROCKS

Introduction

By far the most common and yet least understood mesoscopic planar discontinuities in both undisturbed and deformed sedimentary rocks, are the fracture planes more or less normal to bedding, known as joints. Usage of the term joint varies somewhat; before delving into the various classifications of joints and their possible modes of origin the definition of the term will now be briefly reviewed.

Billings (1954, p. 106), Hills (1963, p. 150), and Metz (1957, p. 59) defined joints as fractures normal to bedding, or nearly so, along which no visible movement has taken place. However, since all open joints have undergone movement at right angles to their surface and since joints are planes of weakness along which movement can readily occur, the definitions set forth by Turner (1948, p. 181), Price (1959, p. 149) and the A.G.I. Glossary Supplement (1960, p. 35) are perhaps preferable. The A.G.I. Glossary Supplement definition reads as follows: "Joints - fractures in rocks, generally more or less vertical or transverse to bedding, along which no appreciable movement has taken place."

Classification

Geometric classification. On the basis of their attitude with respect to bedding, joints have been classified as strike, dip, and oblique or diagonal joints (Billings, 1954, p. 107). Similarly the terms longitudinal, transverse or cross joints, and diagonal joints have been used as geometric classifications when the basis of classification was taken to be the attitude with respect to fold axes (Hills, 1963, pp. 281-282).

The most satisfactory geometric classification of joints, and the one which is followed in this thesis, is based on a system of orthogonal fabric axes a, b, and c which are related to the symmetry elements on the mesoscopic scale (Turner and Weiss, 1963, p. 88). The great flexibility of this classification and its facility in the correlation of minor and major tectonic elements, remove the ambiguities of the other geometric classifications. The designations of the various types of joints and their equivalents are listed below (Fig. 1):

hk0 joints = diagonal joints, oblique joints

h0l joints = strike joints, longitudinal joints

h00 joints = bc joints

0kl joints = cross joints, transverse joints, dip joints

0k0 joints = ac joints

hkl joints = joints not paralleling a fabric axis

Genetic classification. More commonly used than the geometric classification is the genetic classification of joints. As is the pitfall of all genetic classifications, a mode of origin has to be postulated before this classification can be applied. A great deal of uncertainty still exists as to the exact origin of joints in sedimentary rocks and the widespread use of a genetic terminology at the geometric stage of structural analysis is unfortunate. The two genetic classes of joints generally recognized are shear (hk0) and tension (h0l or 0kl) joints.

Shear joints are usually thought to form obliquely to the principal stress axis. Commonly they are smooth, extensive, and planar. They generally occur in two complementary sets, one of which may show right-hand displacement and the other left-hand displacement.

Tension joints are thought to form normal to the direction of least principal stress. They are commonly rough, warped, and show great variability in strike.

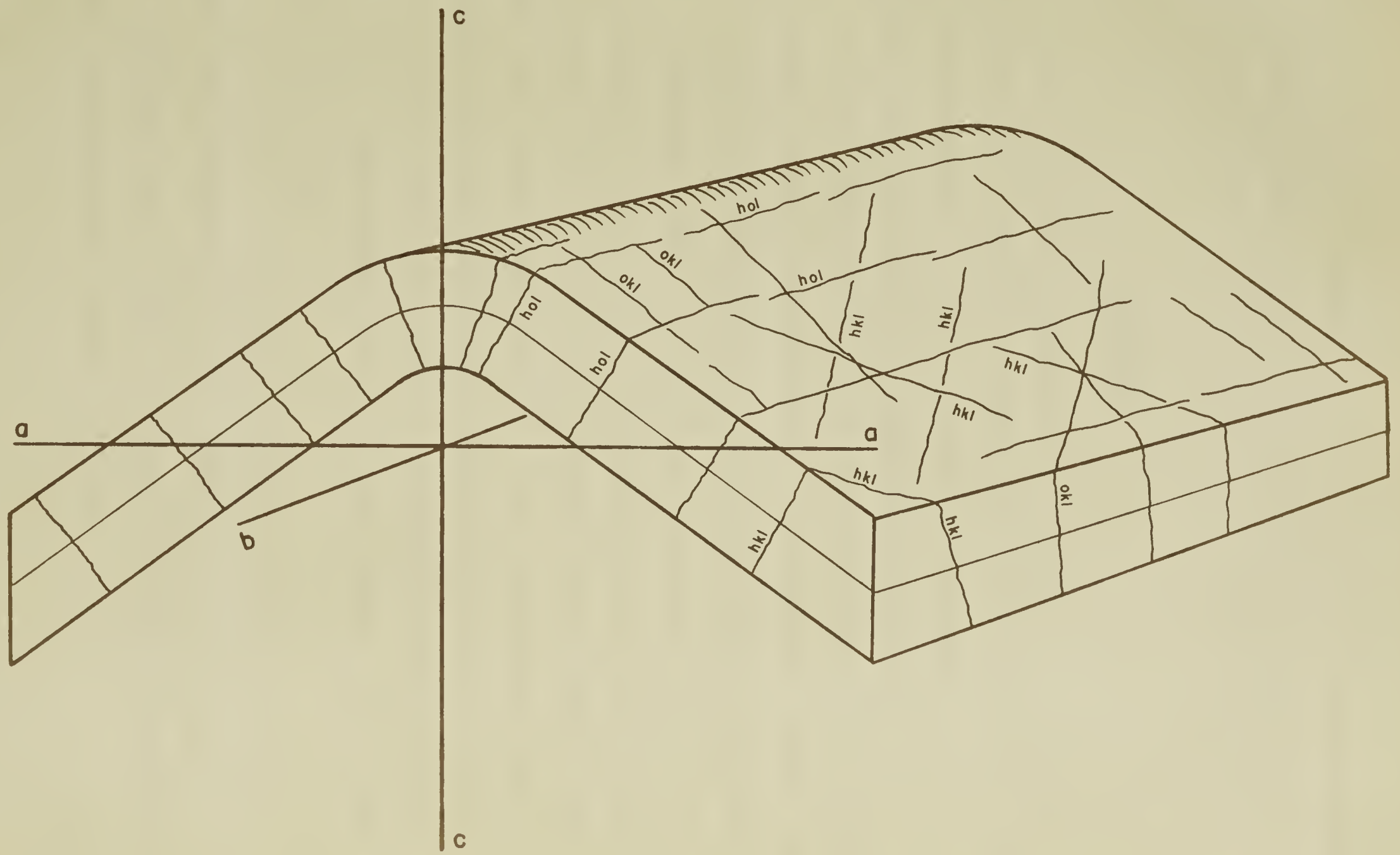

FIGURE 1

The least principal stress in the formation of this type of fracture does not necessarily have to be tensile (Griggs and Handin, 1960, pp. 350-351), but may be compressional. The use of the term extension joint may, therefore, be preferable.

Morphology

Joints which have not undergone relative movement and have not been weathered extensively often display a number of distinctive surface features. The classification and genetic significance of the various structures found on joint surfaces has recently been reviewed by Hodgson (1961c) and Robertson (1961).

Structures falling on the main joint surface can be differentiated from these on the periphery or fringe of the joint. The main joint face is transversed by a central axis from which rays or plumes diverge toward the edge of the joint plane (Robertson 1961, p. 483; Hodgson, 1961c p. 494). The plumes consist of a series of shallow rises and hollows on the joint surface. The central axis approximately parallels the upper and lower boundaries of the rock unit in which it occurs (Hodgson, 1961c, p. 499). In the peripheral regions of the joint plane, large numbers of small en echelon fractures classified as f-joints (Hodgson, 1961c, p. 501) or b-planes (Robertson, 1961, p. 483) can be observed. Perpendicular to the b-planes are a series of rough, irregular fractures known as c-planes (Robertson, 1961, p. 484; Hodgson, 1961c, p. 496).

In the opinion of some authors, the presence of plumose structures is limited to joints of "shear" origin. (Parker, 1942, p. 397; Robertson, 1961, p. 486). Muehlberger (1961, p. 215), on the other hand, cited plumose markings as criteria for the recognition of "extension" fractures.

Origin

Syntectonic theory of origin. The theory of joint formation most widely accepted among structural geologists postulates that joints in folded and faulted rocks can be directly attributed to syntectonic stresses. The existence of a gradual transition from joints showing no motion to faults is also presumed (de Sitter, 1956, p. 122). The orientation of the possible joint sets should, therefore, be predictable by the Coulomb-Navier theory of fracture. Complementary sets of shear joints should develop parallel to the intermediate stress axis at an angle of $45 - \phi/2$ degrees to the maximum principal stress axis; tension joints perpendicular to the minimum principal stress axis. This indeed appears to be the relationship quite frequently observed.

Considerable difficulty arises, however, when the time of development of the fractures is to be determined. Hoeppener (1953) in his studies in the Rheinischen Schiefergebirge concluded that the joints formed at the early stage of folding. The joints are found to be displaced by bedding-plane slip. Hoeppener (ibid.) also thought that these pre-folding or early -folding joints had been rotated with respect to the bedding by slippage along innumerable microscopic fractures parallel to bedding. Maximum rotation was observed for h00 joints and none for 0k0 joints. The amount of rotation for given bedding dips can be calculated theoretically. According to Koebel (1940), the theoretical values of rotation are in excess of those observed; Hoeppener (ibid.) found that the calculated and measured values agreed reasonably well for bedding dips up to 20 degrees.

In the Swiss Jura, Nabholz (1956) found that h00 joints in one tight anticline appear to have been rotated 9 degrees with respect to bedding, whereas in three similar folds no such rotation could be detected. The amount of rotation, in this case, appeared to be independent of the dip of the beds. Hoeppener's explanation for the apparent rotation of joints therefore does not seem to hold in

all cases.

The variation in the acute angle between sets of shear fractures is of considerable interest in the interpretation of fracture patterns. The Coulomb-Navier theory of fracture predicts that the dihedral angle between conjugate failure planes, regardless of the values of the principal stresses, should be $45 - \phi/2$ degrees. for most rocks can be approximated to be 30 degrees. One would, therefore, expect the acute angle between shear sets to be 60 degrees. Significant deviations from this value have been found by some investigators.

Parker (1942, p. 393) studied the jointing in central and northern New York and northern Pennsylvania and found the acute angle between two shear sets to vary from 13 - 30 degrees. Wager (1931, pp. 392-420) investigated the joint pattern in the vicinity of the North Craven fault and observed that two shear sets were nearly perpendicular to each other. In a very gently folded anticline at Robin Hood's Bay, Zwart 1951, p. 3) found sets of shear joints at an angle of 15 degrees to each other. Hoeppener (1953), in his investigation of joints, noted that the shear joints made an angle of less than 45 degrees to the perpendicular of the fold axis. Duschatko (1953, p. 35) investigated the areal fracture pattern of the Lucero Uplift in New Mexico and found that a single joint set became replaced by two conjugate joint sets at low dihedral angle. The progressive increase in the acute angle up to 65 degrees was recorded. Joint sets with the largest dihedral angles were found to be in the structurally lowest positions.

According to de Sitter (1956, p. 130), the deviation of the acute angle from the expected value may be due to "differences in rock properties or to the weight of the overburden; but on the other hand it may merely indicate that two quite different kinds of shear joints exist." Wager (1931, p. 405) suggested that the explanation for the variability may lie in experiments done on natural materials. T. von Karman (1911) had shown that the angle of shear may be altered by superposing a hydrostatic pressure on the non-uniform pressure required to produce shear

fractures.

Muehlberger (1961, pp. 211-219) discussed the mechanics of conjugate joint sets of small dihedral angel in view of the Mohr theory of fracture. He suggested that for low stresses the Mohr envelope assumes a parabolic configuration and intersects the normal stress axis at right angles. Experimental data tends to support this assumption. Under those circumstances there will be a stress circle with radius of curvature equal to that of the parabola at the vertex. This is the largest stress circle for tensile failure. A slight increase in the differential stress in the aforementioned case will move the stress circle off the vertex and it will then be tangent to the envelope at two points. The resulting conjugate fractures would enclose a small dihedral angle. Within a small range of increasing stress differences, the angle would increase to the usual angle of shear failure.

Post-tectonic theory of origin. One of the theories that attempts to explain the formation of joints in both undeformed and deformed rocks postulates that unloading, or the decrease in geostatic pressure, is one of the major factors in the formation of joints. It was noted by Hills (1963, p. 157) that, unless compensated for by the increase of density due to compaction, the formation of tension joints involves an increase in volume of the affected rock mass. This increase in volume suggests that many joints may form with decreasing, rather than increasing, stress due to relief of loading by erosion. Price (1959, p. 158) demonstrated that tensile stresses, equal to half the change in gravitational load, will develop during unloading.

Price (1959, pp. 149-167) used the Mohr theory of fracture to develop a model of events during unloading. The model is based on the assumption that competent rocks act as brittle materials in the upper crust and obey the elastic theory. Price (1959, pp. 156-157) postulated that the elastic strain energy remains stored in the rock and residual stresses may exist which in quantity and direction

are equal to the stresses which acted at the end of the main tectonic phase. Rocks are elastico-viscous bodies and the residual stresses will tend to relax with time. Very little is known, however, about the viscosity of rocks. It may, therefore, be quite possible that the relaxation time may be in the order of 10 million years. This means that the residual stresses would relax to 1% of their original value in 50 million years (Price, 1959, p. 157). Rocks may also have a fundamental strength, that is, they will not deform continuously unless a critical differential stress is reached. Undissipated stresses would then be stored as residual stresses.

Price (ibid.) further showed that if the initial conditions of the rock mass approximate the hydrostatic state the rocks actually go into tension and develop vertical tension joints, provided uplift accompanies erosion. These tension joints will be randomly orientated if all horizontal stresses are equal at each depth level. When horizontal stresses are present, the tension joints will form at right angles to the axis of least principal stress. As soon as fracture has occurred, the least principal stress is replaced by a compressive stress, and the intermediate principal stress becomes the least principal stress. A second set of tension fractures will develop upon further uplift. The two sets will form an orthogonal system. In cases where the tectonic stresses were not relaxed after an initial period in which the greatest principal stress was horizontal, the vertical load would change from being the least principal stress to being the intermediate principal stress at some level. With further uplift, a set of conjugate shear fractures will form which reduces the residual stresses considerably. The conditions discussed in the previous example will be satisfied as uplift continues and the rocks may pass into tension and develop a system of orthogonal tension fractures. In cases where the residual stresses have not been affected by subsequent tectonic events, the joints will still faithfully reflect the stress conditions as they existed during the main tectonic phase. Equally plausible is the situation where the stress conditions may become upset by

subsequent events, in which case the orientation of the joints bears no relationship to the geometry of the structures developed during the main tectonic phase.

Formation of joints by earth tides. The presence of well developed joint sets in relatively undeformed and even flat-lying sedimentary rocks has led some authors to believe that the tension and shear hypotheses are inadequate in explaining the formation of joints. Hodgson (1961, pp. 1-38), investigating the jointing in the Comb Ridge-Navajo Mountain region, found as many as six well developed joint sets in very gently folded rocks. The fractures bear no obvious geometrical relationship to the folding and a number of different stress systems would have to be invoked, if one were to explain these fractures by compressive stresses. Hodgson (ibid.) concluded that the fractures represent fatigue phenomena resulting from the application of external stresses. Most other investigators of fracture patterns in flat-lying rocks also advocate the formation of joints in response of an external stress field (Blanchet, 1957, p. 1754; Mollard, 1958, p. 111; Haman, 1961, p. 9).

Kendall and Briggs (1933) were the first to suggest that semi-diurnal earth tides produce joints by a torsion mechanism. In addition to the semi-diurnal lunar tides, Blanchet (1957, p. 1755) also mentioned the possible effect of the lunar diurnal tides, the solar diurnal tides, and the solar semi-diurnal tides, each with their own period and wave length. The effects of the body tides on the continental crust are as follows:

a) They cause periodic increases and decreases in the porosity of near-surface rocks, which results in a corresponding rise and fall of the local water table (Robinson, 1939, pp. 656-666).
b) They cause the cyclic variation in the flow of some hot springs (Vorster, 1956).
c) They cause the detectable independent tilting of static fault blocks (Nishimura, 1950, p. 359).

d) They cause crustal rise and fall of a magnitude which has been variously estimated at 6 - 21 inches (Holmes, 1963, p. 1411) and 9 - 14 inches (Blanchet, 1957, p. 1754).

Under this hypothesis joints are considered to represent fatigue phenomena resulting from the cyclic repetition of small stresses. Earth tides act approximately four times a day or 1 1/2 billion times per million years. The similarity between the orientation of plumose structures found on joint surfaces and structures on the surfaces of fatigue fractures in metals and concrete was taken as evidence by Hodgson (1961, p. 23) for this mode of origin of joints.

Kendall and Briggs (1933) postulated that earth tides controlled both the formation of the joints and their direction. The chief directions of jointing in the northern hemisphere should, therefore, be northeast and northwest, in coincidence with directions of maximum shearing stress caused by the tidal forces. Joint patterns do not always show such a pattern and modern workers have adopted the hypothesis that the direction, possibly even the original formation of the joints, could be regionally controlled. Holmes (1963, p. 1411) pointed out that the orientation of the developing systems of fractures is probably controlled by independent stresses and that the continuous tidal stresses would extend the fracture pattern under a minimum of internal stress. Hodgson (1961, p. 36) considered the possibility that the fracture pattern could be inherited by each newly deposited rock unit from the jointed rock beneath, advocating thereby the upward migration of joints. In the Bright Angel area, Arizona, Hodgson (1961b, pp. 95-97) found that joints in sedimentary rocks overlying Precambrian metamorphic rocks, in part, reflect the major structural directions found in the Archean metamorphic complex. This seems to indicate that the Precambrian fracture pattern has been imposed on each successive younger rock unit.

COLLECTION OF FIELD DATA

Selection of Localities

Previous joint studies have shown that the structural setting, lithology, and bedding thickness play important roles in both the development and frequency of jointing (Harris, Taylor, and Walper, 1960, pp. 1859-1860; Fitzgerald, 1963, p. 131). One of the primary goals of this investigation was to establish the relationship between the regional structure and the macroscopic fractures. It was desirable to keep both lithology and bedding thickness constant. Other factors influencing the choice of sampling locations included accessibility, nature of the outcrop, and the presence of well developed fractures.

The sandstone units in the Cardium formation of the Foothills of southwestern Alberta most nearly satisfied these requisites. Sandstones in the Cardium formation have a fairly constant lithology for considerable distances along regional strike, although they may change rapidly across it. Joint orientations in these sandstone units were obtained in six anticlines along the Bow River, one anticline on the Red Deer River, the limb of a syncline at South Creek, and a monocline at Cripple Creek (Fig. 3).

Work done in the Eastern and Main Ranges of the Rocky Mountains was on a reconnaissance basis to investigate the feasibility of more extensive studies in the future. Joints were measured in the competent units of the Palliser, Alexo, Banff, and Rundle formations in a number of different thrust sheets of the Eastern Ranges (Fig. 3). Sampling in the Main Ranges was confined to one locality situated in the Eldon formation on the east limb of the Bow River anticline.

Sampling Procedures

In addition to the strike and dip, the size and relative regularity of each joint were noted. Also recorded were the attitude of the slickensides both along the joints and the bedding planes; the relative movement along slickensides wherever discernible; the attitude of the bedding planes; and the thickness, lithology, and stratigraphic position of the fractured unit.

In order to avoid subjective selection in the fractures measured, all the fractures which were planar, or could be approximated by a plane, were measured. Exceptions were fractures smaller than a few square inches in surface area, fractures in the immediate proximity of known faults, curviplanar fractures, and fractures definitely due to blasting. Errors in the measurement of the strike and dip are estimated to be between one and five degrees, depending on the irregulatiry of the fracture surface.

No quantitative measurements of the fracture frequency were made in the course of the study. In order to yield meaningful results, joint frequency studies should be carried out in areas with large outcrops of bedding planes or at least two dimensions of the rock body. In the writer's opinion the exposure in the areas investigated did not warrant this type of study. Only general observations on the fracture frequency were made.

A domain, as used in this study, represents any three dimensional rock body statistically homogeneous with respect to the fracturing. Outcrops were divided into a number of subdomains of approximately 10 foot radius. Subdomains were chosen to have no noticeable changes in lithology or bedding attitude. A number of bedding attitudes and all of the joints were measured in each subdomain. Subdomains showing no appreciable difference in the bedding or fracture attitudes were then grouped into domains containing 200-300 joint orientations. Orientation diagrams were prepared for all domains.

Number of Observations Required

The number of observations of fracture attitudes required to produce valid orientation diagrams poses a critical question in any sampling program for joints. Mueller (1933) concluded that 200 observations were needed and that possibly more should be measured in areas of unknown character. Pincus (1951, p. 101) considered 80 orientations per locality to be the minimum value, while Spencer (1959, p. 475) used 100-120 measurements. The values quoted by Pincus and Spencer represent the minimum number of fracture attitues necessary to establish the general pattern, but not the optimum number of observations required for good accuracy in the quantitative evaluation of the fracture data.

In the writer's opinion the number of observations required depends both on the number of fracture sets present in a particular outcrop, and the dispersion shown by each of these sets. The dependence of the number of fractures needed in the analysis on the dispersion can be illustrated by plotting the number of fractures versus the confidence raius about the mean, for a number of fracture sets (Fig. 2). Fracture sets having different precision parameters (Fisher, 1953, p. 303), that is, different dispersions, can be seen to form independent plots. In the accompanying diagram set 1 has a low dispersion, while sets 2 and 3 have a higher but equal dispersion. The plots show that the number of fractures required to reach a specified value of the confidence radius about the mean depends on the dispersion. It should also be noted that any increase in the number of observations will result in an increase in the confidence in the mean fracture orientations. An optimum number of observations has only a minimal effect on the confidence radius. In the example illustrated (Fig. 2), this number appears to be 55 observations for set 1 and 65 observations for both sets 2 and 3. As approximately 10 per cent of the observed fractures in this area do not fall within one of the fracture sets, 205 joint attitudes should be obtained at this locality.

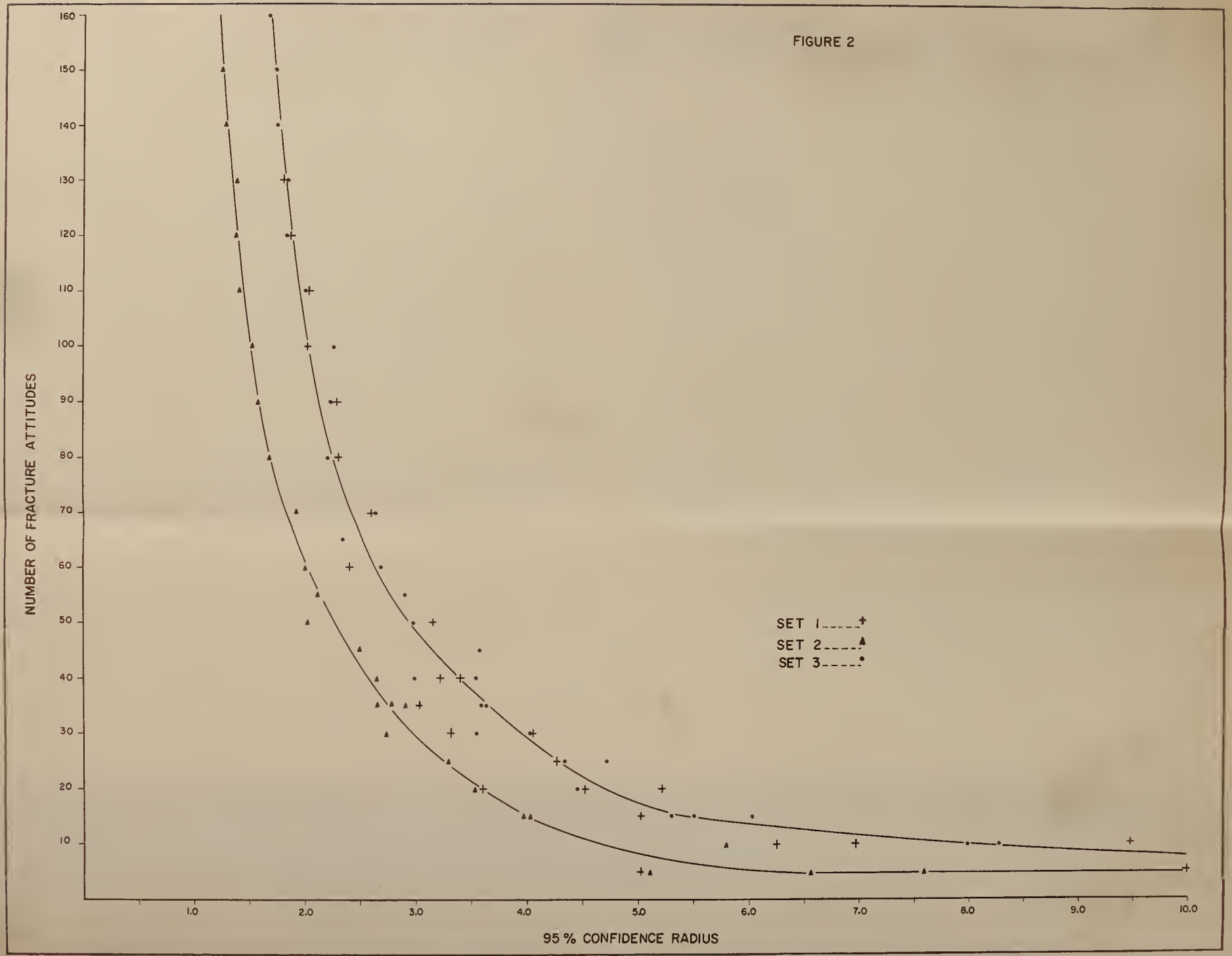
FIGURE 2
NUMBER OF FRACTURE ATTITUDES
160
150
140
130
120
110
100
90
80
70
60
50
40
30
20
10
1.0
2.0
3.0
4.0
5.0
6.0
7.0
8.0
9.0
10.0
95 % CONFIDENCE RADIUS
SET 1
SET 2
SET 3

Because the dispersion was one of the parameters to be investigated, it was found necessary to determine how many observations per joint set would be required to arrive at a consistent value of the precision parameter (Fisher, 1953, p. 303). A plot of the precision parameter of various fracture sets versus the number of fracture orientations reveals that 70 observations per set are required to arrive at a consistent value of the precision parameter. When the dispersion of the fractures is to be investigated, 230 fracture orientations should be measured at this locality.

The dispersion of the fractures can vary considerably from outcrop to outcrop, not all sets are equally developed in any one outcrop, and the number of fracture sets present is not always known beforehand. It was, therefore, attempted to measure 250-300 joints per domain.

DATA PROCESSING

Introduction

In view of the large number of bits of information to be processed, it was found that conventional methods of analysis were unsatisfactory. A number of computer programs were designed to aid in the preparation and evaluation of the orientation diagrams.

The equipment used consisted of the IBM 1620 Data Processing System at the University of Alberta, Edmonton, with 1622 Card Read Punch. 1623 Core Store Unit with one 60K module and a 407 Line Printer.

The programs were written in FORTRAN II and compiled with a floating-point word length of 8 characters and a fixed-point word length of 4 characters. Program and monitor statements conform with specifications set forth in the "FORTRAN II for the Magnetic Tape 1620" manual of the Computing Center, University of Alberta, Edmonton.

Preparation of Pole Density Diagrams: Program 913107-001

Introduction. Joint studies in structural geology originated in the latter half of the nineteenth century in regions where joints showed a great degree of regularity and could easily be defined by a single observation of their attitude. Soon investigators found, however, that in areas, where the joint pattern is less clearly defined, the joints also exhibit definite preferred orientations. In such cases, geologists found it necessary to estimate the mean orientation of the joints in the outcrop; a method which is still widely used today.

Salomon (1911) and his students conducted extensive joint surveys along the Rhine graben. By careful and detailed cartography they were able to define

regional patterns in the jointing. Although they took only a few readings per outcrop, this school laid the foundation for the statistical treatment of joints.

Stiny (1925, p. 873) postulated that the mean attitudes of joints could not be estimated accurately in the field, and he was the first to advocate the measurement of a large number of joints per outcrop, in order to determine the true joint direction. His ideas were readily accepted. Soon various methods were designed to evaluate statistical numbers of joint attitudes. Strike frequency diagrams and rectangular coordinates were frequently used. These methods were found to be unsuitable in most cases. however, because they only illustrate the variation in one variable, whereas the attitude of any plane is defined by two dependent variables.

The attitude of a plane in space can be accurately represented on a stereographic projection. A stereographic net to plot joints was first used by Seitz (1914/17). As equal areas on the reference sphere do not remain equal on the stereographic projection, the pole densities are distorted by this method. To overcome this difficulty, Schmidt (1925) introduced the use of the equal-area projection to petrofabrics. This method of investigation was first used in studying joints by Rueger (1928). In order to facilitate an easier interpretation of the diagrams, it became customary, to count out the diagrams with circular counters and to draw density contours (Knopf and Ingerson, 1938, pp. 245-252).

Strand (1944, p. 112) pointed out that accurate contouring required a change of the unit counting area from circular at the center of the diagram to elliptical towards the margin. Duschatko (1955, p. 1522) designed a counter consisting of a number of ellipses. with increasing ellipticity toward the periphery of the projection, in order to eliminate some of the distortion introduced during the counting out process. A large number of ellipses would be necessary to obtain true pole densities.

Statement of problem. Ideally petrofabric diagrams should not be counted out in their projection, but on the reference sphere. Pole densities obtained on the reference sphere can then be projected onto the equatorial plane and will faithfully reflect the true pole densities. Until recent years, this type of analysis would have been impossible for large numbers of observations. Problems involving repetitive intricate calculations are ideally suited for modern high-speed digital computers. A computer program was designed to count out petrofabric diagrams on the reference sphere and to print out the projections of the densities onto the equatorial plane.

Method. In order that a number (NCDS) of attitudes of planes or lineations can be processed by this program, each attitude has to be in one of the following forms: strike (NSTR), dip (NDIP), and direction (NDIR); trend (NTR) and plunge (NPL); or direction cosines (A, B, G). When in one of the above forms, the attitude will be referred to as a data reading. The computer converts the strike, dip, and direction of a plane to the trend (TR) and plunge (PL) of the normal to the plane. All the trends and plunges are then changed into direction cosines λ_i, μ_i, and γ_i of unit length using the relationships:

$$\lambda_i = \cos TR_i * \cos PL_i \quad (1)$$

$$\mu_i = \sin TR_i * \cos PL_i \quad (2)$$

$$\gamma_i = \sin PL_i \quad (3)$$

The counting out of the poles in the reference sphere is accomplished by the use of a circular cone with semivertical angle of α. The value of α is determined by the value of P, the percentage of the total area of the projection which the counter is required to cover. The value of P and the number (N) of counting locations have to be chosen such that the counting cones overlap in such a manner as to assure that all points on the sphere are counted. At the same time P should be kept small in order to obtain the best possible definition of any differences in

the densities of the points. In most petrofabric studies P has been taken to be 1.0 and N as 317.

The centre of the counting cone is placed at specified and previously calculated locations. If the direction cosines of the counting locations are $\lambda_c, \mu_c,$ and $\gamma_c,$ and of the data readings $\lambda_i, \mu_i,$ and γ_i then the angle between their directional lines is given by

$$\beta = (\lambda_c * \lambda_i + \mu_c * \mu_i + \gamma_c * \gamma_i) \qquad (4)$$

If $(\alpha - \beta) \geq 0$ the data reading falls within the counting cone. The number of data readings in each data set falling within the counting cone at each counting locality is noted, and converted into the percentage of the total number of points processed.

In order to facilitate a simple output format using the IBM 407 Line Printer, the counting locations were chosen to form a regular grid with a spacing of R/10 (R = radius of the reference sphere) on the equatorial plane. For the convenience of accurate contouring, these were augmented by 14 additional points near the periphery of the projection. The counting points are projected only from the lower hemisphere of the reference sphere onto the equatorial plane by equal-area projection.

Limitations on parameters.

		NCDS	$\leq$	500
0	$\leq$	NSTR	$\leq$	180
0	$\leq$	NDIP	$\leq$	90
0	$\leq$	NDIR	$\leq$	2
0	$\leq$	NTR	$\leq$	360
0	$\leq$	NPL	$\leq$	90
-1.0	$\leq$	A	$\leq$	1.0
-1.0	$\leq$	B	$\leq$	1.0
0.0	$\leq$	G	$\leq$	1.0

Input. (a) Parameter card

Column	Content	Format
1	blank	1X
2 - 4	NCDS	I3
5	blank	1X
6	Code	I1
7	blank	1X
8 - 10	Run No.	I3

The following code has been employed in column 6 of the parameter card:

0 if the input data consists of the strike, dip, and direction planes;

1 if the input data consists of the trend and plunge of linears;

2 if the input data consists of the direction cosines of lines (output from Program 913107-003 or 004).

(b) Data cards

Data cards differ in format according to the code used in column 6 of the parameter card as follows:

Code = 0

Column	Content	Format
1	blank	1X
2 - 4	NSTR	I3
5	blank	1X
6 - 7	NDIP	I2
8	blank	1X
9	NDIR	I1
10 - 15	blank	7X
16 - 80	can be used for coding and sorting.	

The direction of dip (NDIR) of planes has been coded in the following manner:

0 if the dip is 90 degrees;

1 if the dip direction is N, NE, NW, or W;

2 if the dip direction is S, SE, SW, or E.

N and S are only valid for strikes of 90 degrees, and similarly E and W for strikes of 0 and 180 degrees; otherwise the NE, NW, SE, or SW quadrants have to be specified. For example, 179/85 W is an invalid data reading and should read 179/85 SW.

Code = 1

Column	Content	Format
1	blank	1X
2 - 4	NTR	I3
5	blank	1X
6 - 7	NPL	I2
8 - 15	blank	10X
16 - 80	can be used for coding and sorting.	

Code = 2

Column	Content	Format
1 - 7	blank	7X
8 - 18	A	F11.8
19 - 29	B	F11.8
30 - 40	G	F11.8

(c) Termination card

Column	Content	Format
1 - 14	blank	14X
15	5	I1

Order of cards.

(a) Program 913107-001 (pp. 25-27)

(b) Direction cosines of counting locations (Appendix I)

(c) Parameter card

(d) Data cards

Repeat (c) and (d) for each subsequent run.

(e) Termination card

Output. The output of this program consists of two grids of numbers, one representing the per cent density of poles per counting cone, and the other the actual number of points counted per counting cone. The grids, when circumscribed by a circle of 10 inch diameter, represents the densities of points at counting points on the reference sphere that have been projected onto the equatorial plane.

The numerals are right-hand orientated and contours should be placed through the center of the right-hand digit.

Test data and results. The accompanying output sample (pp. 28-29) represents 237 attitudes of joint planes measured on the east limb of Kananaskis anticline. The contoured output (Fig. 5) of the computer can be compared with a similar diagram (Fig. 4) prepared by the conventional graphic methods using a circular counter. In general the agreement is excellent in the central regions of the diagram. Marked differences exist in the peripheral regions if the graphical counter used is circular rather than elliptical.

```
..I  913107  POINT DENSITY DIAGRAMS      G.K.MUECKE
..I PLEASE SAVE CARDS.
..LOAD FORTRAN EXECUTE DUMP
      DIMENSION COSA(333),COSB(333),COSG(333),ND(333)
      DIMENSION A(500),B(500),G(500)
 1    READ INPUT TAPE 5,50,NDENS
      DO 2 I=1,NDENS
 2    READ INPUT TAPE 5,51,COSA(I),COSB(I),COSG(I)
      READ INPUT TAPE 5,52,KPCA
      DA=KPCA
      TEST=1.-DA*.01
      THET=ATANF(SQRTF(1./(TEST*TEST)-1.))
 3    DO 4 I=1,NDENS
 4    ND(I)=0
      NZ=0
      PI=3.1415926
      R180=1./180.
      CF=PI*R180
      IX=1
      READ INPUT TAPE 5,50,NCDS,NZ,NSTN,NUTS
      IF(NUTS)45,46,45
 45   CALL EXIT
 46   FNCDS=NCDS
      RNCDS=100./FNCDS
      NZ=NZ+1
      GO TO (47,47,1200),NZ
 47   DO 12 I=1,NCDS
      GO TO (5,10),NZ
 5    READ INPUT TAPE 5,53,NSTR,NDIP,NDIR
      PL=90-NDIP
      IF(NDIR-1)8,7,8
 7    TR=NSTR+90
      GO TO 11
 8    TR=NSTR-90
      IF(TR)9,11,11
 9    TR=TR+360.
      GO TO 11
 10   READ INPUT TAPE 5,53,NTR,NPL
      TR=NTR
      PL=NPL
 11   PL=PL*CF
      TR=TR*CF
      A(I)=COSF(TR)*COSF(PL)
      B(I)=SINF(TR)*COSF(PL)
      G(I)=SINF(PL)
 12   CONTINUE
      GO TO 1202
1200  DO 1201 I=1,NCDS
1201  READ INPUT TAPE 5,51,A(I),B(I),G(I)
1202  PMAX=0.
      DO 124 I=1,NCDS
      IF(PMAX-G(I))123,124,124
123   PMAX=G(I)
124   CONTINUE
      PMAX=PMAX+TEST
      DO 15 I=1,NDENS
```

```
      CSG=COSG(I)
      IF(PMAX-CSG)15,15,125
  125 CSA=COSA(I)
      CSB=COSB(I)
      DENS=0.
      AT=CSG+TEST
      BT=CSG-TEST
      DO 14 J=1,NCDS
      GEE=G(J)
      IF(GEE-BT)14,122,121
  121 IF(AT-GEE)14,122,122
  122 PEST=ABSF(CSA*A(J)+CSB*B(J)+CSG*GEE)
      IF(TEST-PEST)13,13,14
   13 DENS=DENS+1.
   14 CONTINUE
   15 ND(I)=DENS
      KLIK=1
   16 WRITE OUTPUT TAPE 6,58,ND(1)
      WRITE OUTPUT TAPE 6,66,ND(318),ND(319),ND(320),ND(321)
      WRITE OUTPUT TAPE 6,68,NSTN
      WRITE OUTPUT TAPE 6,59,(ND(I),I=2,10)
      WRITE OUTPUT TAPE 6,57
      WRITE OUTPUT TAPE 6,57
      WRITE OUTPUT TAPE 6,60,(ND(I),I=11,23)
      WRITE OUTPUT TAPE 6,57
      WRITE OUTPUT TAPE 6,57
      WRITE OUTPUT TAPE 6,61,(ND(I),I=24,38)
      WRITE OUTPUT TAPE 6,57
      WRITE OUTPUT TAPE 6,57
      WRITE OUTPUT TAPE 6,62,(ND(I),I=39,55)
      WRITE OUTPUT TAPE 6,57
      WRITE OUTPUT TAPE 6,57
      WRITE OUTPUT TAPE 6,62,(ND(I),I=56,72)
      WRITE OUTPUT TAPE 6,57
      WRITE OUTPUT TAPE 6,57
      WRITE OUTPUT TAPE 6,63,(ND(I),I=73,91)
      WRITE OUTPUT TAPE 6,57
      WRITE OUTPUT TAPE 6,57
      WRITE OUTPUT TAPE 6,63,(ND(I),I=92,110)
      WRITE OUTPUT TAPE 6,57
      WRITE OUTPUT TAPE 6,57
      WRITE OUTPUT TAPE 6,63,(ND(I),I=111,129)
      WRITE OUTPUT TAPE 6,67,ND(322),ND(323)
      WRITE OUTPUT TAPE 6,57
      WRITE OUTPUT TAPE 6,63,(ND(I),I=130,148)
      WRITE OUTPUT TAPE 6,67,ND(324),ND(325)
      WRITE OUTPUT TAPE 6,57
      WRITE OUTPUT TAPE 6,64,(ND(I),I=149,169)
      WRITE OUTPUT TAPE 6,57
      WRITE OUTPUT TAPE 6,67,ND(326),ND(327)
      WRITE OUTPUT TAPE 6,63,(ND(I),I=170,188)
      WRITE OUTPUT TAPE 6,57
      WRITE OUTPUT TAPE 6,67,ND(328),ND(329)
      WRITE OUTPUT TAPE 6,63,(ND(I),I=189,207)
      WRITE OUTPUT TAPE 6,57
      WRITE OUTPUT TAPE 6,57
```

```
      WRITE OUTPUT TAPE 6,63,(ND(I),I=208,226)
      WRITE OUTPUT TAPE 6,57
      WRITE OUTPUT TAPE 6,57
      WRITE OUTPUT TAPE 6,63,(ND(I),I=227,245)
      WRITE OUTPUT TAPE 6,57
      WRITE OUTPUT TAPE 6,57
      WRITE OUTPUT TAPE 6,62,(ND(I),I=246,262)
      WRITE OUTPUT TAPE 6,57
      WRITE OUTPUT TAPE 6,57
      WRITE OUTPUT TAPE 6,62,(ND(I),I=263,279)
      WRITE OUTPUT TAPE 6,57
      WRITE OUTPUT TAPE 6,57
      WRITE OUTPUT TAPE 6,61,(ND(I),I=280,294)
      WRITE OUTPUT TAPE 6,57
      WRITE OUTPUT TAPE 6,57
      WRITE OUTPUT TAPE 6,60,(ND(I),I=295,307)
      GO TO (17,18),KLIK
17    WRITE OUTPUT TAPE 6,54
      GO TO 19
18    WRITE OUTPUT TAPE 6,69
19    WRITE OUTPUT TAPE 6,70,KPCA
      WRITE OUTPUT TAPE 6,59,(ND(I),I=308,316)
      WRITE OUTPUT TAPE 6,57
      WRITE OUTPUT TAPE 6,66,ND(330),ND(331),ND(332),ND(333)
      WRITE OUTPUT TAPE 6,65,ND(317)
      GO TO (20,22),KLIK
20    DO 21 I=1,333
      XND=ND(I)
21    ND(I)=XND*RNCDS+.5
      KLIK=2
      GO TO 16
22    GO TO 3
50    FORMAT(1X,I3,1X,I1,1X,I3,I5)
51    FORMAT(7X,3F11.8)
52    FORMAT(I3)
53    FORMAT(1X,I3,1X,I2,1X,I1)
54    FORMAT(21H      NUMBER OF POINTS)
57    FORMAT(1X)
58    FORMAT(21H1DENSITY DISTRIBUTION,29X,I5)
59    FORMAT(30X,9I5)
60    FORMAT(20X,13I5)
61    FORMAT(15X,15I5)
62    FORMAT(10X,17I5)
63    FORMAT(5X,19I5)
64    FORMAT(21I5)
65    FORMAT(50X,I5)
66    FORMAT(39X,I5,I6,I10,I6)
67    FORMAT(I6,93X,I5)
68    FORMAT(12H STATION NO.,I4)
69    FORMAT(21H PERCENTAGE OF POINTS)
70    FORMAT(4H PER,I3,13H PERCENT AREA)
      END
```

DENSITY DISTRIBUTION

STATION NO. 105

								0	7	14	45	55								
					4	0	1	4	8	26	44	49	12							
			21	11	3	0	0	0	0	2	5	5	3	0	2					
		45	18	2	0	0	0	0	0	0	0	0	0	1	2	6				
	46	25	5	0	0	0	0	0	0	0	0	0	0	1	4	7	8			
	31	6	1	0	0	0	0	0	0	0	0	0	0	0	2	4	8			
8	5	2	0	0	0	0	0	0	0	0	0	0	0	0	0	4	11	7		
2	1	0	0	0	0	0	0	0	0	0	0	0	0	0	0	1	10	11		
0	0	0	0	0	0	0	0	0	0	0	0	0	0	0	0	1	7	8		
0	0	0	0	0	0	0	0	0	0	0	0	0	0	0	0	0	1	2		7
1	1	0	0	0	0	0	0	0	0	0	0	0	0	0	0	0	0	0	1	1
2	2	0	0	0	0	0	0	0	0	0	0	0	0	0	0	0	0	0	0	
6	5	4	0	0	0	0	0	0	0	0	0	0	0	0	0	0	0	0	0	
	5	4	1	0	0	0	0	0	0	0	0	0	0	0	0	0	0	0		
	4	4	1	0	0	0	0	0	0	0	0	0	0	0	0	0	3	8		
		6	2	0	0	0	0	0	0	0	0	0	0	0	0	1	19			
		8	4	2	0	0	0	0	0	0	0	0	0	0	1	7	46			
			5	2	1	0	0	0	0	0	0	0	0	1	3	40				
				2	0	0	0	0	0	0	0	0	0	1	21					
						7	9	4	5	0	0	0	0	1						
								53	20		1	0								

NUMBER OF POINTS
PER 1 PERCENT AREA

DENSITY DISTRIBUTION

STATION NO. 105

									0	3	6	19	23										
						2	0	0	2	3	11	19	21	5									
				9	5	1	0	0	0	0	1	2	2	1	0	1							
			19	8	1	0	0	0	0	0	0	0	0	0	0	1	3						
		19	11	2	0	0	0	0	0	0	0	0	0	0	0	2	3	3					
		13	3	0	0	0	0	0	0	0	0	0	0	0	0	1	2	3					
	3	2	1	0	0	0	0	0	0	0	0	0	0	0	0	0	2	5	3				
	1	0	0	0	0	0	0	0	0	0	0	0	0	0	0	0	0	4	5				
	0	0	0	0	0	0	0	0	0	0	0	0	0	0	0	0	0	3	3				
0																				3			
	0	0	0	0	0	0	0	0	0	0	0	0	0	0	0	0	0	0	1				
0																				0			
0	0	0	0	0	0	0	0	0	0	0	0	0	0	0	0	0	0	0	0	0			
1																				0			
	1	0	0	0	0	0	0	0	0	0	0	0	0	0	0	0	0	0	0				
3																				0			
	2	2	0	0	0	0	0	0	0	0	0	0	0	0	0	0	0	0	0				
	2	2	0	0	0	0	0	0	0	0	0	0	0	0	0	0	0	0	0				
	2	2	0	0	0	0	0	0	0	0	0	0	0	0	0	0	0	1	3				
		3	1	0	0	0	0	0	0	0	0	0	0	0	0	0	0	8					
		3	2	1	0	0	0	0	0	0	0	0	0	0	0	0	3	19					
			2	1	0	0	0	0	0	0	0	0	0	0	0	1	17						
				1	0	0	0	0	0	0	0	0	0	0	0	9							

PERCENTAGE OF POINTS
PER 1 PERCENT AREA

						3	4	2	2	0	0	0	0	0									
								22	8		0	0											

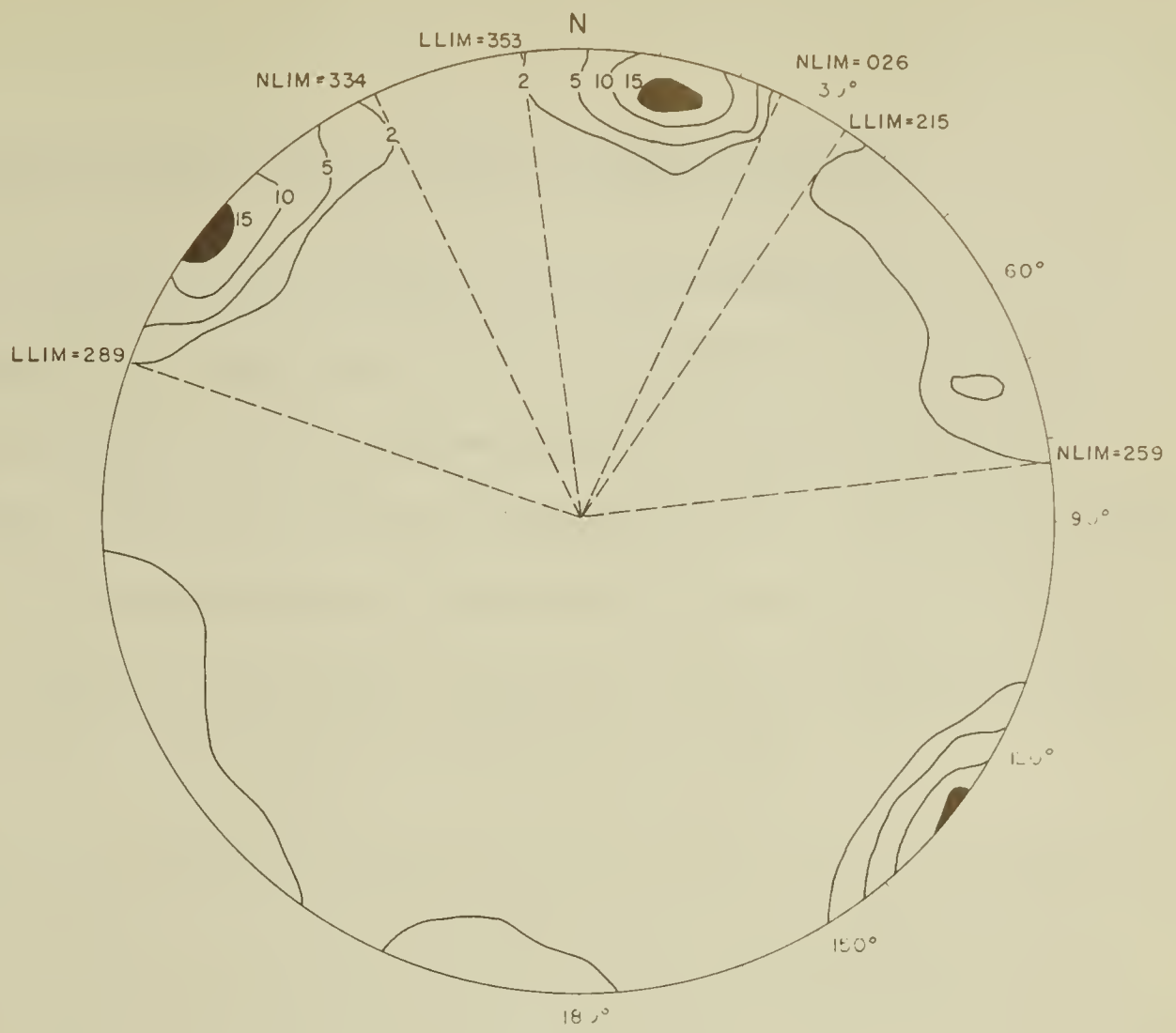
N
LLIM=353
NLIM=334
NLIM=026
LLIM=215
LLIM=289
NLIM=259
2
5
10
15
60°
150°

FIG. 4

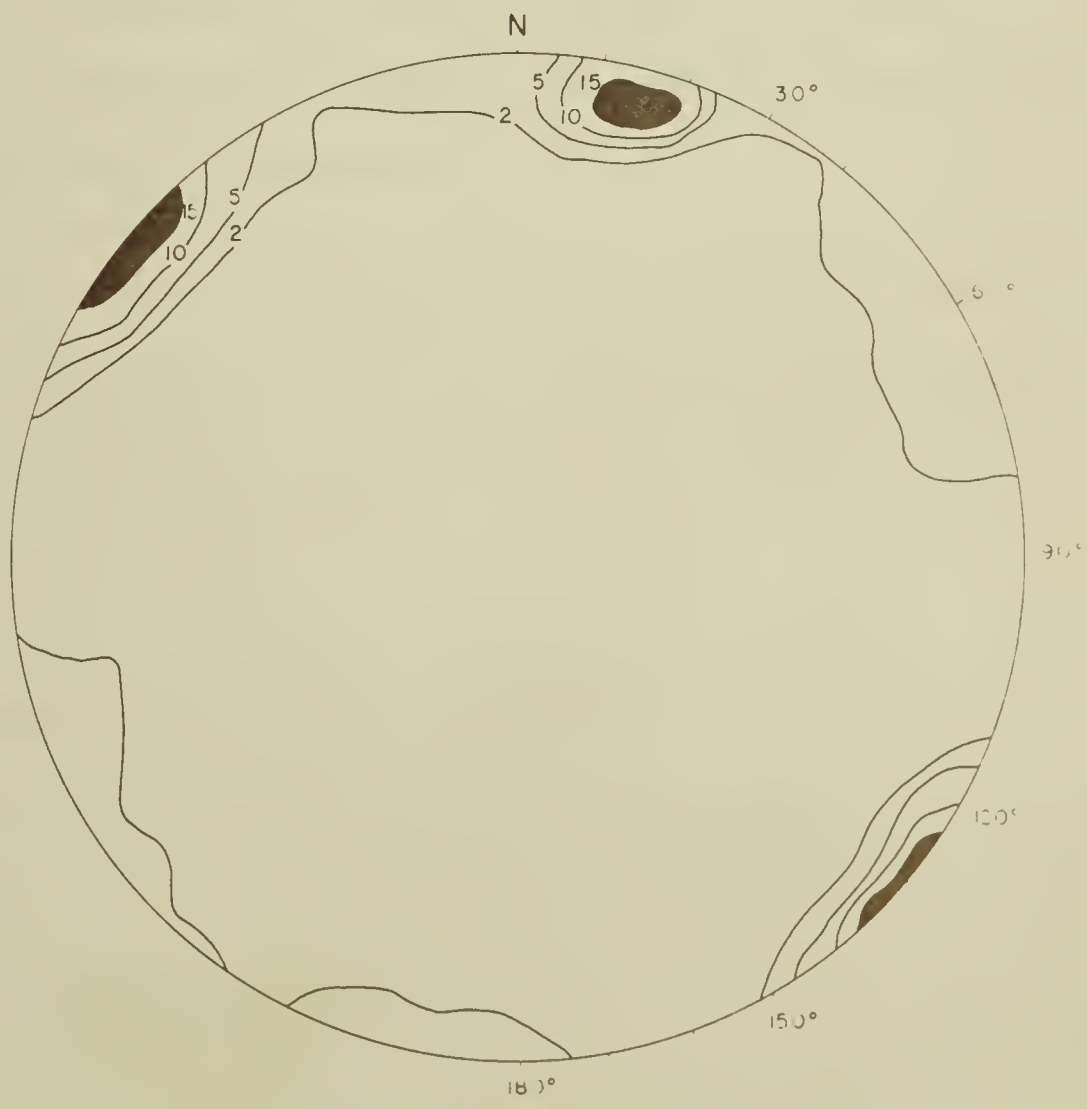
N
2
5
10
15
30°
150°

FIG.5

Determination of Mean Fracture Planes: Program 913107-002

Introduction. The quantitative evaluation of orientation diagrams has received considerable attention in recent years. In fracture analysis the determination of the mean fracture planes, which are represented by the observed maxima, is of utmost importance. These have previously been determined by empirically choosing the peak value of the concentration, or by estimating centers of gravity (Pincus, 1951, p. 105; Spencer, 1959, p. 480). Where peak values are not symmetrically centered, significant errors may be introduced by this method.

Statement of problem. Individual maxima can be analyzed using the statistical treatment of the dispersion of points on a sphere, as has been developed by R.A. Fisher (1953). This method of analysis has proved to be a useful took in the analysis of paleomagnetic data. Cox and Doell (1960, p. 669) suggested that this method of analysis could also be applied to other problems involving sets of vectors or lines. The mean value defined by the maximum, the confidence radius about the mean, and the dispersion can be calculated.

Method. The data processed by this program consists of a number (NCDS) of fracture attitudes specified by their strike (NSTR), dip (NDIP), and direction (NDIR). These attitudes are converted by the computer to direction cosines ($\lambda_i, \mu_i, \gamma_i$) by using equations (1), (2), and (3).

When using Fisher's statistics one assumes that the sample was randomly drawn from a population in which the points are distributed with axial symmetry about the true mean direction, and that the density vector decreases with increasing angular displacement ψ from the mean according to the probability density function

$$P = (K/4\pi \sinh K) \exp (K \cos\psi) \qquad (5)$$

K is known as the "precision parameter" and is a measure of the dispersion of the points. K is large for a tight grouping about the mean, and zero for a uniform distribution of the points on the sphere.

Fisher (1953, p. 296) showed that the best estimate (λ, μ, γ) of the true mean direction is the vector sum of the individual directions $(\lambda_i, \mu_i, \gamma_i)$. That is

$$\lambda = \frac{\sum \lambda_i}{R} \qquad \mu = \frac{\sum \mu_i}{R} \qquad \gamma = \frac{\sum \gamma_i}{R} \tag{6}$$

where

$$R^2 = (\sum \lambda_i)^2 + (\sum \mu_i)^2 + (\sum \gamma_i)^2 \tag{7}$$

The azimuth and the inclination of the resultant vector are determined using the relationships (Cox and Doell, 1960, p. 669):

$$\tan D_r = \frac{\sum \mu_i}{R} \qquad \sin I_r = \frac{\sum \gamma_i}{R} \tag{8}$$

where D_r is the declination and I_r the inclination of the resultant vector.

The accuracy of the calculated mean direction (λ, μ, γ) can be estimated by the cosine of the angle between this mean and the true mean. Fisher (1953, p. 303) showed that at a probability level of (1 - P) the true mean direction of the population lies within a circular cone about the resultant vector with a semi-vertical angle α, given for $K > 3$ by the expression

$$\cos \alpha = 1 - \frac{N - R}{R} \left\{ \left[\frac{1}{P} \right] \exp \frac{1}{N-1} - 1 \right\} \tag{9}$$

where N is the total number of vectors included in the analysis. Usually P is chosen to be .05, which means that there is one chance in twenty that the true mean direction lies outside the cone of confidence.

Where $K \leq 3$, Fisher (ibid.) showed that "k", the best estimate of K, is given by

$$k = \frac{N - 1}{N - R} \tag{10}$$

As N is increased without limit, this estimate of the precision parameter approaches the true value of K, α on the other hand becomes infinitely small (Cox and Doell, 1960, p. 671).

Wilson (1959, p. 751) pointed out that Fisher's statistics are based on an assumed Gaussian distribution of density of the measured vectors about the mean direction. However, this type of distribution is not always valid, and in a rigorous analysis the observations should first be fitted to Fisher's distribution. In cases where there is no good fit, any circle of confidence containing the mean direction with a specified probability may contain falsely implied precision. Wilson (1959, p. 755) suggested the use of the root mean square deviation, given by

$$\delta = (2\,(N-R) / N)^{1/2} \tag{11}$$

and the standard deviation of the mean direction, given by

$$\epsilon = \delta / N^{1/2} \tag{12}$$

In some cases it may be advantageous to use δ and ϵ, because no assumptions about the distribution of the line or vector densities have to be made.

Because Fisher's statistics are designed for vectors, lines have to be converted to vectors before proceeding with the analysis. This can be accomplished by dividing the reference sphere into two hemispheres along the equatorial plane, and arbitrarily assigning a positive sense to all the lines falling into the lower hemisphere. In many petrofabric problems planes are steeply dipping and lineations gently plunging. The poles of the same maximum will therefore commonly fall at diametrically opposed positions on the hemisphere. In order to account for this

behaviour in the computer program, a dextral (LLIM) and a sinistral (NLIM) azimuthal limit had to be drawn for each maximum (Fig. 4).

Limitations on parameters.

$$\begin{aligned} & & NCDS &\leq 500 \\ 0 &\leq P &&\leq 10 \\ 180 &\leq LLIM &&\leq 360 \\ 0 &\leq NLIM &&\leq 360 \\ 0 &\leq NSTR &&\leq 180 \\ 0 &\leq NDIP &&\leq 90 \\ 0 &\leq NDIR &&\leq 2 \end{aligned}$$

Input. (a) Parameter cards.

Card 1

Column	Content	Format
1	blank	1X
2 - 4	Station No.	I3
5	blank	1X
6 - 7	Maximum No.	I2
8	blank	1X
9 - 11	NCDS	I3
12	blank	1X
13	P	I1

Card 2

Column	Content	Format
1	blank	1X
2 - 4	LLIM	I3
5	blank	1X
6 - 8	NLIM	I3

(b) Data cards

Column	Content	Format
1	blank	1X
2 - 4	NSTR	I3
5	blank	1X
6 - 7	NDIP	I2
8	blank	1X
9	NDIR	I1

Order of cards.

(a) Program 913107-002 (pp. 36-37)

(b) Parameter card 1

(c) Parameter card 2

(d) Data cards

Repeat (b) to (d) for subsequent runs. Each run of data, except the first, must be preceeded by the following cards: ..1

..BRANCH 0040R

Output. The program puts out the following information:

(a) Station number and number of the maximum under consideration.

(b) Number of data readings included in the analysis.

(c) Declination of the normal to the mean fracture plane in degrees of azimuth.

(d) Inclination of the normal to the mean fracture plane in degrees from the horizontal.

(e) An estimate of the precision parameter.

(f) Confidence radius in degrees about the mean direction, for a specified probability level.

(g) Root mean square deviation in degrees.

(h) Standard deviation from the mean in degrees.

```
..I 913107 MEAN FRACTURE PLANE MODIFIED  G.K.MUECKE
..I PLEASE SAVE DUMP.
..I PLEASE SAVE CARDS.
..LOAD FORTRAN EXECUTE
      DIMENSION A(500),B(500),G(500)
      PI=3.1415926
      R180=1./180.
      CF=PI*R180
      READ 50,NSTN,NDEN,NCDS,NP
      P=NP
      READ 51,LLIM,NLIM
      SA=0.0
      SB=0.0
      SG=0.0
 1    DO 12 I=1,NCDS
      READ 52,NSTR,NDIP,NDIR
      PL=90-NDIP
      IF(NDIR-1)3,2,3
 2    TR=NSTR+90
      GO TO 5
 3    TR=NSTR-90
      IF(TR)4,5,5
 4    TR=TR+360.
 5    DLIM=LLIM
      IF(TR-DLIM)6,10,10
 6    SLIM=NLIM
      IF(SLIM-DLIM)8,9,9
 8    IF(TR-90.)10,10,9
 9    TR=TR+180.
      PL=PL*CF
      TR=TR*CF
      A(I)=COSF(TR)*COSF(PL)
      B(I)=SINF(TR)*COSF(PL)
      G(I)=-SINF(PL)
      GO TO 11
10    PL=PL*CF
      TR=TR*CF
      A(I)=COSF(TR)*COSF(PL)
      B(I)=SINF(TP)*COSF(PL)
      G(I)=SINF(PL)
11    SA=SA+A(I)
      SB=SB+B(I)
12    SG=SG+G(I)
      R=SQRTF((SA*SA)+(SB*SB)+(SG*SG))
      SININ=SG/R
      TADE=SB/SA
      REIN=ATANF(SININ/SQRTF(1.-SININ*SININ))
      REIN=REIN/CF
      REIN=ABSF(REIN)
      REDE=ATANF(TADE)
      REDE=REDE/CF
      IF(SG)121,122,122
121   SA=-(SA)
      SB=-(SB)
122   IF(SA)15,13,13
13    IF(SB)16,17,17
```

```
15    REDE=180.+REDE
      GO TO 17
16    REDE=360.+REDE
17    CDS=NCDS
      XK=(CDS-1.)/(CDS-R)
      PUNCH 60,NSTN,NDEN
      PUNCH 65,NCDS
      PUNCH 63,REDE
      PUNCH 62,REIN
      PUNCH 61,XK
      PERC=(100.-P)
      P=P*.01
      Q=1./(CDS-1.)
      RR=(CDS-R)/R
      PP=((1./P)**Q)-1.
      RR=RR*PP
      COSAL=1.-RR
      FUN=ABSF((1.-COSAL*COSAL)/(COSAL))
      FUN=SQRTF(FUN)
      AL=ATANF(FUN)
      AL=AL/CF
      DELTA=SQRTF(2.*(CDS-R)/CDS)
      ETA=DELTA/SQRTF(CDS)
      DELTA=DELTA/CF
      ETA=ETA/CF
      PUNCH 64,PERC,AL
      PUNCH 66,DELTA
      PUNCH 67,ETA
50    FORMAT(1X,I3,1X,I2,1X,I3,1X,I1)
51    FORMAT(1X,I3,1X,I3)
52    FORMAT(1X,I3,1X,I2,1X,I1)
60    FORMAT(//8H STATION I4,14H MEAN FRACTURE I3)
61    FORMAT(20H PRECISION PARAMETER,12X,F8.3)
62    FORMAT(22H RESULTANT INCLINATION,10X,F8.3)
63    FORMAT(22H RESULTANT DECLINATION,10X,F8.3)
64    FORMAT(1X,I2,1X,28H PER CENT CONFIDENCE RADIUS F8.3)
65    FORMAT(//13H MEASUREMENTS I23)
66    FORMAT(14H RMS DEVIATION,18X,F8.3)
67    FORMAT(19H STANDARD DEVIATION,13X,F8.3)
      CALL EXIT
      END
```

Test data and results. An example solved by Fisher (1935, p. 304) which consists of nine paleomagnetic directions determined by Hospers (1953) was chosen to test the program. The answers derived by Fisher and the computer are identical. (pp. 39-40)

Determination of Beta Axes and the Preparation of Beta Diagrams: Program 913107-003

Introduction. The most pronounced tendency of any particular set of s-surfaces in a tectonite body is to intersect along a common axis. Where the s-surfaces are folded cylindrically, these intersections tend to cluster around a mean value, known as the β-axis, which defines the axis of folding B (Turner and Weiss, 1963, pp. 154-155).

Conventional methods of analysis involve the determination of lines of intersections on an equal-area net, and the contouring of the diagram. The peak value or center of gravity of the resulting maximum is then taken to define the β-axis.

Statement of problem. It is desired to determine a large number of planar intersections, to calculate their mean direction, and to produce an equal-area projection showing the distribution of these intersections.

Method. The data processed by this program consists of a number (NCDS) of attitudes of s-surfaces specified by their strike (NSTR), dip (NDIP), and direction (NDIR). These attitudes are converted to direction cosines ($\lambda_i, \mu_i, \gamma_i$) using equations (1), (2), and (3).

The normal equation of any plane passing through the origin, whose normal has the direction cosines λ, μ, and γ, is given by

$$\lambda x + \mu y + \gamma z = 0 \tag{13}$$

For two given planes

$$\lambda_1 x + \mu_1 y + \gamma_1 z = 0 \tag{14}$$

and

$$\lambda_2 x + \mu_2 y + \gamma_2 z = 0 \tag{15}$$

the direction cosines of their line of intersection are given by λ_s, μ_s, and γ_s.

```
..I                    INPUT DATA
..I
..I 913107-002  TEST DATA BY FISHER.
..BRANCH 0040R
 222 02 009 5
 343 062
 073 24 2
 152 21 2
 127 20 2
 117 08 2
 089 11 2
 096 17 2
 140 21 2
 088 31 2
 134 39 2
```

..I PROGRAM OUTPUT
..I
..I 913107-002 TEST DATA BY FISHER.
..BRANCH 0040R

STATION 222 MEAN FRACTURE 2

MEASUREMENTS	9
RESULTANT DECLINATION	24.269
RESULTANT INCLINATION	70.771
PRECISION PARAMETER	35.131
95 PER CENT CONFIDENCE RADIUS	8.755
RMS DEVIATION	12.888
STANDARD DEVIATION	4.296

It can then be shown that

$$\mu \frac{\lambda_s}{\mu_1 \gamma_2 - \mu_2 \gamma_1} = \lambda \frac{\mu_s}{\lambda_2 \gamma_1 - \lambda_1 \gamma_2} = \lambda \frac{\gamma_s}{\lambda_1 \mu_2 - \lambda_2 \mu_1} \tag{16}$$

or

$$\lambda_s = \frac{\mu_1 \gamma_2 - \mu_2 \gamma_1}{K} \tag{17}$$

$$\mu_s = \frac{\lambda_2 \gamma_1 - \lambda_1 \gamma_2}{K} \tag{18}$$

$$\gamma_s = \frac{\lambda_1 \mu_2 - \lambda_2 \mu_1}{K} \tag{19}$$

where $$K = (\mu_1 \gamma_2 - \mu_2 \gamma_1)^2 + (\lambda_2 \gamma_1 - \lambda_1 \gamma_2)^2 + (\lambda_1 \mu_2 - \lambda_2 \mu_1)^{2\ 1/2} \tag{20}$$

The β -axis is then found by calculating the vector sum of all the individual directions and using equations (6), (7), and (8). The confidence radius about the β-axis and the precision parameter are calculated from equations (9) and (10) respectively.

The number of mutual intersections of N non-parallel planes is given by

$$N(N - 1)/2 \tag{21}$$

It should be noted that the program will put out the direction cosines of any specified number (IFINI) of intersections. The format of this output is compatible with the input specifications for Program 913107-001. The output of the present program can, therefore, be used directly as data cards in the counting out of a beta diagram.

Limitations on parameters. The limitations are the same as for Program 913107-002, with the exception of $0 \leq IFINI \leq 9999$.

Input. (a) Parameter cards

Card 1

Column	Content	Format
1	blank	1X
2 - 4	Station No.	I3
5	blank	1X
6 - 8	NCDS	I3
9	blank	1X
10	P	I1
11	blank	1X
12 - 15	IFINI	I4

Card 2 has the same format as in Program 913107-002.

(b) Data cards have the same format as in Program 913107-002.

Order of cards.

(a) Program 913107-003 (pp. 43-45)

(b) Parameter card 1

(c) Parameter card 2

(d) Data cards

Repeat (b) to (d) for each subsequent run. Each run of data, except the first, must be preceded by the following cards:

..I

..BRANCH 0040R

Output. The following information is put out by the program:

(a) direction cosines of a specified number of intersections

(b) station number,

(c) number of s-surfaces used in the analysis,

```
..I 913107  BETA DETERMINATIONS          G.K.MUECKE
..I   SAVE CARDS. PLEASE RECORD RUNNING TIME
..LOAD FORTRAN EXECUTE
      DIMENSION A(300),B(300),G(300),AINT(300),BINT(300),GINT(300)
      PI=3.1415926
      R180=1./180.
      CF=PI*R180
      READ 50,NSTN,NCDS,NP,IFINI
      P=NP
      READ 51,LLIM,NLIM
      SA=0.0
      SB=0.0
      SG=0.0
      K=0
 1    DO 11 I=1,NCDS
      READ 52,NSTR,NDIP,NDIR
      PL=90-NDIP
      IF(NDIR-1)3,2,3
 2    TR=NSTR+90
      GO TO 10
 3    TR=NSTR-90
      IF(TR)4,10,10
 4    TR=TR+360.
10    TR=TR*CF
      PL=PL*CF
      A(I)=COSF(TR)*COSF(PL)
      B(I)=SINF(TR)*COSF(PL)
11    G(I)=SINF(PL)
20    DO 21 J=1,NCDS
      AA=A(J)
      BA=B(J)
      GA=G(J)
      GA=G(J)
30    DO 39 L=1,NCDS
      AB=A(L)
      BB=B(L)
      GB=G(L)
      IF(AA-AB)33,31,33
31    IF(BA-BB)33,32,33
32    IF(GA-GB)33,37,33
33    DTRE=(AA*BB)-(AB*BA)
      DONE=(BA*GB)-(BB*GA)
      IF(DTRE)37,332,331
332   IF(DONE)37,331,331
331   DTWO=(AB*GA)-(AA*GB)
      DIVI=SQRTF((DONE*DONE)+(DTWO*DTWO)+(DTRE*DTRE))
      K=K+1
      AINT(L)=DONE/DIVI
      BINT(L)=DTWO/DIVI
      GINT(L)=DTRE/DIVI
      IF (K-IFINI)40,40,41
40    PUNCH 71,AINT(L),BINT(L),GINT(L)
41    IF(AINT(L))338,337,338
338   TRINT=ATANF(BINT(L)/AINT(L))/CF
      IF(AINT(L))335,333,333
333   IF(BINT(L))334,336,336
```

```
334   TRINT=360.+TRINT
      GO TO 336
335   TRINT=180.+TRINT
      GO TO 336
337   IF(BINT(L))339,340,340
339   TRINT=90.
      GO TO 336
340   TRINT=270.
336   DLIM=LLIM
      IF(TRINT-DLIM)34,38,38
34    SLIM=NLIM
      IF(SLIM-DLIM)35,36,36
35    IF(TRINT-90.)38,38,36
36    AINT(L)=-AINT(L)
      BINT(L)=-BINT(L)
      GINT(L)=-GINT(L)
      GO TO 38
37    AINT(L)=0.0
      BINT(L)=0.0
      GINT(L)=0.0
38    SA=SA+AINT(L)
      SB=SB+BINT(L)
39    SG=SG+GINT(L)
21    AA=A(J)
      R=SQRTF((SA*SA)+(SB*SB)+(SG*SG))
      SININ=SG/R
      TADE=SB/SA
      REIN=ATANF(SININ/SQRTF(1.-SININ*SININ))
      REIN=REIN/CF
      REIN=ABSF(REIN)
      REDE=ATANF(TADE)
      REDE=REDE/CF
      IF(SG)121,122,122
121   SA=-(SA)
      SB=-(SB)
122   IF(SA)16,14,14
14    IF(SB)17,18,18
16    REDE=180.+REDE
      GO TO 18
17    REDE=360.+REDE
18    ZINT=K
      XK=(ZINT-1.)/(ZINT-R)
      PUNCH 60,NSTN
      PUNCH 65,NCDS
      PUNCH 66,K
      PUNCH 61,XK
      PUNCH 63,REDE
      PUNCH 62,REIN
      P=P*.01
      Q=1./(ZINT-1.)
      RR=(ZINT-R)/R
      PP=((1./P)**Q)-1.
      RR=RR*PP
      COSAL=1.-RR
      FUN=ABSF((1.-COSAL*COSAL)/(COSAL))
      FUN=SQRTF(FUN)
```

```
      AL=ATANF(FUN)
      AL=AL/CF
      PUNCH 64,AL
50    FORMAT(1X,I3,1X,I3,1X,I1,1X,I4)
51    FORMAT(1X,I3,1X,I3)
52    FORMAT(1X,I3,1X,I2,1X,I1)
60    FORMAT(//8H STATIONI4,4X,24H BETA AXIS DETERMINATION)
61    FORMAT(21H PRECISION PARAMETER F10.3)
62    FORMAT(23H RESULTANT INCLINATION F8.3)
63    FORMAT(23H RESULTANT DECLINATION F8.3)
64    FORMAT(19H CONFIDENCE RADIUS F12.3)
65    FORMAT(//13H MEASUREMENTSI14)
66    FORMAT(14H INTERSECTIONSI13)
71    FORMAT(7X,3F11.8)
      CALL EXIT
      END
```

(d) number of intersections calculated and used in calculating the mean,

(e) precision parameter,

(f) azimuth of the delination of the β -axis in degrees,

(g) inclination of the β -axis in degrees from the horizontal,

(h) confidence radius about the β -axis for a specified probablility level.

Test data and results. Four planes which intersect along a common line on the stereographic net were chosen as test data. The attitude of their intersection agrees closely with the value calculated by the computer. (pp. 47-48)

Determination of Cleavage-Bedding Intersections: Program 913107-004

Statement of problem. The intersection between two different sets of s-surfaces may sometimes yield useful structural information. The intersection between bedding and axial plane cleavage may be used to define the axis of folding B, or it may be desired to find the lines of intersection of different fracture sets.

Method. The data processed by this program consists of a number (NCDS) of attitudes of s-surfaces specified by their strike (NSTR), dip (NDIP), and direction (NDIR). These attitudes are converted to direction cosines $(\lambda_i, \mu_i, \gamma_i)$ using equations (1), (2), and (3).

Intersections are calculated using equations (17), (18), (19), and (20). The program differs from 913107-003 in that intersections of chosen planes are calculated, rather than all the possible intersections of a set of s-surfaces.

Limitations on parameters.

	NCDS	300
0	NSTR	180
0	NDIP	90
0	NDIR	2

```
..I                    INPUT DATA
..I
..I 913107  BETA DETERMINATIONS          G.K.MUECKE
..BRANCH 0040R
 999 004 5
 180 270
 179 30 2
 146 26 2
 086 46 2
 054 90 0
```

```
..I                  PROGRAM OUTPUT
..I
..I 913107  BETA DETERMINATIONS              G.K.MUECKE
..BRANCH 0040R


 STATION 999      BETA AXIS DETERMINATION


 MEASUREMENTS                 4
 INTERSECTIONS                6
 PRECISION PARAMETER     1510.026
 RESULTANT DECLINATION    235.695
 RESULTANT INCLINATION     26.388
 CONFIDENCE RADIUS          1.724
```

Input. (a) Parameter card

Column	Content	Format
1	blank	1X
2 - 4	Station N	I3
5	blank	1X
6 - 8	NCDS	I3

(b) Data cards have the same format as in Program 913107-002. Each data set should consist of a series of pairs of data cards, each pair being a bedding attitude followed by a cleavage attitude.

Order of cards.

(a) Program 913107-004 (pp. 50-51)

(b) Parameter card

(c) Data cards

Repeat (b) and (c) for subsequent runs. Each run of data, except the first, must be preceded by the following cards:

..I

..BRANCH 0040R

Output. The following information is put out by the program:

(a) station number,

(b) intersection number,

(c) bedding attitude,

(d) cleavage attitude,

(e) trend of the cleavage-bedding intersection,

(f) plunge of the cleavage-bedding intersection,

(g) direction cosines of the cleavage-bedding intersection.

It should be noted that the program puts out the direction cosines of the inter-

```
..I 913107  BEDDING-CLEAVAGE INTERSECTIONS  G.K.MUECKE
..I PLEASE SAVE CARDS.
..LOAD FORTRAN DUMP
      DIMENSION A(300),B(300),G(300),KSTR(300),KDIP(300),KDIR(300)
      PI=3.1415926
      R180=1./180.
      CF=PI*R180
      READ 100,NSTN,NCDS
      PUNCH 200,NSTN
      IFINI=NCDS-1
      K=0
 1    DO 11 I=1,NCDS
      READ 101,NSTR,NDIP,NDIR
      KSTR(I)=NSTR
      KDIP(I)=NDIP
      KDIR(I)=NDIR
      PL=90-NDIP
      IF(NDIR-1)3,2,3
 2    TR=NSTR+90
      GO TO 10
 3    TR=NSTR-90
      IF(TR)4,10,10
 4    TR=TR+360.
 10   TR=TR*CF
      PL=PL*CF
      A(I)=COSF(TR)*COSF(PL)
      B(I)=SINF(TR)*COSF(PL)
 11   G(I)=SINF(PL)
 20   DO 21 J=1,IFINI,2
      AA=A(J)
      BA=B(J)
      GA=G(J)
      JSTR=KSTR(J)
      JDIP=KDIP(J)
      JDIR=KDIR(J)
      L=J+1
      AB=A(L)
      BB=B(L)
      GB=G(L)
      LSTR=KSTR(L)
      LDIP=KDIP(L)
      LDIR=KDIR(L)
      IF(AA-AB)33,31,33
 31   IF(BA-BB)33,32,33
 32   IF(GA-GB)33,43,33
 33   DTRE=(AA*BB)-(AB*BA)
      DONE=(BA*GB)-(BB*GA)
      DTWO=(AB*GA)-(AA*GB)
      DIVI=SQRTF((DONE*DONE)+(DTWO*DTWO)+(DTRE*DTRE))
      K=K+1
      AINT=DONE/DIVI
      BINT=DTWO/DIVI
      GINT=DTRE/DIVI
      TIP=AINT
      TAP=BINT
      TOE=GINT
```

```
      IF(AINT)36,40,36
36    TRINT=ATANF(BINT/AINT)/CF
      GO TO 50
40    IF(BINT)41,42,42
41    TRINT=90.
      GO TO 420
42    TRINT=270.
420   PLINT=ATANF(GINT/SQRTF(1.-GINT*GINT))
      PLINT=ABSF(PLINT/CF)
      GO TO 65
43    AINT=0.0
      BINT=0.0
      GINT=0.0
50    PLINT=ATANF(GINT/SQRTF(1.-GINT*GINT))
      PLINT=ABSF(PLINT/CF)
      IF(GINT)60,61,61
60    AINT=-AINT
      BINT=-BINT
61    IF(AINT)63,62,62
62    IF(BINT)64,65,65
63    TRINT=180.+TRINT
      GO TO 65
64    TRINT=360.+TRINT
65    PUNCH 201,K
      PUNCH 202,JSTR,JDIP,JDIR
      PUNCH 203,LSTR,LDIP,LDIR
      PUNCH 204,TRINT
      PUNCH 205,PLINT
21    PUNCH 206,TIP,TAP,TOE
100   FORMAT(1X,I3,1X,I3)
101   FORMAT(1X,I3,1X,I2,1X,I1)
200   FORMAT(//8H STATIONI4,4X,30H CLEAVAGE-BEDDING INTERSECTION)
201   FORMAT(//17H INTERSECTION NO.,I3)
202   FORMAT(/17H BEDDING ATTITUDE,7X,I3,1X,I2,1X,I1)
203   FORMAT(18H CLEAVAGE ATTITUDE,6X,I3,1X,I2,1X,I1)
204   FORMAT(20H INTERSECTION TREND F11.3)
205   FORMAT(21H INTERSECTION PLUNGE F10.3)
206   FORMAT(7X,3F11.8)
      CALL EXIT
      END
```

sections in a format compatible to the input for Program 913107-001. The direction cosines can, therefore, be used directly to produce orientation diagrams.

Test data and results. A data set consisting of four pairs of bedding and cleavage attitudes respectively was used to test the program. Results obtained by the computer program check with those obtained using the stereographic net. (pp. 53-54)

Preparation of Lineation Diagrams

A method, which permits the illustration of linears and their relationship to the plane in which they occur, has been devised by Hoeppener (1957, pp. 19-20). The attitude of the slickensides, the joint plane in which they occur, and the relative movement can be shown in one diagram.

The attitude of any plane passing through the center of the reference sphere can be defined by the penetration pole of the normal to the plane. A linear lying in the plane can be defined by a family of great circles in which the linear lies. There is, however, only one great circle which is common to both the penetration pole of the plane and the penetration pole of the linear. This unique great circle plus the penetration pole of the plane clearly show the relationship between the plane and the linear. On the projection it is usually sufficient to give the great circle only in the vicinity of the penetration pole on the sphere. The sense of relative movement, if known, can then be given by marking the direction of movement of the hanging wall by an arrow.

```
..I                    INPUT DATA
..I
..I 913107 TEST DATA
..BRANCH 0040R
 999 008
 160 16 2              BDG
 108 20 1              CLE
 020 78 2              BDG
 064 80 1              CLE
 055 24 2              BDG
 135 28 2              CLE
 170 36 2              BDG
 070 50 2              CLE
```

```
..I                 PROGRAM OUTPUT
..I
..I 913107  BEDDING-CLEAVAGE INTERSECTIONS  G.K.MUECKE

 STATION 999     CLEAVAGE-BEDDING INTERSECTION

 INTERSECTION NO.  1

 BEDDING ATTITUDE        160 16 2
 CLEAVAGE ATTITUDE       108 20 1
 INTERSECTION TREND      310.687
 INTERSECTION PLUNGE       7.991
         .64559932 -.75091602  .13902055

 INTERSECTION NO.  2

 BEDDING ATTITUDE         20 78 2
 CLEAVAGE ATTITUDE        64 80 1
 INTERSECTION TREND       44.155
 INTERSECTION PLUNGE      62.551
        -.33070879 -.32110202 -.88742617

 INTERSECTION NO.  3

 BEDDING ATTITUDE         55 24 2
 CLEAVAGE ATTITUDE       135 28 2
 INTERSECTION TREND      178.977
 INTERSECTION PLUNGE      20.264
        -.93795415  .01673619  .34635526

 INTERSECTION NO.  4

 BEDDING ATTITUDE        170 36 2
 CLEAVAGE ATTITUDE        70 50 2
 INTERSECTION TREND      221.502
 INTERSECTION PLUNGE      29.623
         .65104118  .57603689 -.49429434
```

GENERAL GEOLOGY

Introduction

Joints were measured in three of the structural sub-provinces of the Canadian Rocky Mountains (Fig. 3). The Foothills sub-province, bound to the east by the undisturbed Interior Plains and to the west by the McConnell fault, is composed mainly of Mesozoic sedimentary rocks. Closely spaced west-dipping thrust faults and tight folds are the most prominent macroscopic structural elements. The Eastern Ranges, which border the Foothills to the west, consist predominantly of Upper Paleozoic strata. Imbricate thrust sheets, showing usually only a minor amount of folding, predominate in this region. The Castle Mountain thrust forms the eastern boundary of the Main Range sub-province. Rocks in the Castle Mountain thrust sheet are of Lower Paleozoic age and form gently undulating structures.

Bow River Area

Previous work. The general geology along the Bow River between Kananaskis Falls and Morley was previously studied by Cairnes (1914), Rutherford (1927), and Beach (1943). A limited number of observations on the mesocscopic structures were made by Roeder (1960, p. 591) in the vicinity of Kananaskis Falls.

The writer's investigations were confined to a seven mile long strip along the Bow River, east of Kananaskis Falls (Fig. 6).

Stratigraphy. All beds observed in the course of this study belong to the Upper Cretaceous Alberta group, which can be divided into the following formations:

Upper Cretaceous	Wapiabi formation	1775'
	Cardium formation	220' - 230'
	Blackstone formation	700' - 800'


OLDFORT CREEK
HIGHWAY NO. 1A
HORSESHOE FALLS
DAM
KANANASKIS ANTICLINE
HORSESHOE ANTICLINE
OLDFORT ANTICLINE
FLATTOP ANTICLINE
TIGHT ANTICLINE
BOW RIVER
KANANASKIS FALLS
SEEBE
4219
OZADA
4164
C.P.R. RAILWAY
TRANS-CANADA HIGHWAY
KANANASKIS RIVER
LEGEND
UPPER CRETACEOUS
WAPIABI FORMATION
CARDIUM FORMATION
BLACKSTONE FORMATION
LOWER CRETACEOUS
BLAIRMORE FORMATION
ORIENTATION DIAGRAM LOCATIONS
N
0 1/4 1/2 1 2
MILES

FIGURE 6

Fracture measurements were carried out in the Cardium formation, which can be further subdivided using distinctive changes in lithology. A section of the Cardium formation measured by Cairnes (1914, pp. 27-28) at the mouth of Oldfort Creek may be summarized as follows:

Overlying beds - Blackstone formation

Cardium formation

Upper sandstone unit	70'
Dark shale unit	60'
Middle sandstone unit	30'
Dark shale unit	20'
Lower sandstone unit	40'

Underlying beds - Wapiabi formation

The middle sandstone unit thins to the east and is represented only by an argillaceous sandstone in the eastern portions of the region.

Lithology of sandstone units. The sandstones of the Cardium formation are brownish grey to grey, rusty red to brown weathering, generally fine grained, quartzose, and well cemented. Cross-stratification in all the sandstone units was found to be more common than previously reported. Bedding thicknesses are 1/2 inch to 1 foot in the upper sandstone unit, 1 foot to 4 feet in the middle sandstone unit, and 1/2 inch to 3 feet in the lower sandstone unit.

Structural setting. The area is located in the severely disturbed Foothills sub-province. The resistant sandstone members of the Cardium formation produce readily traceable ridges north and south of the Bow River, and excellent outcrops are found along the banks of the Bow River. The beds are deformed into folds which trend north 30 degrees west and plunge to the northwest. Six of the anticlines were investigated in detail.

Three thrust faults, striking from north 30 degrees west to north-south, can be inferred from the abrupt terminations of Cardium outcrops. Thrust planes, although not exposed, are thought to dip steeply to the southwest.

Red Deer River Area

The Red Deer anticline is situated north of the junction of the Red Deer River and the Alberta Forestry Trunk Road (Fig. 7). The area lies within the Foothills and its stratigraphy is identical to that discussed for the Bow River region. Joints were measured in the upper and lower sandstone units of the Cardium formation. 25 feet of the upper and 20 feet of the lower sandstone unit are exposed. The sandstones are grey in color, rusty weathering, fine grained, well sorted, and quartzitic. Cross-stratification is common. The thickness of the beds varies from 2 inches to 2 1/2 feet in the upper unit, and from 6 inches to 3 feet in the lower unit.

The beds are in a large anticlinal fold which has a well exposed eastern limb and only poor exposures in the western limb. The fold is asymmetric and its axial plane dips steeply to the southwest. The anticlinal axis trends approximately north 40 degrees west and plunges 10 degrees to the northwest.

Cripple Creek Area

Erdman (1946) has investigated the general geology of this section of the Foothills. Fractures were measured in the Cardium Formation, which is 375 feet thick at this locality. The Cardium formation can be subdivided into the following units (Erdman, 1946, p. 2):

Overlying beds - Wapiabi formation

Cardium formation

Upper sandstone unit	75'
Middle sandy shale unit	200'
Lower sandstone unit	100'

Underlying beds - Blackstone formation

FIGURE 7

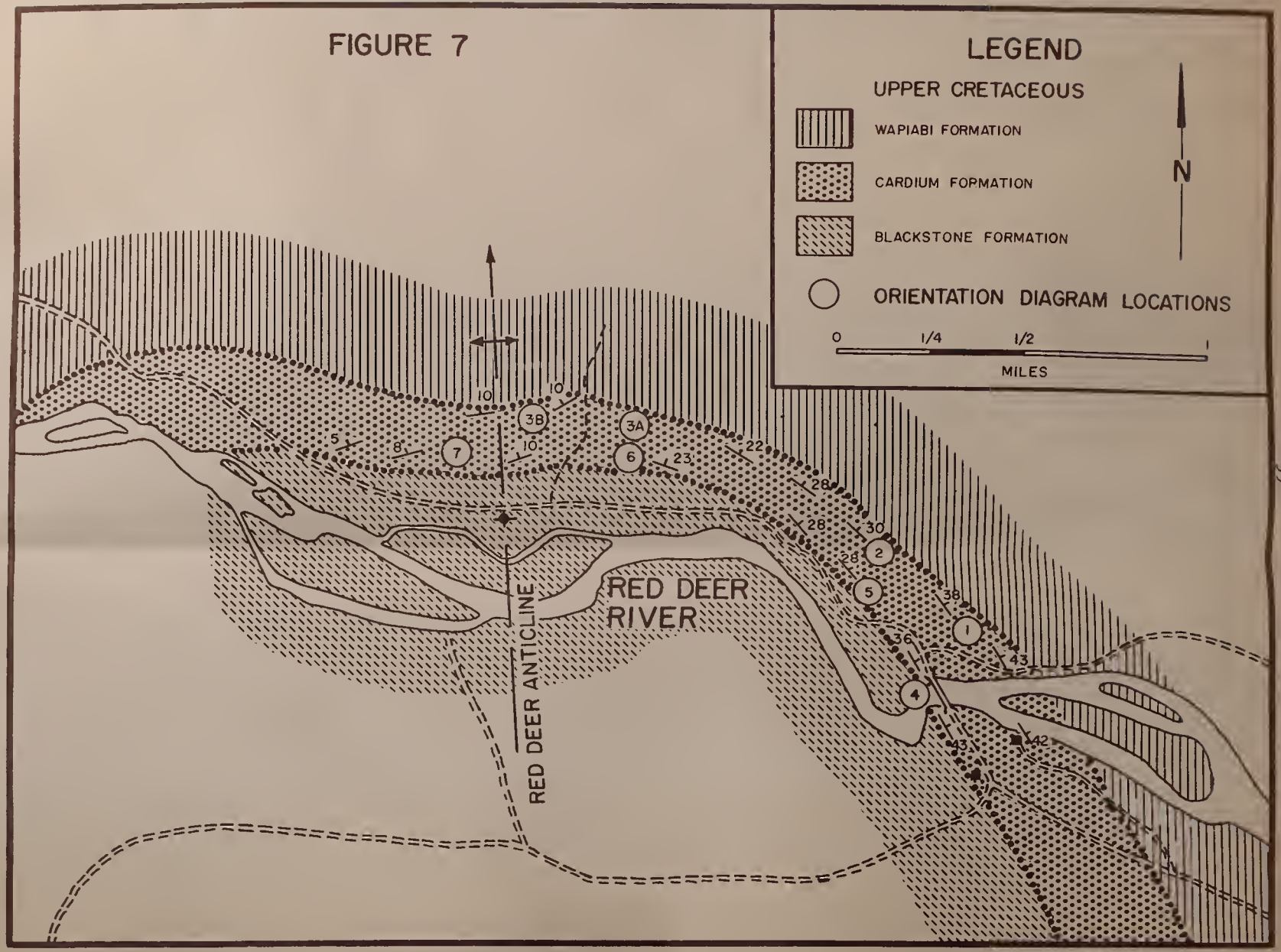
LEGEND
UPPER CRETACEOUS
WAPIABI FORMATION
CARDIUM FORMATION
BLACKSTONE FORMATION
ORIENTATION DIAGRAM LOCATIONS
0
1/4
1/2
1
MILES
N
RED DEER ANTICLINE
RED DEER RIVER
10
10
5
8
10
22
28
28
28
30
38
36
43
43
42
23
1
2
3A
3B
4
5
6
7

The sandstones are grey, rusty weathering, fine grained, and quartzitic. Cross-stratification and ripple marks are present, and the bedding thickness ranges from 4 inches to 2 1/2 feet.

The sampling locality is situated in a southwest-dipping monoclinal thrust sheet. The thrust shows a maximum stratigraphic throw os 5000' a few miles south of the area investigated (Erdman, 1946, p. 3).

South Creek Area

Joints were measured in the lower sandstone unit of the Cardium formation. The sandstones attain a thickness of 60' at this location and are brownish grey in color, rusty brown to orange brown weathering, fine grained, and show frequent cross-stratification. Beds range from 2 inches to 4 feet in thickness.

Fractures were measured at two locations two miles apart, but in identical structural positions on the east limb of a syncline trending north 35 degrees west.

Exshaw Area

Fracturing in the Exshaw thrust sheet of the Eastern Ranges was investigated at one locality on Highway No. 1A (Fig. 8). The resistant, massive limestones of the upper part of the Palliser formation are exposed along the road and show excellent fracture development. The lithology is a dark grey, light grey weathering bio-pelmicrites.

The Exshaw fault in this area dips approximately 60 degrees to the west (Clark, 1954, p. 44). Beds in the thrust sheet show a monoclinal dip of 40 to 65 degrees to the west.

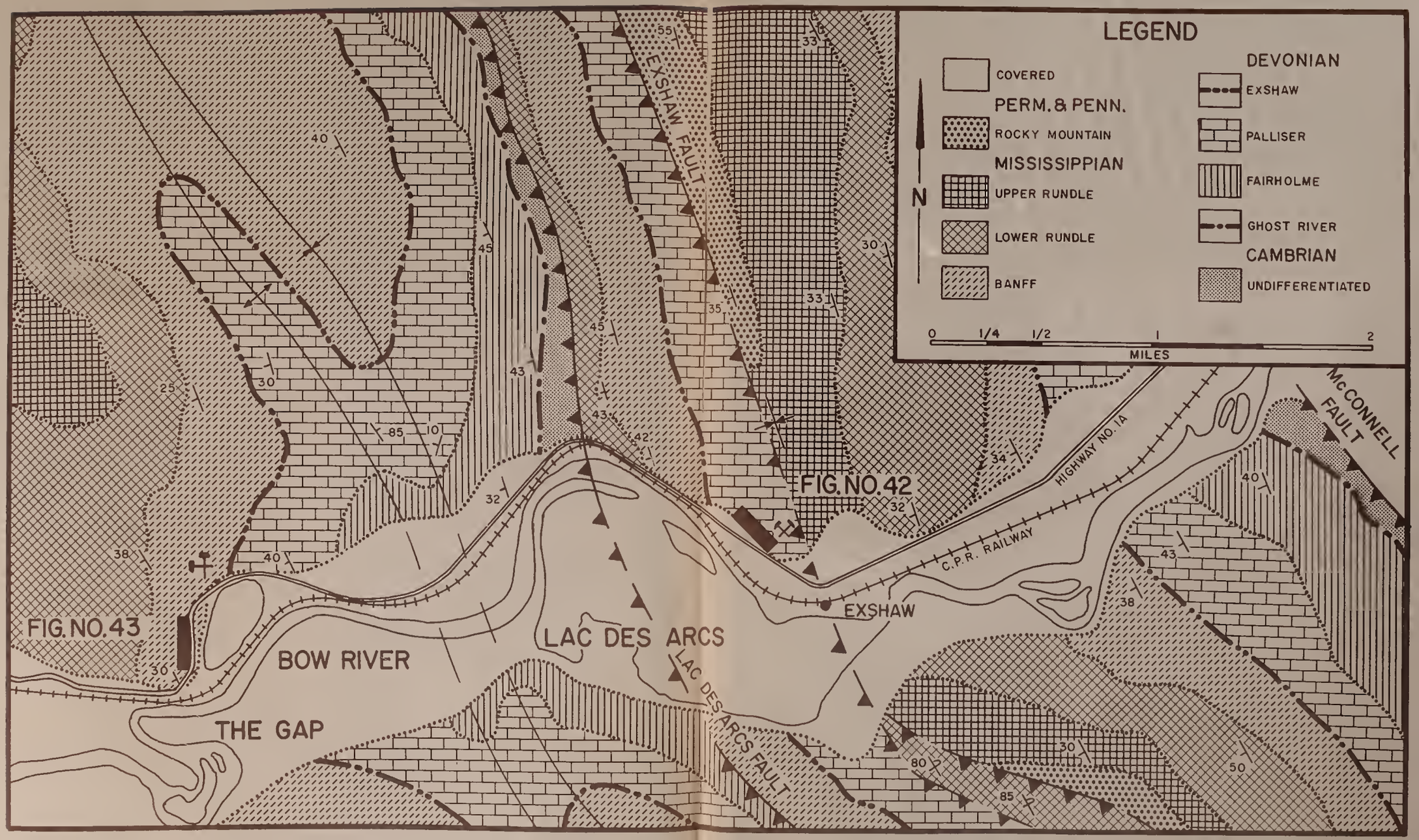
LEGEND
COVERED
PERM. & PENN.
ROCKY MOUNTAIN
MISSISSIPPIAN
UPPER RUNDLE
LOWER RUNDLE
BANFF
DEVONIAN
EXSHAW
PALLISER
FAIRHOLME
GHOST RIVER
CAMBRIAN
UNDIFFERENTIATED
N
0 1/4 1/2 1 2
MILES
EXSHAW FAULT
McCONNELL FAULT
HIGHWAY NO. 1A
C.P.R. RAILWAY
FIG. NO. 42
FIG. NO. 43
LAC DES ARCS
LAC DES ARCS FAULT
BOW RIVER
THE GAP
EXSHAW

FIGURE 8

The Gap Area

The upper portion of the Banff formation in the Lac des Arcs thrust sheet (Fig. 8) shows some fracturing in a road outcrop along Highway No. 1A. The beds are mainly dark grey, medium grained, argillaceous biocalcarenites, and dark grey calcilutites. Frequent stringers of black chert, up to 3 inches thick, are found near the top of the exposure. Heavy calcite veining sub-parallel to the bedding is common.

The Lac des Arcs thrust sheet of the Eastern Ranges has been folded along axes trending nearly parallel to the trace of the fault. Fracture orientations were obtained on the western limb of an anticline (Fig. 8).

Roche Miette Area

The area investigated belongs to the Disaster Point thrust sheet of the Eastern Ranges. This area has previously been mapped by Mountjoy (1959). Fractures were measured in the massive beds of the Devonian Palliser formation. The lithology consists of dark grey, crypto- to fine crystalline, dolomitic limestones. Bedding thickness varies from 6 inches to 5 feet.

The beds lie in the overturned west limb of an anticline. Although the Disaster Point fault dips to the east in the vicinity of the sampling location, it is asssumed to dip to the southwest at depth.

Morro Peak Area

Road outcrops along the Jasper-Edmonton highway in the Colin thrust sheet show extensive fracturing. Separate sets of measurements were made for the Palliser and the Alexo formation. The Palliser formation is composed of dark grey, crypto- to fine crystalline, slightly argillaceous limestones. Bedding ranges from 1 inch to 4 feet in thickness. The Alexo formation consists predominantly of yellowish grey,

calcareous siltstones in beds from 6 inches to 5 feet thick. The beds of the Colin thrust sheet show a uniform dip to the southwest in this area.

Mount Murchison Area

The Mount Murchison area is situated in the Main Ranges of the Rocky Mountains and forms part of the Castle Mountain thrust sheet. Joints were measured in a road outcrop of the Eldon formation which consists of grey, medium to coarse crystalline dolomites showing conspicuous mottling and pseudo-algal structures. Beds are from 1 foot to 2 1/2 feet thick. The area is located on the east limb of the Bow River anticline.

GEOMETRIC ANALYSIS

Introduction

In order to facilitate the classification and correlation of the mesoscopic structures, three orthogonal fabric axes a, b, and c were defined in each area. Rules adopted in the selection of the fabric axes were as follows (Turner and Weiss, 1963, p. 88):

a) In folded beds the fold axis = b; b is normal to the plane ac; a is horizontal (Fig. 1).

b) In uniformly dipping beds the plane of symmetry = ac; the normal to ac lying in the bedding plane = b; a is horizontal.

The relationship of the fabric axes to uniformly dipping beds is taken to be identical to that of the fabric axes to the limbs of folds (Fig. 1). The choice of fabric axes is completely free of any kinematic or dynamic implications.

Bow River Area

Folding. Six anticlines in the competent sandstone units of the Cardium formation were examined in detail (Fig. 6). The folds are bilaterally symmetric across the axial plane. Kananaskis anticline and Horseshoe anticline approach orthorhombic symmetry, while all other folds display a definite monoclinic symmetry.

Kananaskis anticline (Fig. 9), Horseshoe anticline (Fig. 10), and Flattop anticline (Fig. 13) are open folds with axial planes that are steeply inclined to the southwest. Oldfort anticline (Fig. 11), Cutoff anticline (Fig. 12), and Tight anticline (Fig. 14) have thrust-faulted northeastern limbs which display steep dips. The east limb of Tight anticline is overturned to the southwest. Axial planes of these folds show a definite southwesterly dip.

The bedding poles of each fold were plotted on a stereographic projection

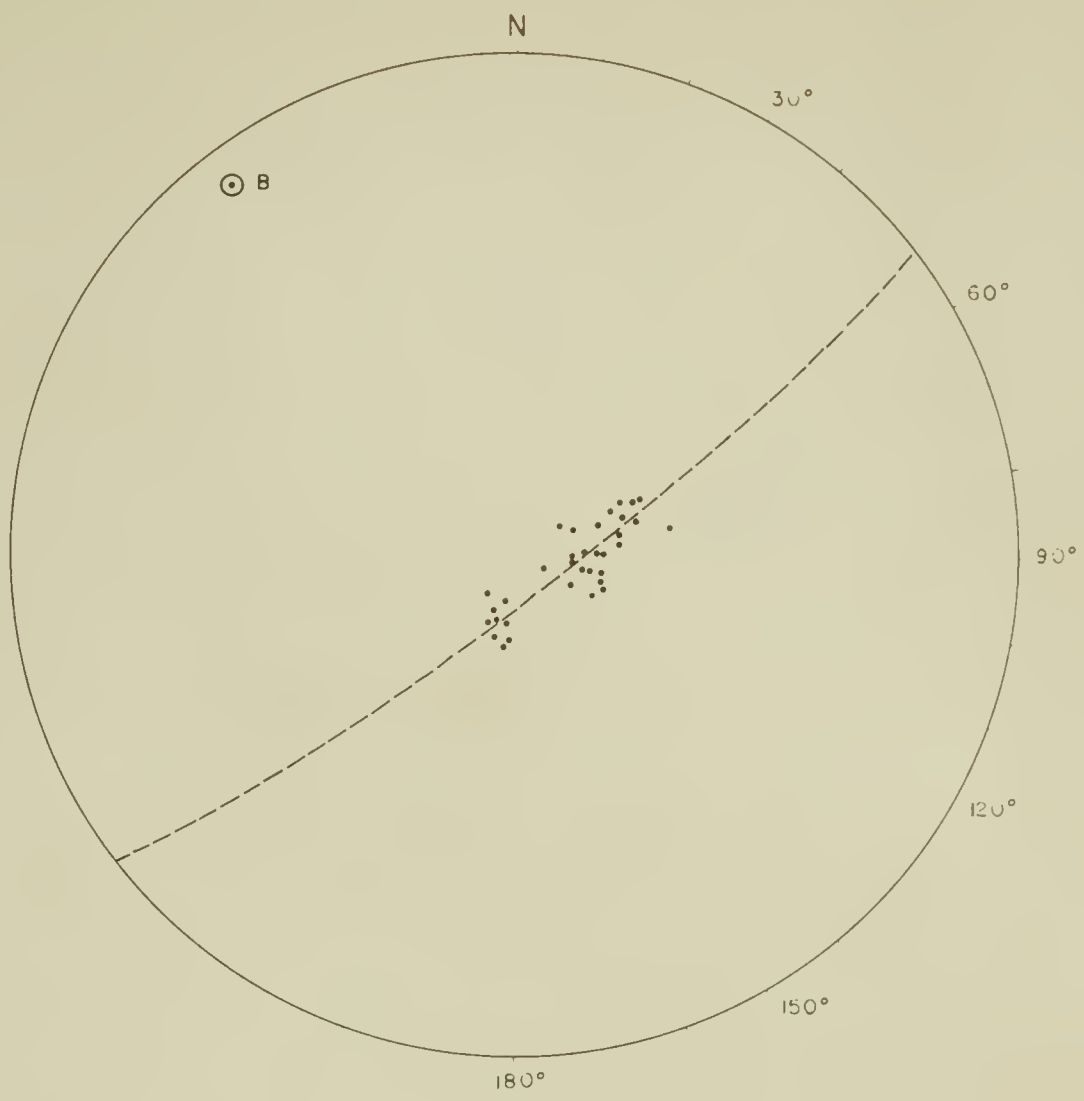

FIG. 9

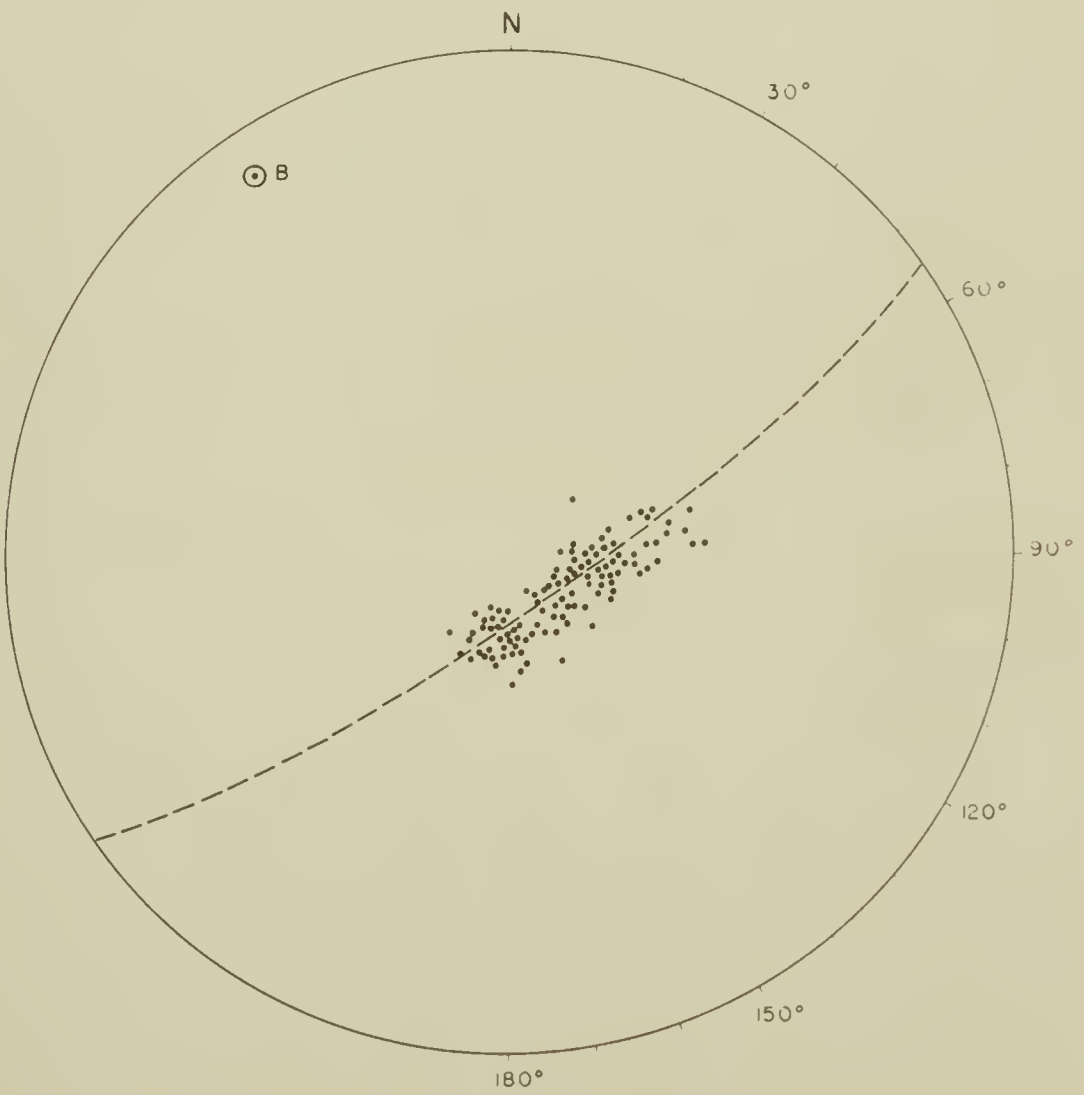

FIG. 10

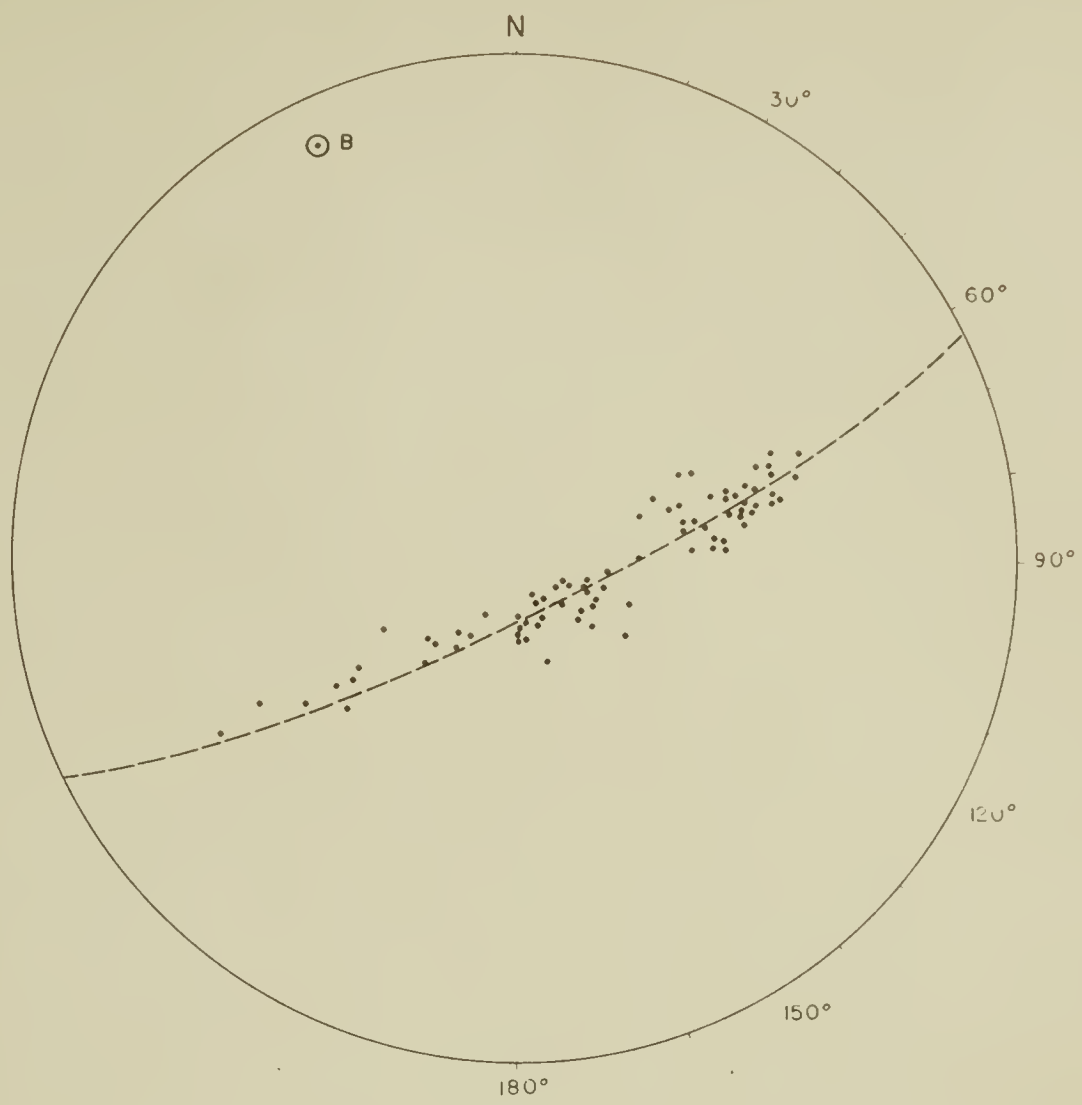

FIG. 11

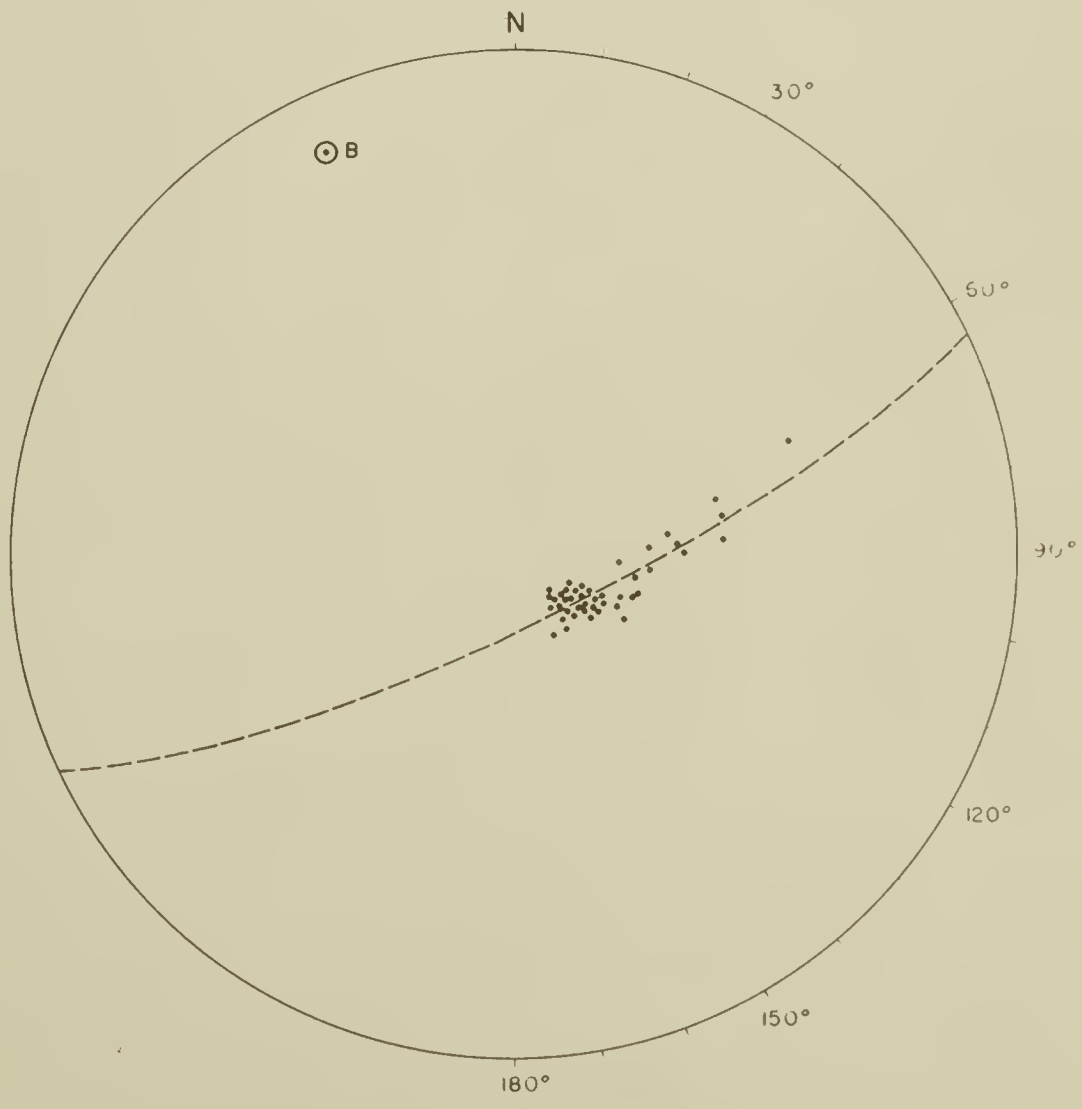

FIG. 12

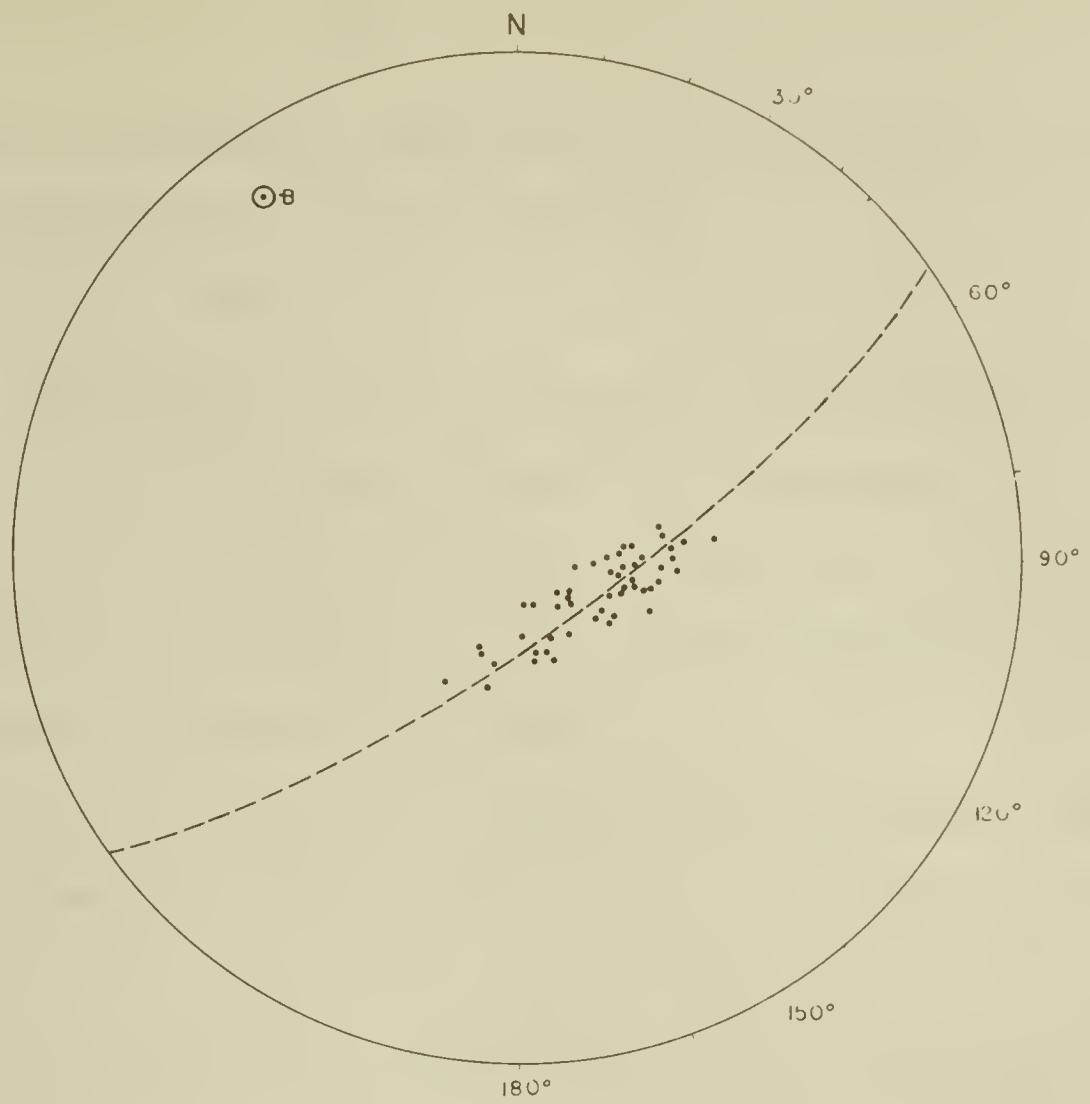

FIG. 13

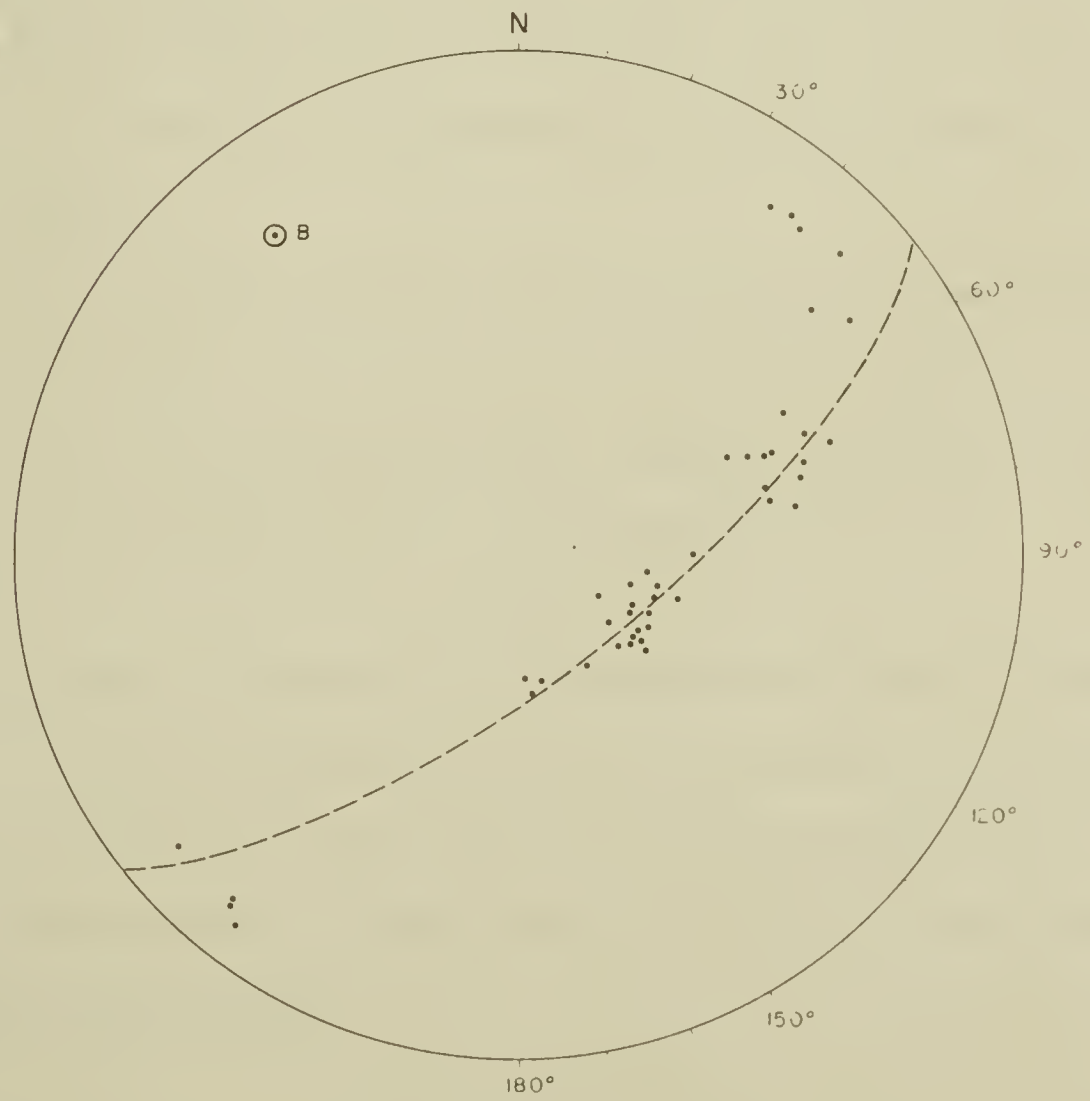

FIG. 14

(Fig. 9-14). For each fold the bedding poles tend to fall along one great circle on the stereonet. Cylindrical folding requires that all bedding poles lie in the plane normal to the fold axis. In the folds analyzed, the poles tend to scatter about the ideal great circle. The scatter may represent the deviation of the folding from truly cylindrical folding. Large scale irregular warping of the bedding surfaces, as observed at several localities, would tend to confirm this assumption. On the other hand, cross-stratification in the sandstone units may hve influenced bedding plane determinations sufficiently to account for the scatter.

All the folds can be considered to be essentially planar cylindrical folds. There appears to be no apparent thickening of the sandstone units in the axial regions, or thinning in the limbs. The folds are of the concentric type.

β -intersections were found to yield spurious results when used for the determination of the fold axis. The results obtained varied widely and showed a strong dependence on the positions of the measurements on the folded surface, and on the number of bedding attitudes measured on each limb. When several thousand intersections were used, results usually corresponded closely with value for the β -axis obtained from point diagrams.

The attitudes of the fold axes (B) were determined from the stereographic plots of the bedding planes (Fig. 9-14). The trends of anticlinal fold axes range from N 26° W to N 40° W. All folds plunge to the northwest at angles from 7 to 20 degrees. The plunges of the folds increase progressively from west to east.

Bedding -plane slickensides. Slickensides along bedding planes throughout the area trend from N 42° E to N 80° E. The average trend of the slickensides is perpendicular to the mean fold axis of the area. At some localities more than one generation of slickensides can be differentiated on the same bedding plane; their directions usually do not differ by more than 15 degrees.

Bedding plane slickensides represent a stress release along bedding planes during folding. The presence of several generations of movement implies discontinuous strain during folding.

Joints have not been displaced by the bedding-plane slip.

Joints. The maximum number of joint sets is observed in the most westerly domain of the area investigated. Four sets of joints can be differentiated in the west limb of Kananaskis anticline (Fig. 15). Because the joints in this domain are well exposed and typical of the joints found throughout the area, they will be discussed in detail.

a) Two conjugate hkl joint sets (N 32 E/81 SE and N 77 W/82 NE) have a dihedral angle of 72 degrees and an acute bisectrix trending N 68° E. The N 32 E/81 SE set shows abundant evidence of shear-type movement and the fractures are smooth and planar. The N 77 W/82 NE set shows only rare indications of shear-type movement and is the most common.

b) An h0l joint set (N 30 W/82 NE) consists of irregular fractures which are nevertheless large and prominent. Evidence of normal-type movement is abundant. In rare cases fractures belonging to this set show plumose markings on the fracture surface.

c) A 0kl joint set (N 66E/88 SE) contains some planar fractures up to 50 feet long. Evidence of movement along the joints is rare and can be both of the shear-type and the normal-type. Plumose markings on the joint surface can be observed. The joint set parallels the bisectrix of the conjugate hkl sets.

Only three of the fracture sets observed on the west limb of the anticline are present on the eastern limb (Fig. 16). The 0kl set is found to be absent. The dihedral angle between the conjugate hkl joint sets has decreased to 60 degrees.

Two domains on the western limb of Horseshoe anticline illustrate the influence of lithology, bedding thickness, and outcrop conditions on the fracture


N
30°
60°
90°
120°
150°
180°
10
5
2
5
2
2
5
⊙ = BEDDING POLE
GIRDLE AXIS

FIG. 15

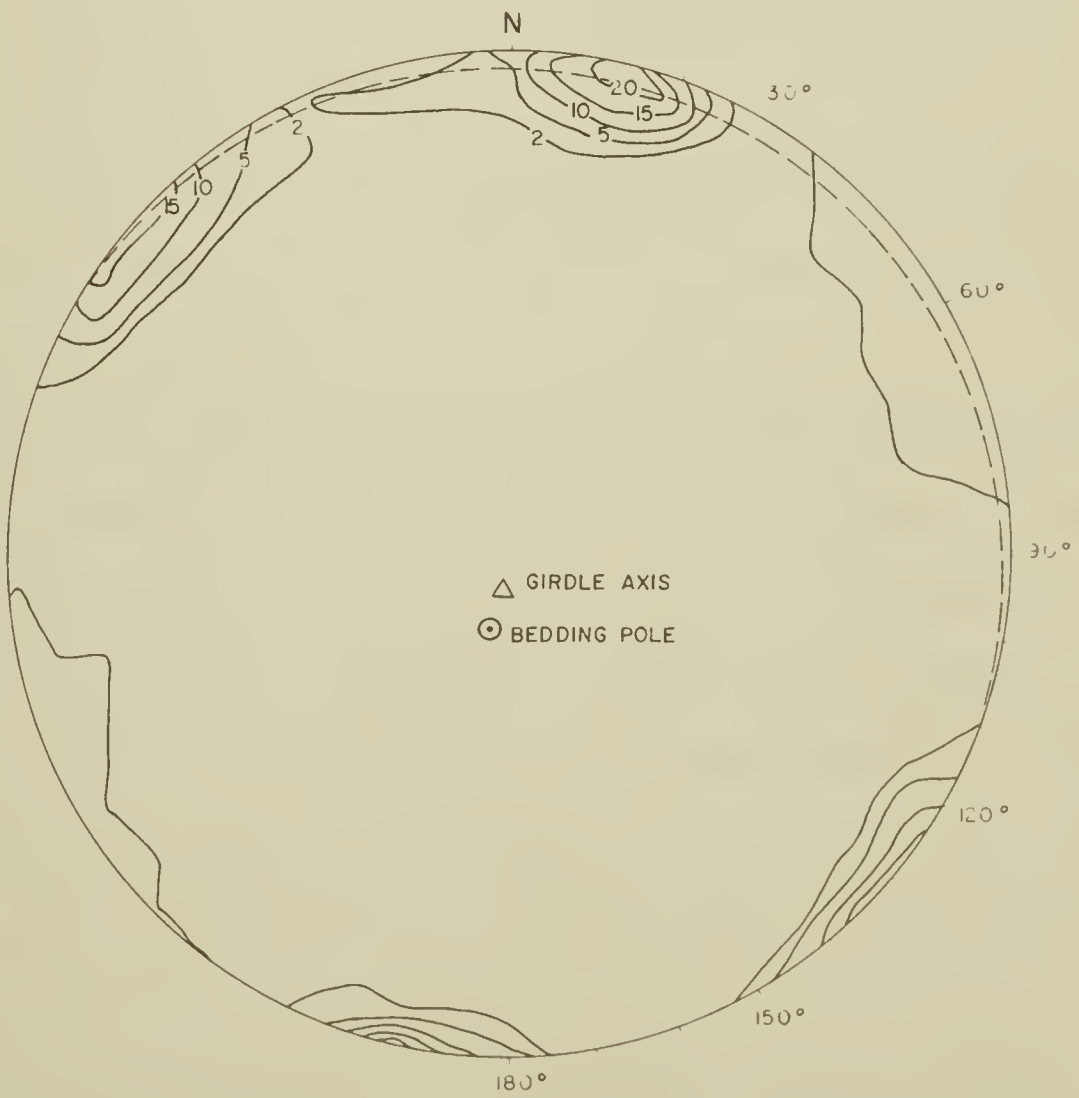
N
30°
60°
90°
120°
150°
180°
20
15
10
5
2
2
5
10
15
△ GIRDLE AXIS
⊙ BEDDING POLE

FIG. 16

development. The domains are located in structurally equivalent positions. One domain includes fractures measured in the upper and middle sandstone units (Fig. 17) of the Cardium formation, while the other represents fractures in the lower sandstone unit (Fig. 18). The mean orientation of a very strong maximum, due to one of the hkl sets (N 83 W/87 NE), is essentially identical in both domains. Marked differences are apparent in the weaker maxima. The complementary hkl set is nearly absent in the lower sandstone unit. The strike of bedding can be seen to change by 90 degrees across the crest of Horseshoe anticline (Fig. 19). The orientations of the joint sets change only slightly across the same interval. The strike of the bedding has no influence on the orientation of the joints (Fig. 17-21).

The reproducibility of results was tested on the eastern limb of Horseshoe anticline. Joints were measured in equivalent structural positions and stratigraphic units on both banks of the Bow River (Fig. 20 and 21). Circles of confidence about the mean orientations of the two domains intersect for each joint set. The two orientation diagrams are therefore equivalent.

Three joint sets are present in all domains on Horseshoe anticline. The dihedral angle between conjugate hkl sets decreases from 48 degrees in the west limb to 33 degrees in the east limb.

In the west limb of Oldfort anticline the upper and middle sandstone units show different fracture patterns. Two conjugate hkl joint sets in the upper sandstone unit (Fig. 23) are being represented by a single 0kl joint set in the middle sandstone unit (Fig. 24). The conjugate sets intersect with a dihedral angle of 33 degrees.

Only two maxima can be differentiated in the western limb of Cutoff anitcline (Fig. 25 and 26) and the east and west limbs of Flattop anticline (Fig. 27 and 28). The maximum, occupying the position of the two conjugate hkl sets found west of these domains, shows an unusually large dispersion in strike. The maximum is interpreted to represent two merging maxima. Two conjugate hkl sets intersecting at

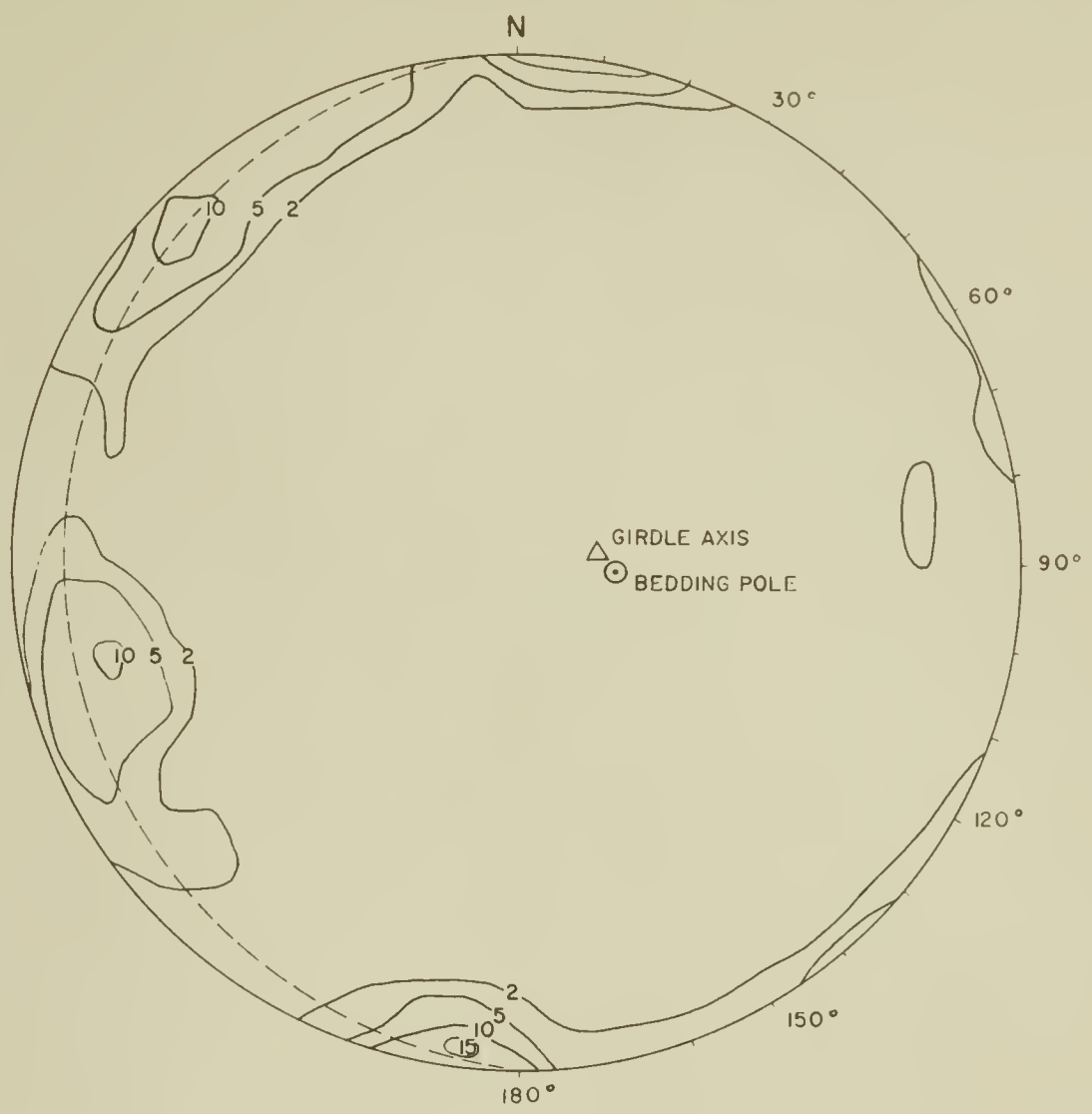
N
30°
60°
90°
120°
150°
180°
10 5 2
10 5 2
GIRDLE AXIS
BEDDING POLE
2
5
10
15

FIG. 17

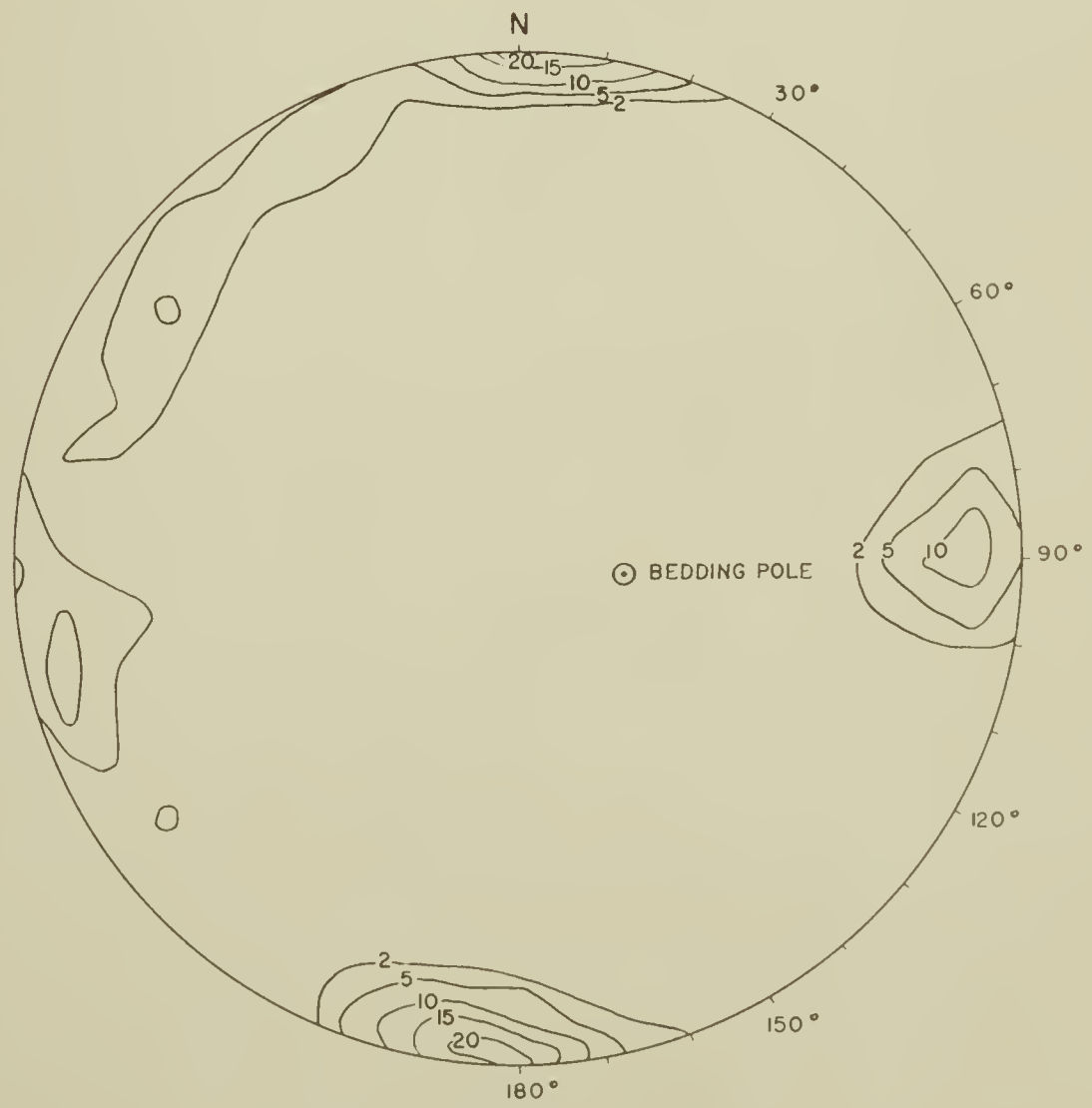
N
20 15 10 5 2
30°
60°
90°
120°
150°
180°
BEDDING POLE
2 5 10
2
5
10
15
20

FIG. 18

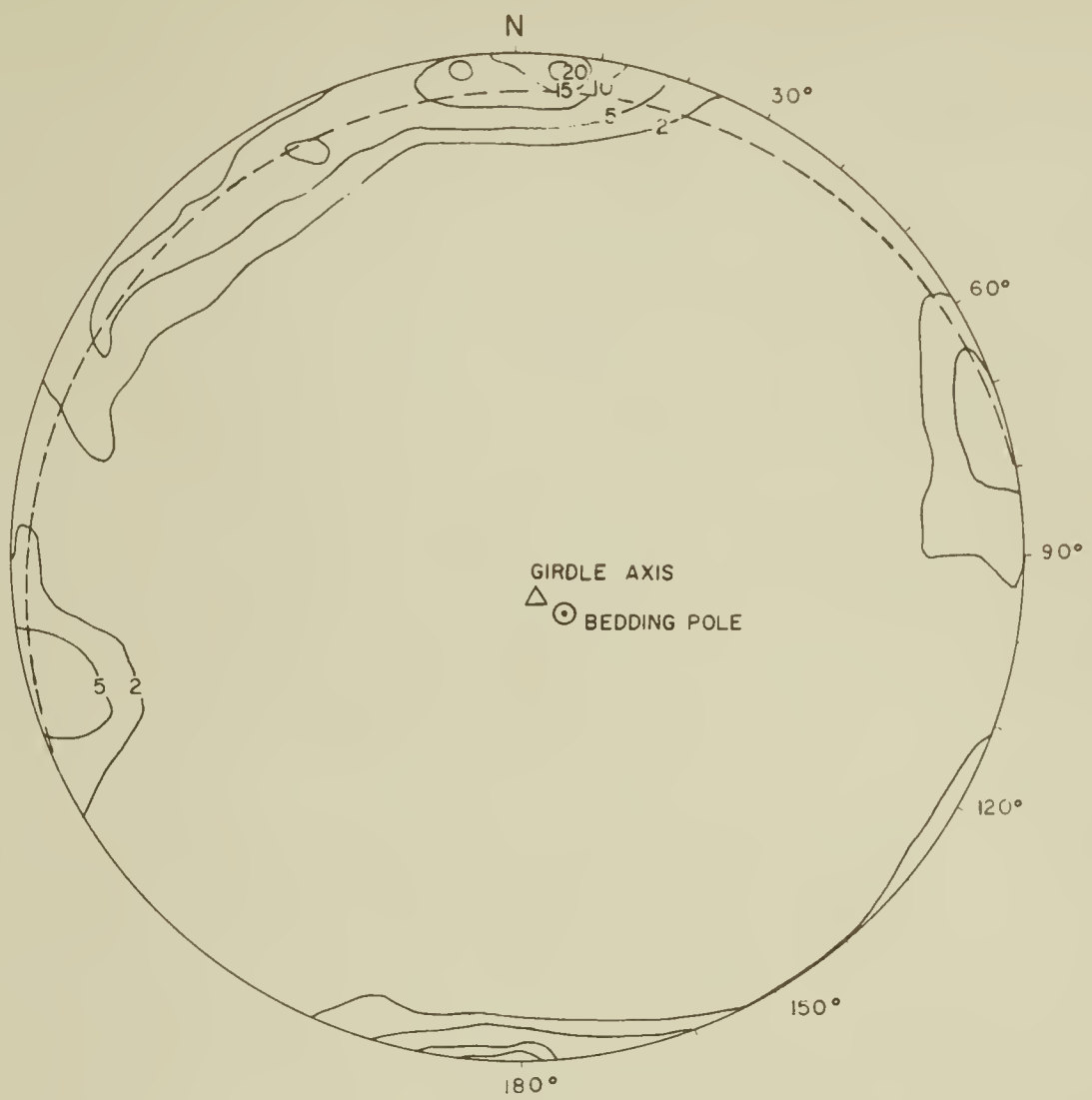
N
30°
60°
90°
120°
150°
180°
20
15
10
5
2
5
2
GIRDLE AXIS
BEDDING POLE

FIG. 19

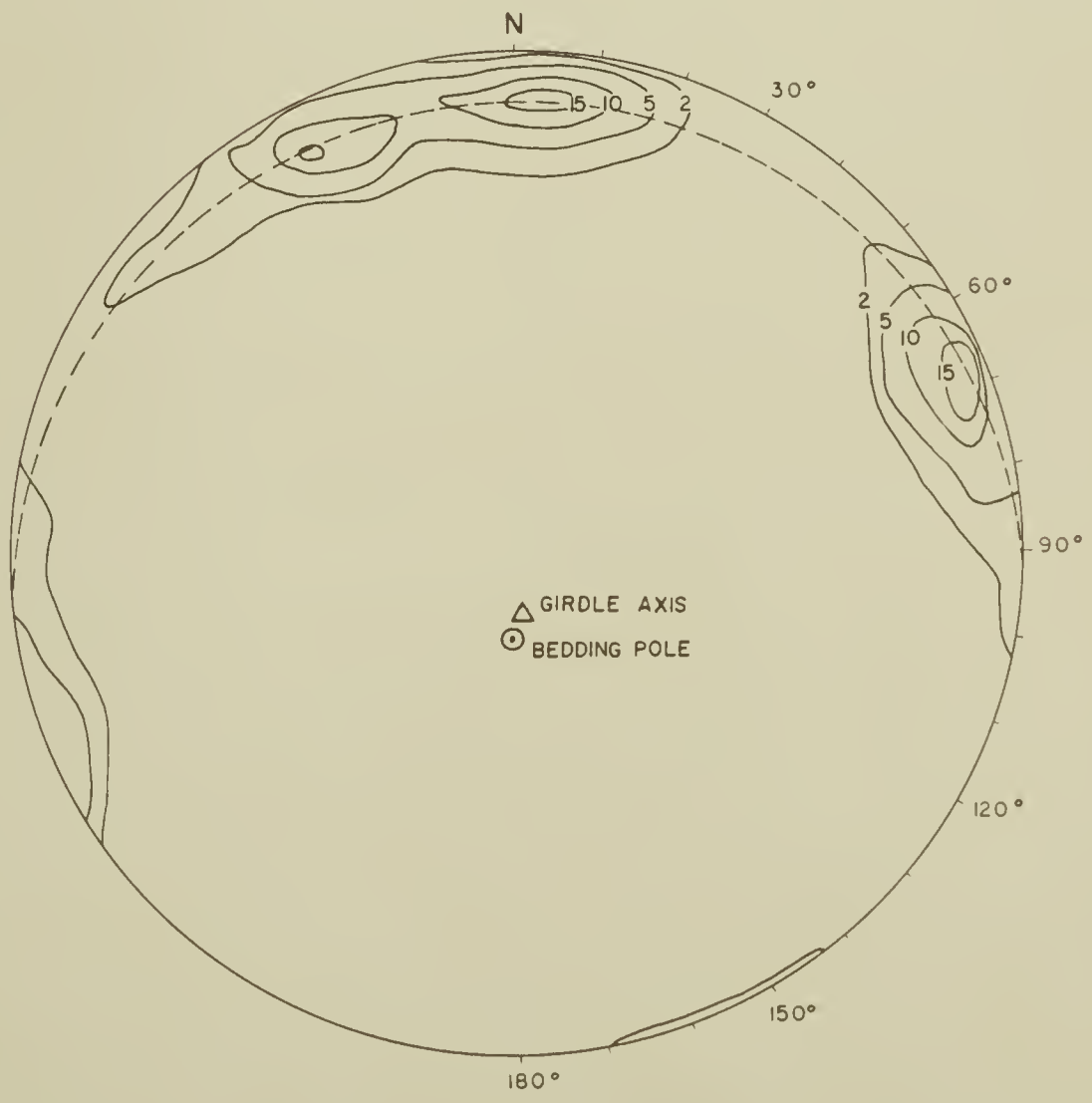
N
30°
60°
90°
120°
150°
180°
15
10
5
2
2
5
10
15
GIRDLE AXIS
BEDDING POLE

FIG. 20

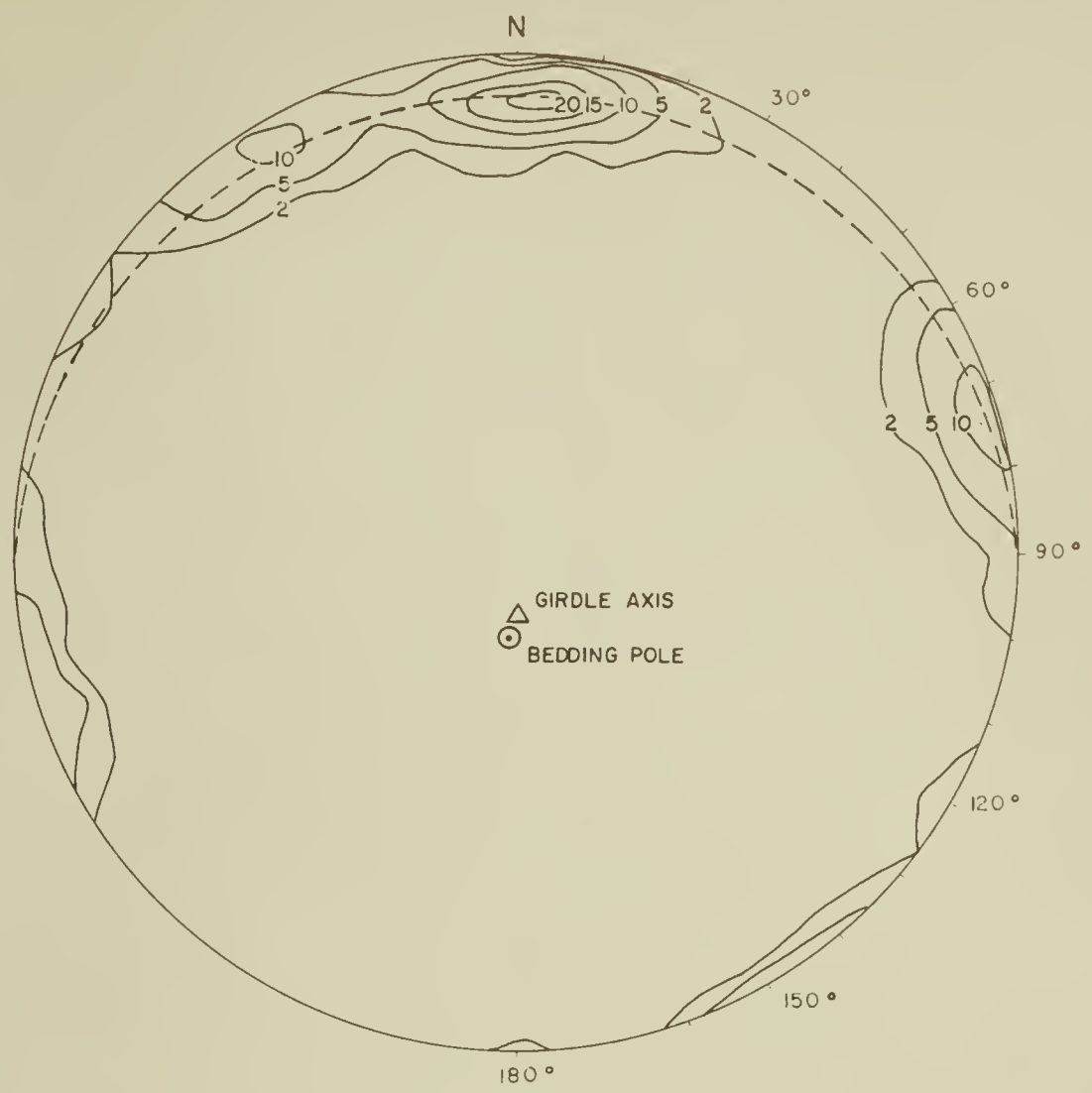
N
30°
60°
90°
120°
150°
180°
20
15
10
5
2
10
5
2
2
5
10
GIRDLE AXIS
BEDDING POLE

FIG. 21


N
30°
60°
90°
120°
150°
180°
15
10
5
2
2
5
10
GIRDLE AXIS
BEDDING POLE

FIG. 22


N
30°
60°
90°
120°
150°
180°
15
10
5
2
GIRDLE AXIS
BEDDING POLE
2
5
10
15

FIG. 25

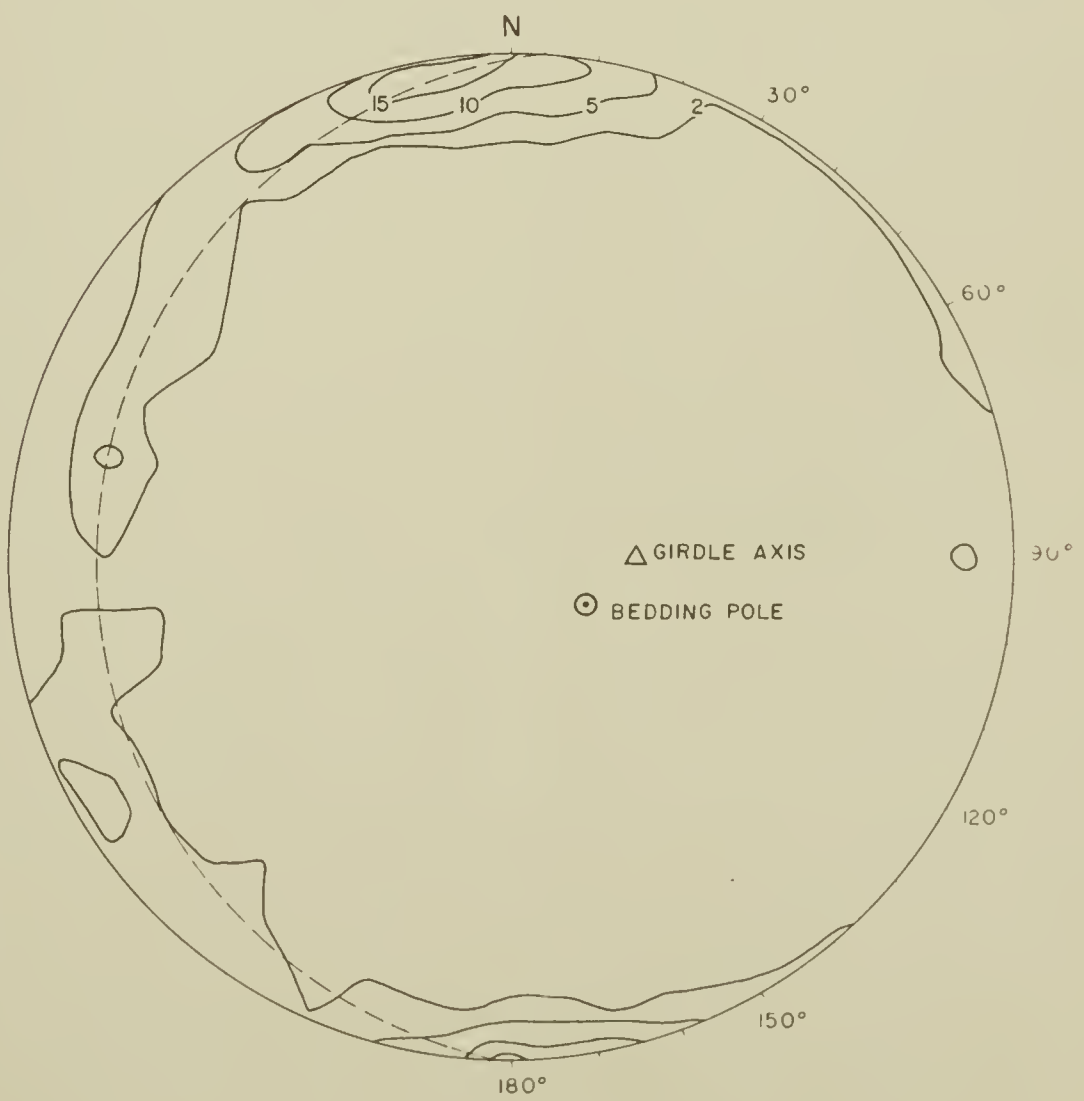
N
30°
60°
90°
120°
150°
180°
15
10
5
2
GIRDLE AXIS
BEDDING POLE

FIG. 26

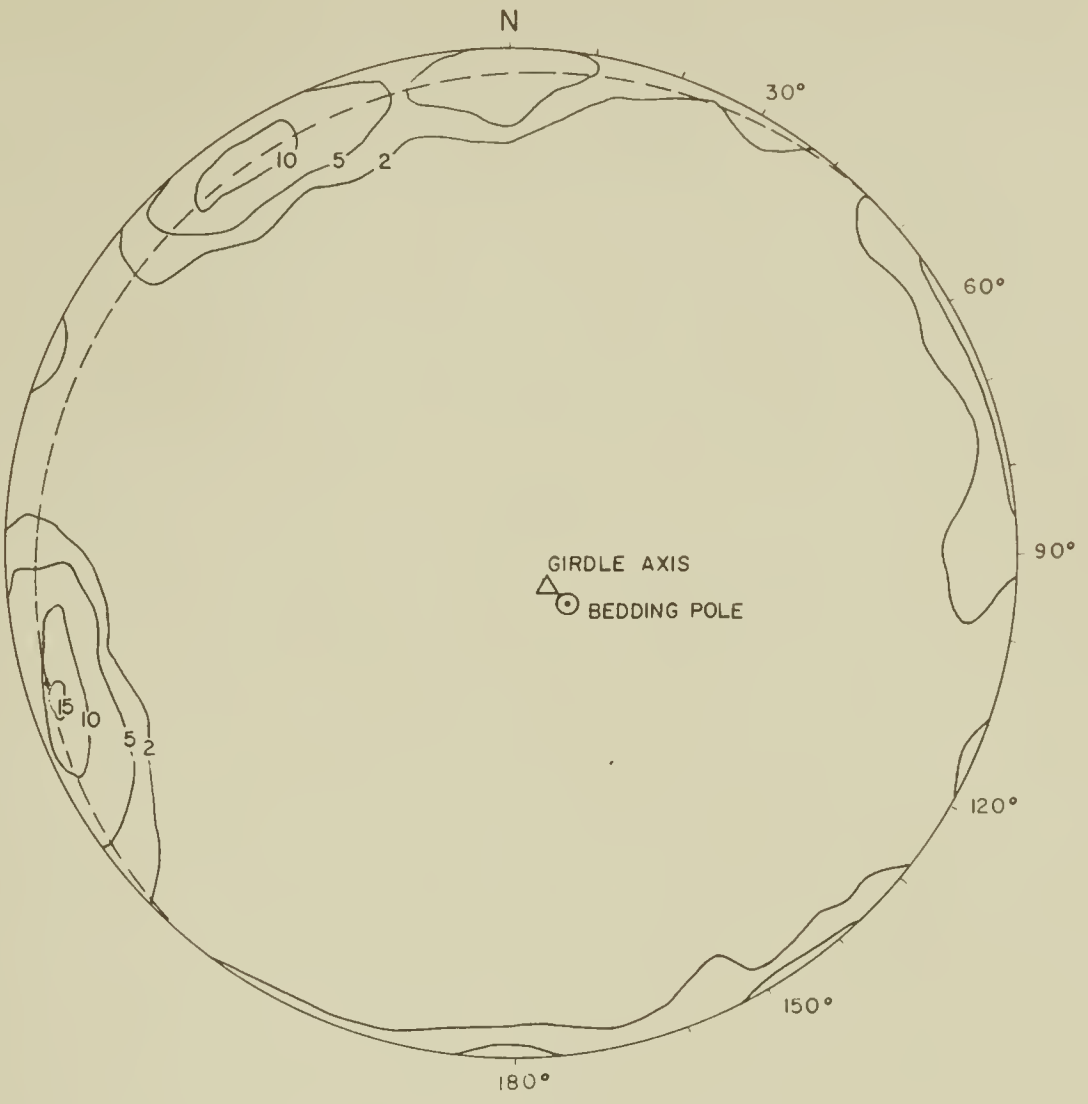
N
30°
60°
90°
120°
150°
180°
10
5
2
GIRDLE AXIS
BEDDING POLE
15
10
5
2

FIG. 23

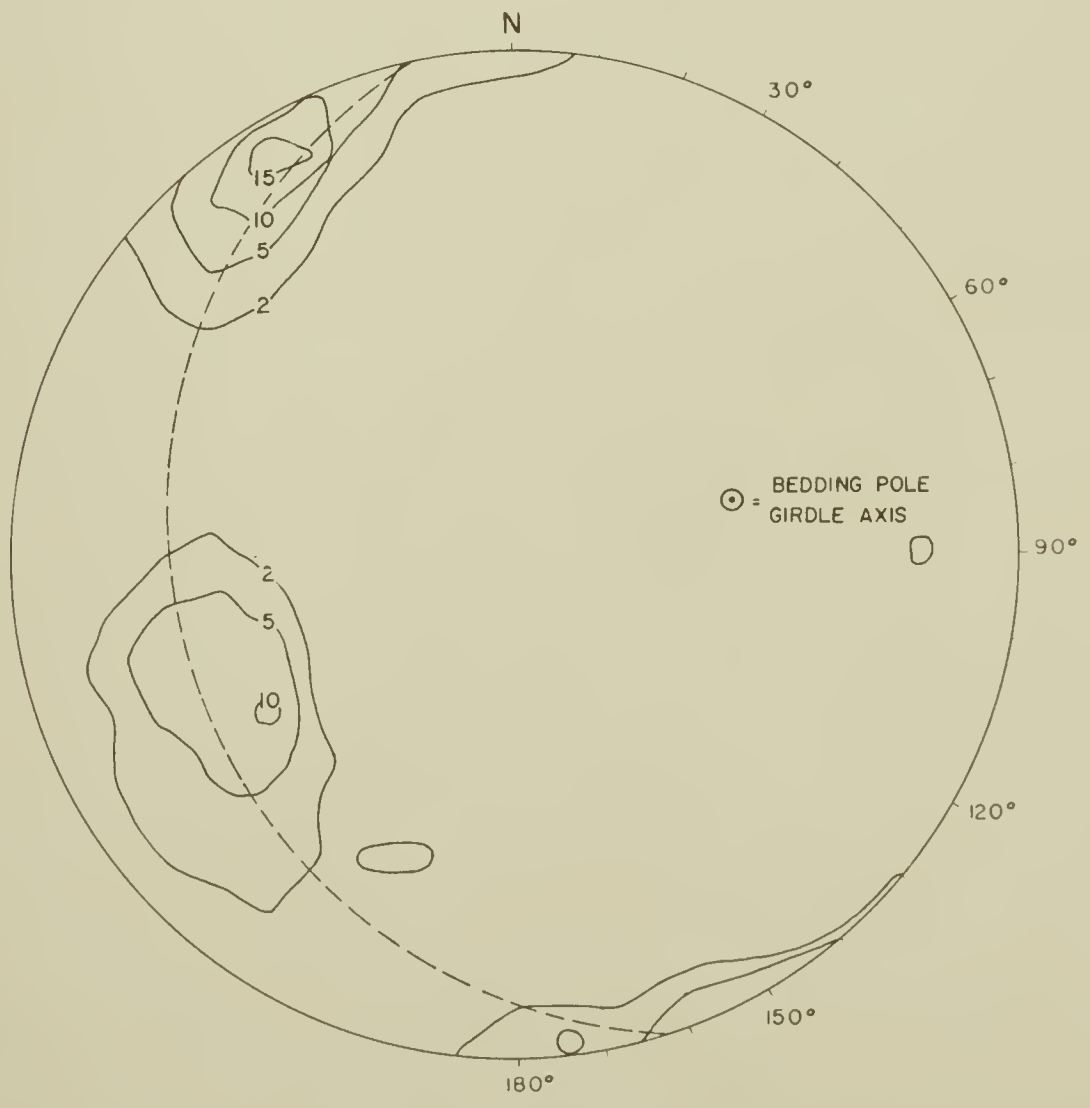
N
30°
60°
90°
120°
150°
180°
15
10
5
2
⊙ = BEDDING POLE
GIRDLE AXIS
2
5
10

FIG. 24

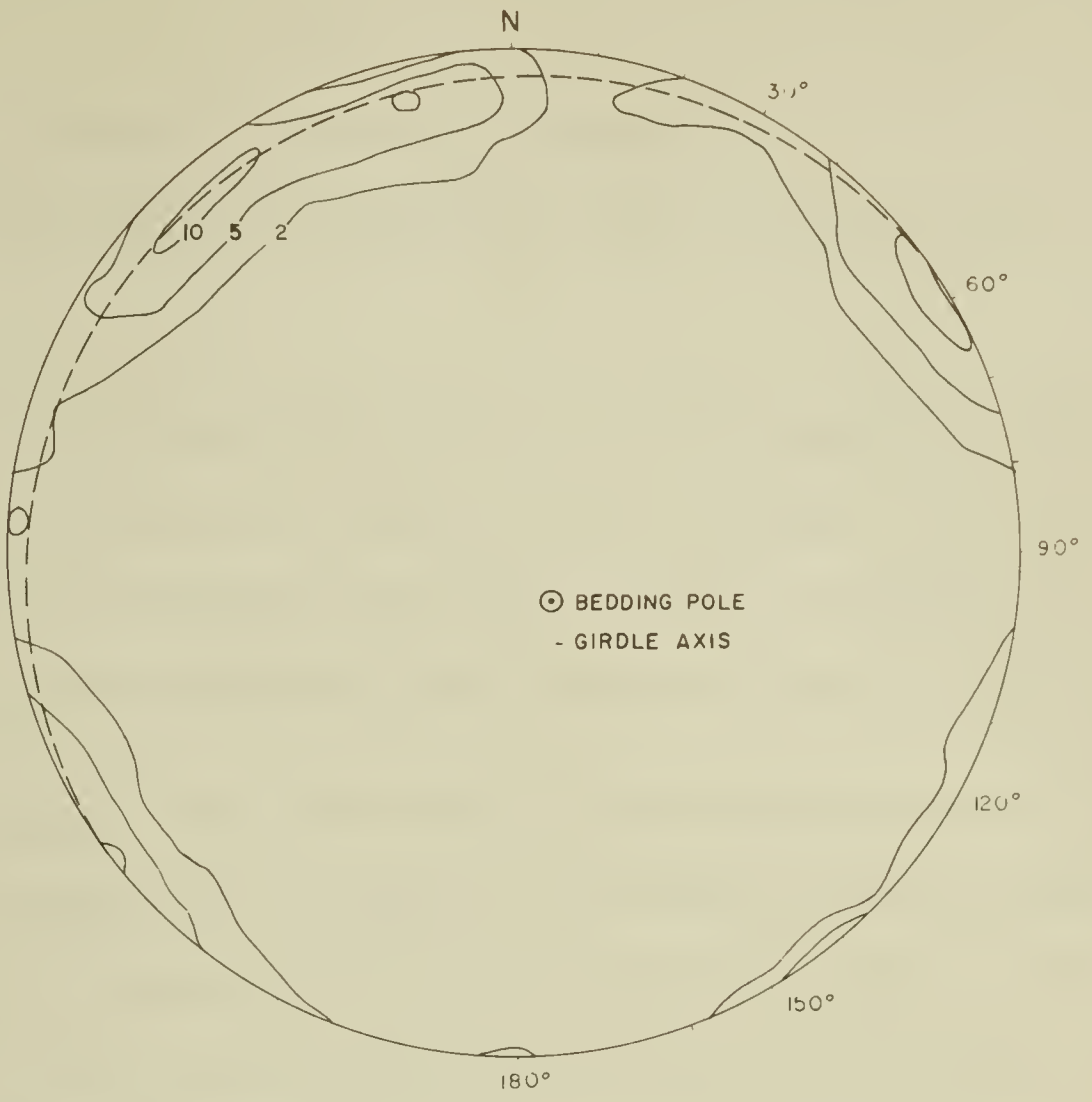
N
30°
60°
90°
120°
150°
180°
10
5
2
⊙ BEDDING POLE
- GIRDLE AXIS

FIG.27

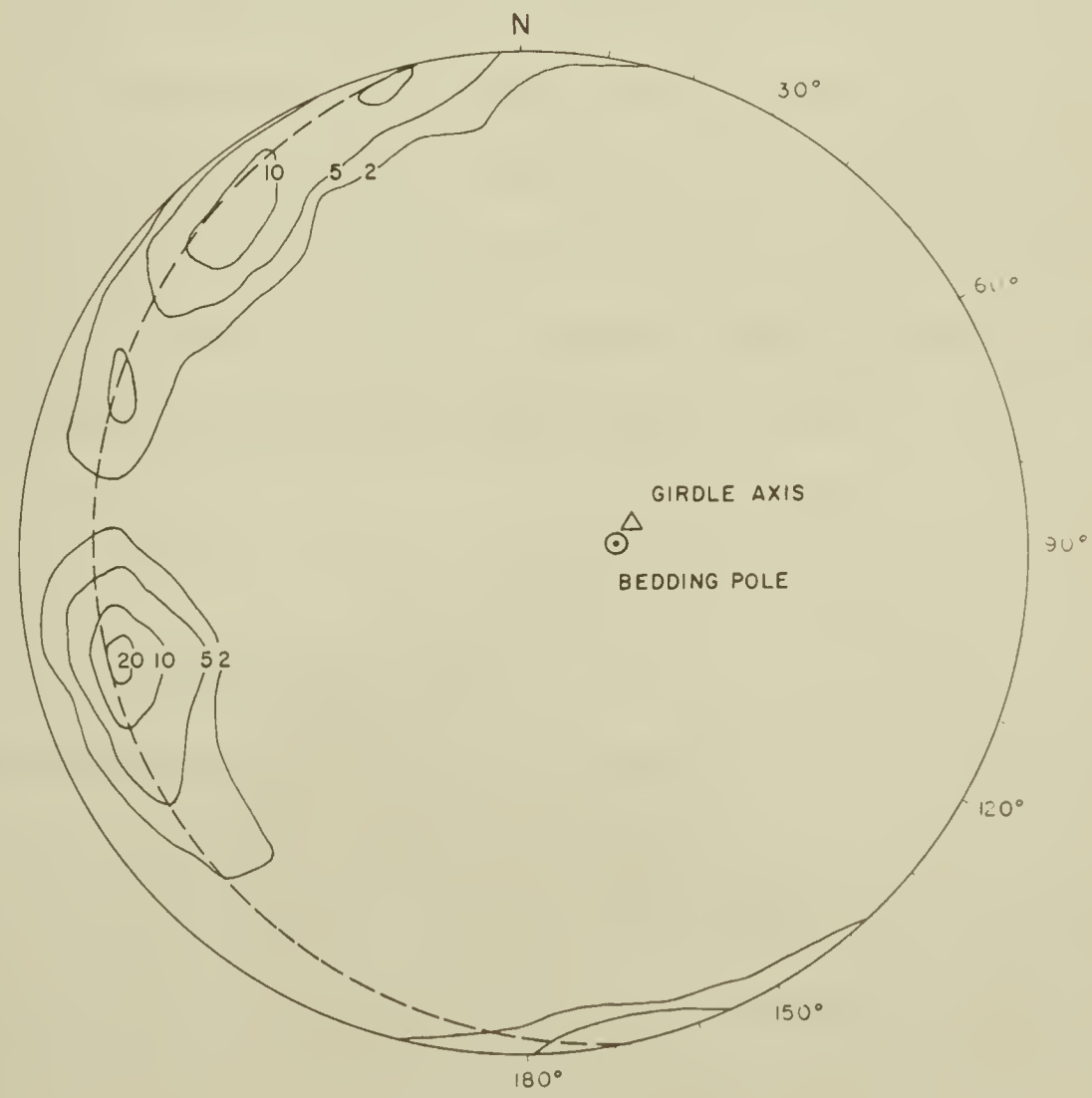
N
30°
60°
90°
120°
150°
180°
10
5
2
GIRDLE AXIS
BEDDING POLE
20
10
5
2

FIG.28

low dihedral angles are thought to be present in these localities.

Joints on the west limb of Tight anticline fall into an h0l and a 0kl set (Fig. 29 and 30).

Joint intersections. Intersections of the two hkl joint sets, and intersections of the orthogonal h0l and 0kl joint sets were calculated for selected domains. The intersections were found to form maxima about the normal to bedding. Intersections of conjugate hkl joint sets show less dispersion than intersections of the 0kl and h0l sets.

Variation in dihedral angle. A plot of the dihedral angle between conjugate hkl sets versus the distance perpendicular to the reguional strike reveals a linear relationship (Fig. 31). For dihedral angles smaller than 35 degrees the maxima of the two hkl sets merge, and the determination of the mean fracture planes and the dihedral angle between them becomes impossible.

Slickensides on joint planes. Nearly 15 per cent of the observed joint planes show signs of movement. All conjugate hkl joints and 0kl joints show shear-type slickensides. These slickensides tend to parallel the intersection between the joints and the bedding plane. No conclusions could be reached about the directions of movement, because the sense of movement deduced from the roughness of the slickensides was often contradictory for two parallel, adjacent joints. h0l joints invariably show normal-type slickensides.

Red Deer River Area

Two orthogonal joint sets predominate in the Red Deer anticline. The mean fracture planes of an h0l joint set strike between N 45° W and N 64° W. Dips of the joints are highly dependent on bedding plane dips (Fig. 32-37). Mean fracture planes of a 0kl set strike between N 22° E and N 36° E. A third joint set, which

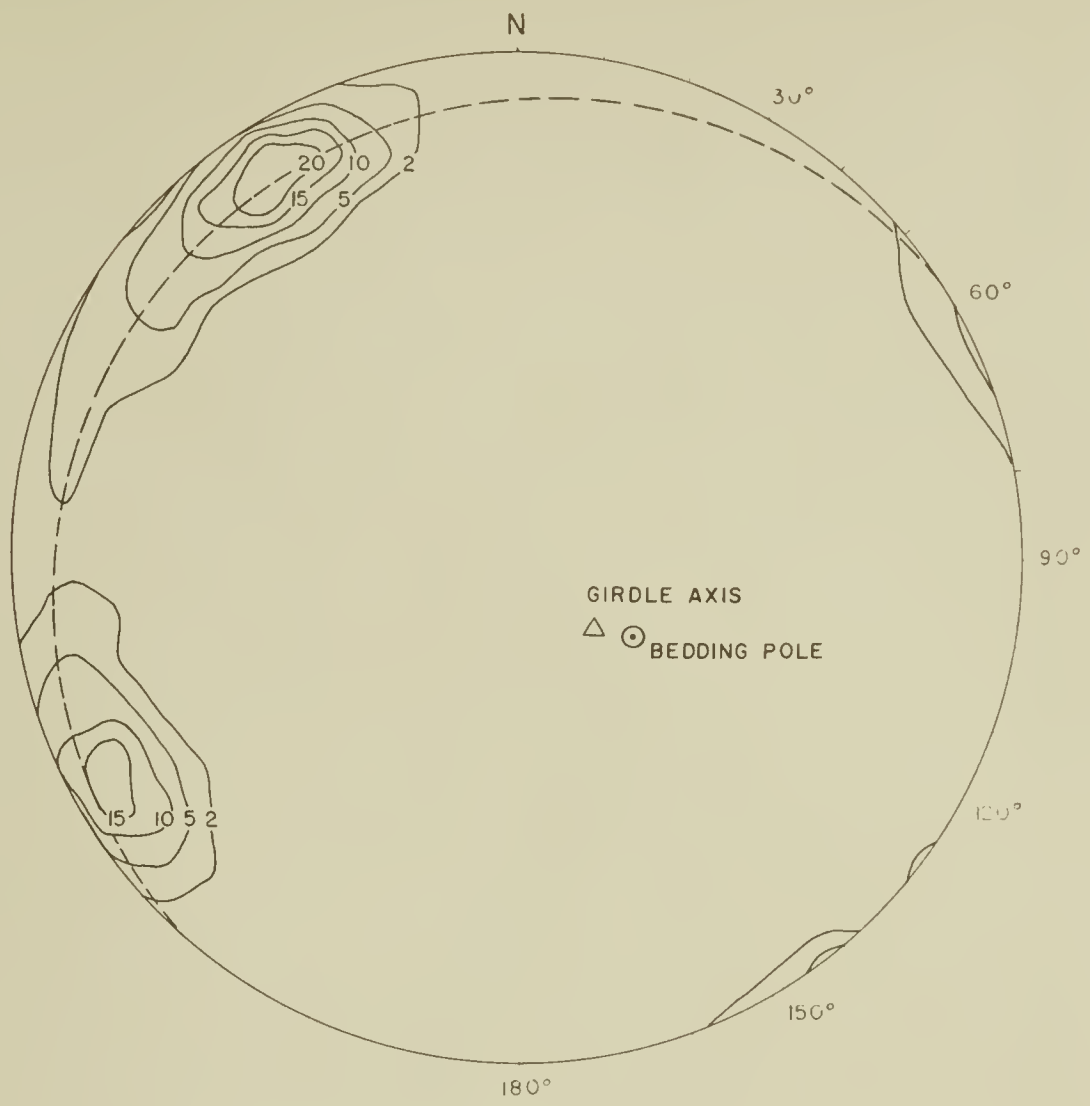
N
30°
60°
90°
120°
150°
180°
20
15
10
5
2
15
10
5
2
GIRDLE AXIS
BEDDING POLE

FIG. 29

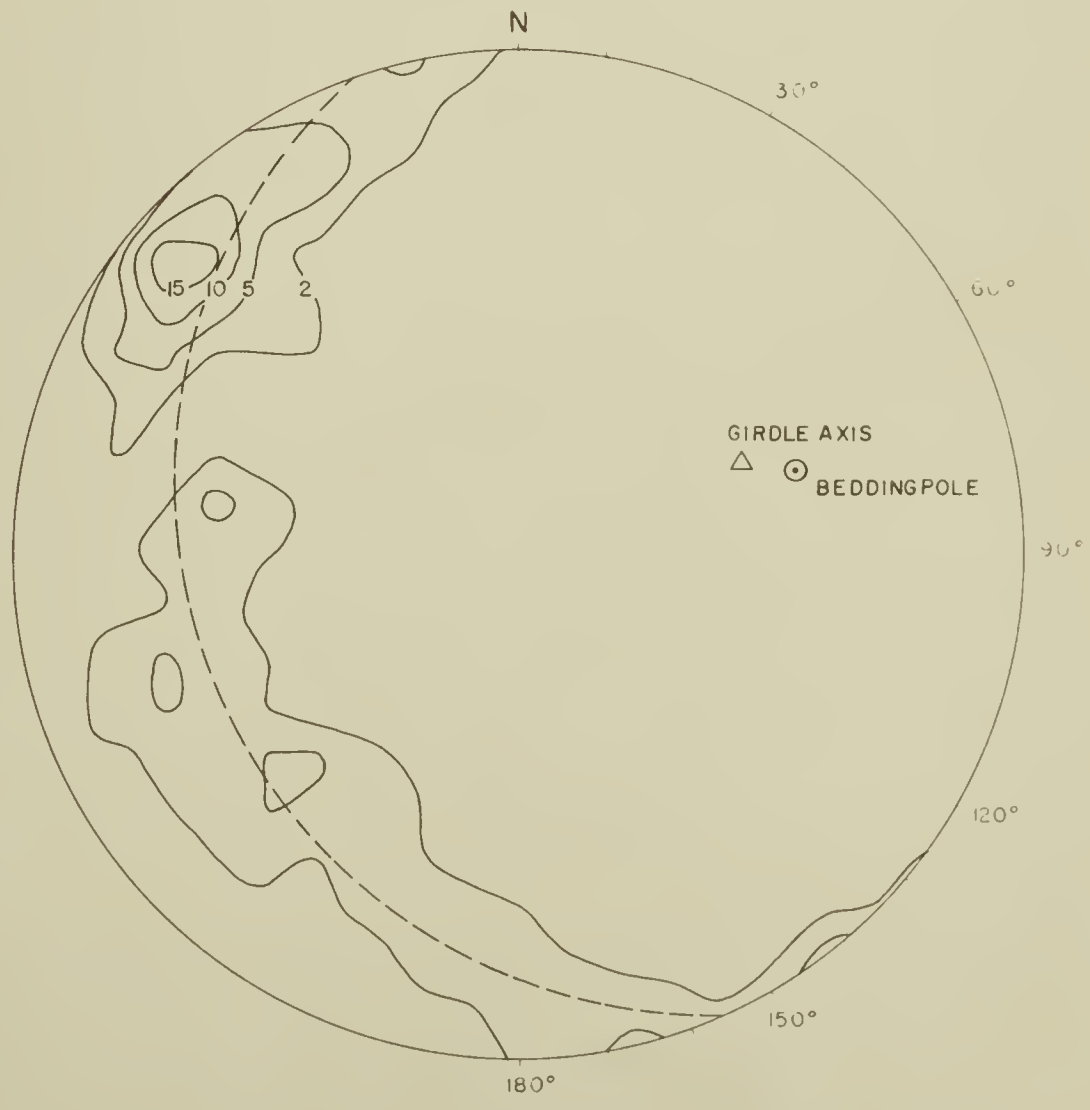
N
30°
60°
90°
120°
150°
180°
15
10
5
2
GIRDLE AXIS
BEDDINGPOLE

FIG. 30

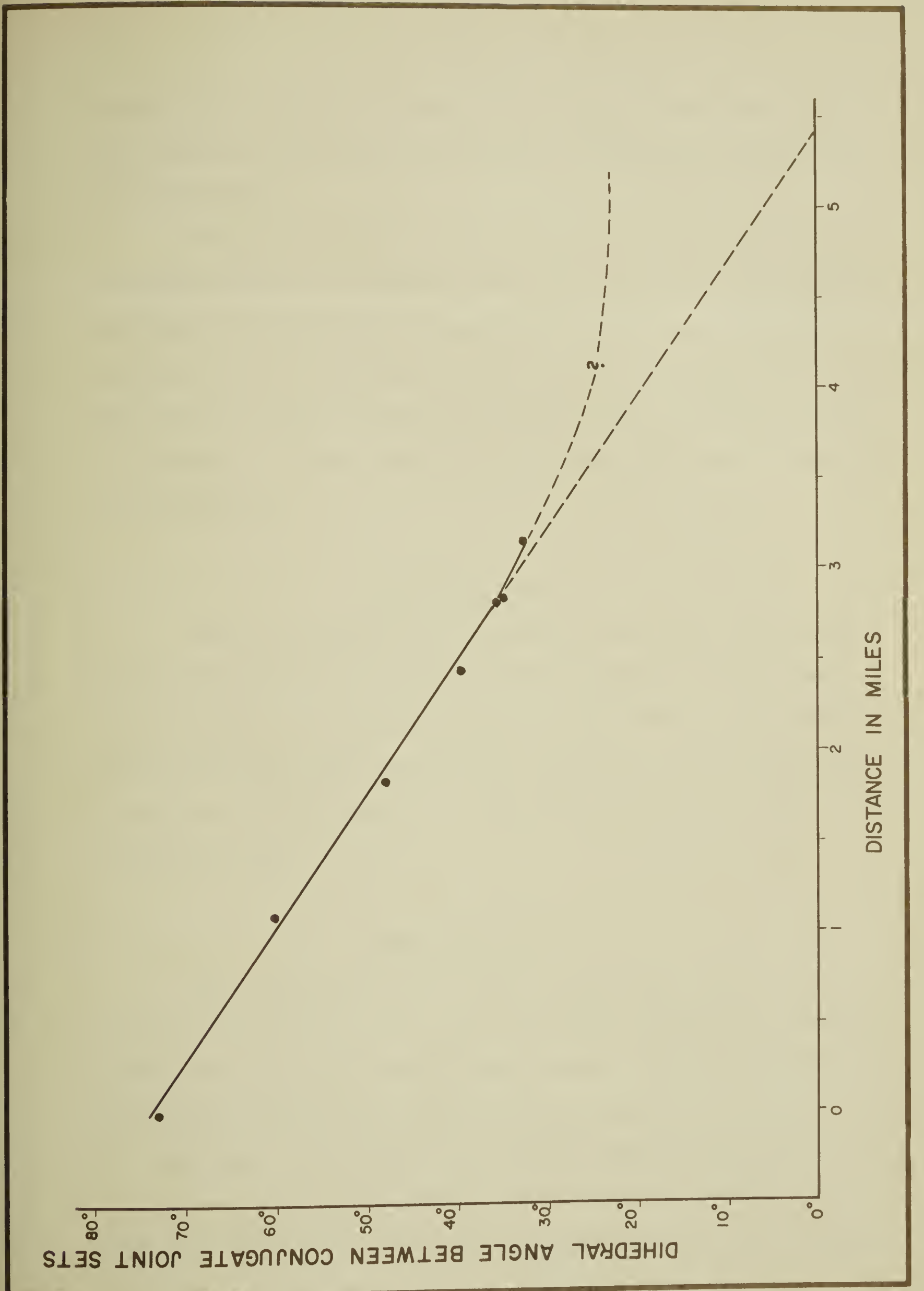
DIHEDRAL ANGLE BETWEEN CONJUGATE JOINT SETS
80°
70°
60°
50°
40°
30°
20°
10°
0°
?
0
1
2
3
4
5
DISTANCE IN MILES

FIGURE 31

is only weakly developed, can be seen in both the upper and lower sandstone units where beds dip over 30 degrees (Fig. 32 and 35). The mean fracture plane of this set trends N 50° E.

0kl maxima are found to be much stronger than h0l maxima in all domains on Red Deer anticline. The predominance of the 0kl joints can be at least partially attributed to outcrop conditions. Exposures in the area fall along a line roughly perpendicular to the fold axis, and 0kl joints are much better exposed than h0l joints. 0kl joints show abundant evidence of shear-type movement. The sense of movement is indeterminate. h0l joints rarely display slickensiding, but movement along them is of the normal type.

Cripple Creek Area

Joints in the Cripple Creek area are found to be irregular and frequently curved. The poles of the joints define a well developed girdle with three weak maxima (Fig. 38). Two conjugate hkl joint sets (N 85 E/80 NE and N 35 E/75 SW) exhibit predominantly shear-type movement. An h0l joint set (n 44 W/48 NE) shows normal movement which appears to have taken place preferentially in a plane striking N 20° W (Fig. 39).

South Creek Area

Joints were measured at two locations in equivalent structural positions on the ast limb of a large syncline. Three sets of joints are present in the western domain, while only two joint sets are found to the east. A 0kl joint set (N 40° E/88 SE) and an h0l joint set (N 33° W/72 NE) are common to both localities (Fig. 40). Shear-type slickensides on the 0kl joints indicates sinistral relative movement and normal-type movement has occurred on the h0l joints (Fig. 41). An hkl joint set (N 77° W/72 NE) observed in the western domain appears to bear

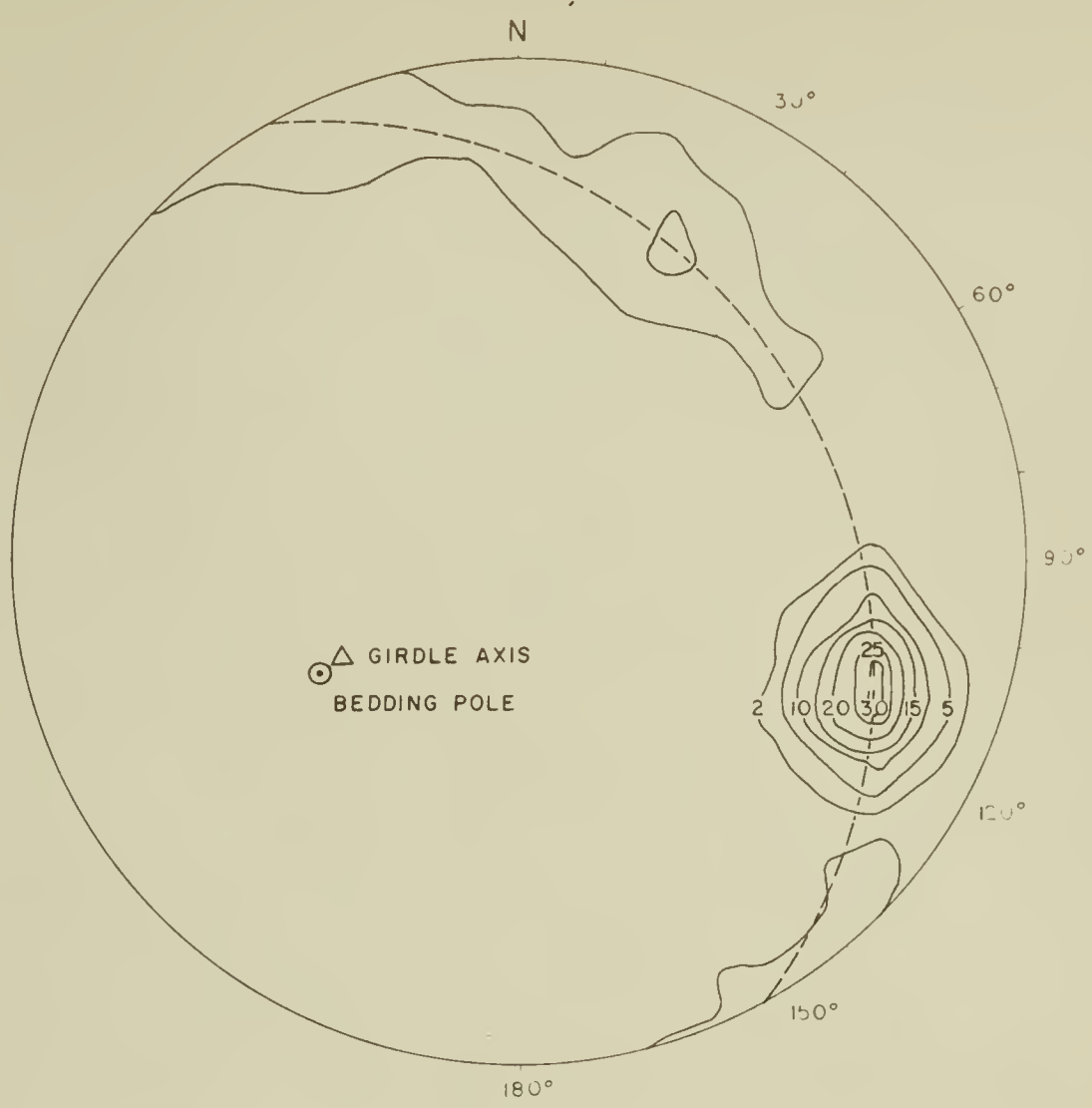
N
30°
60°
90°
120°
150°
180°
GIRDLE AXIS
BEDDING POLE
25
2 10 20 30 15 5

FIG.32

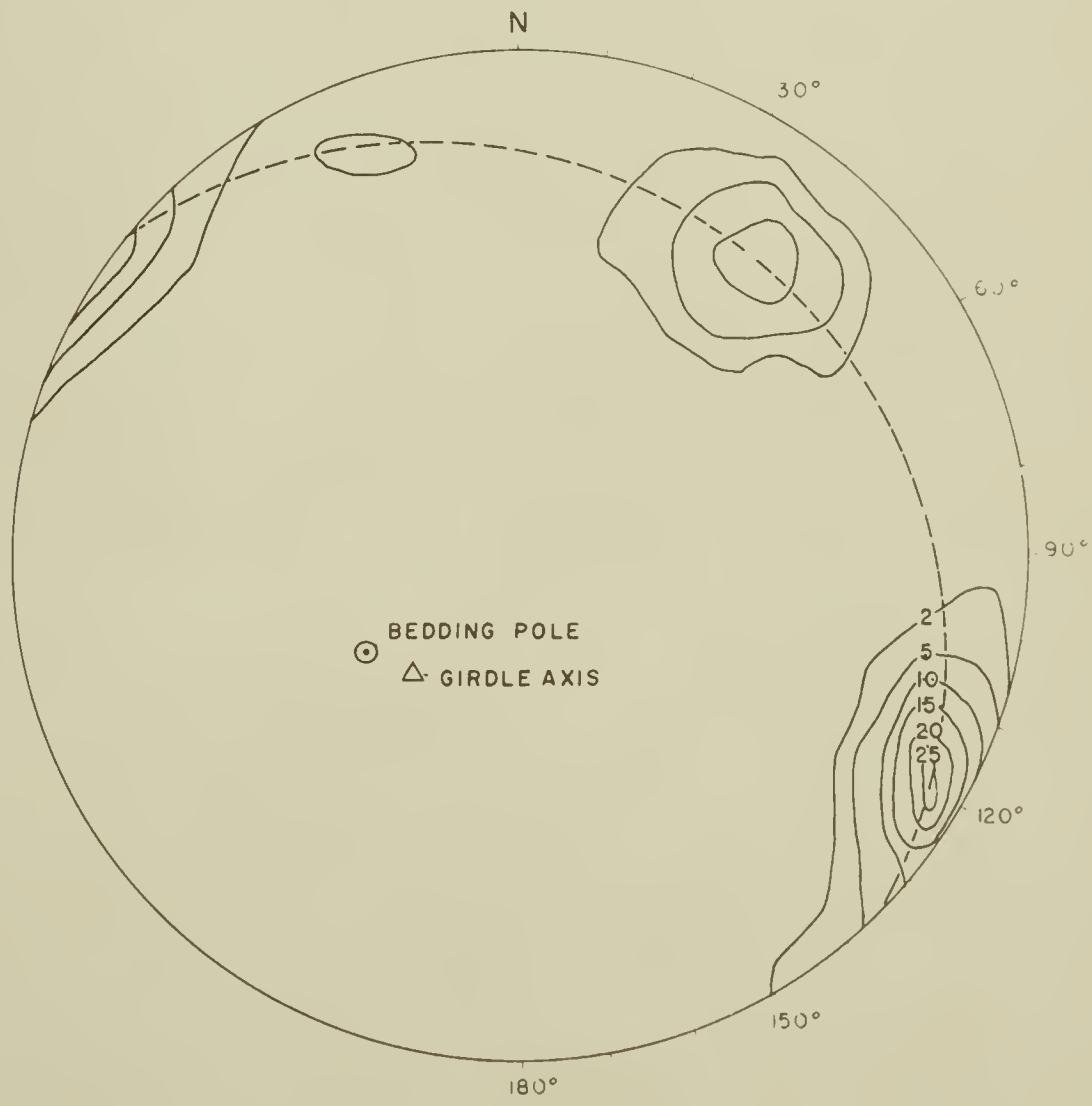
N
30°
60°
90°
120°
150°
180°
BEDDING POLE
GIRDLE AXIS
2
5
10
15
20
25

FIG.33

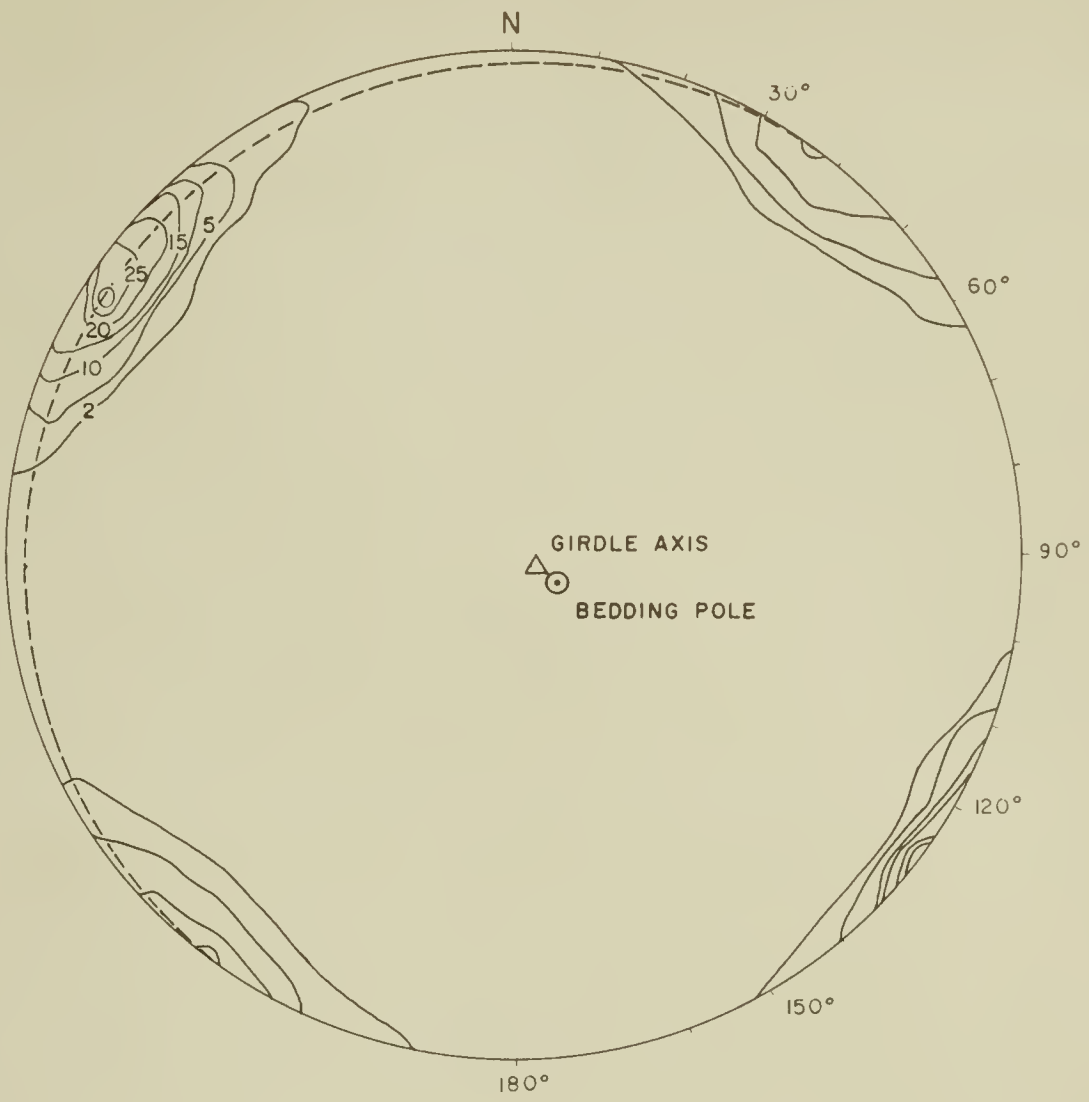
N
30°
60°
90°
120°
150°
180°
25
20
15
10
5
2
GIRDLE AXIS
BEDDING POLE

FIG.34

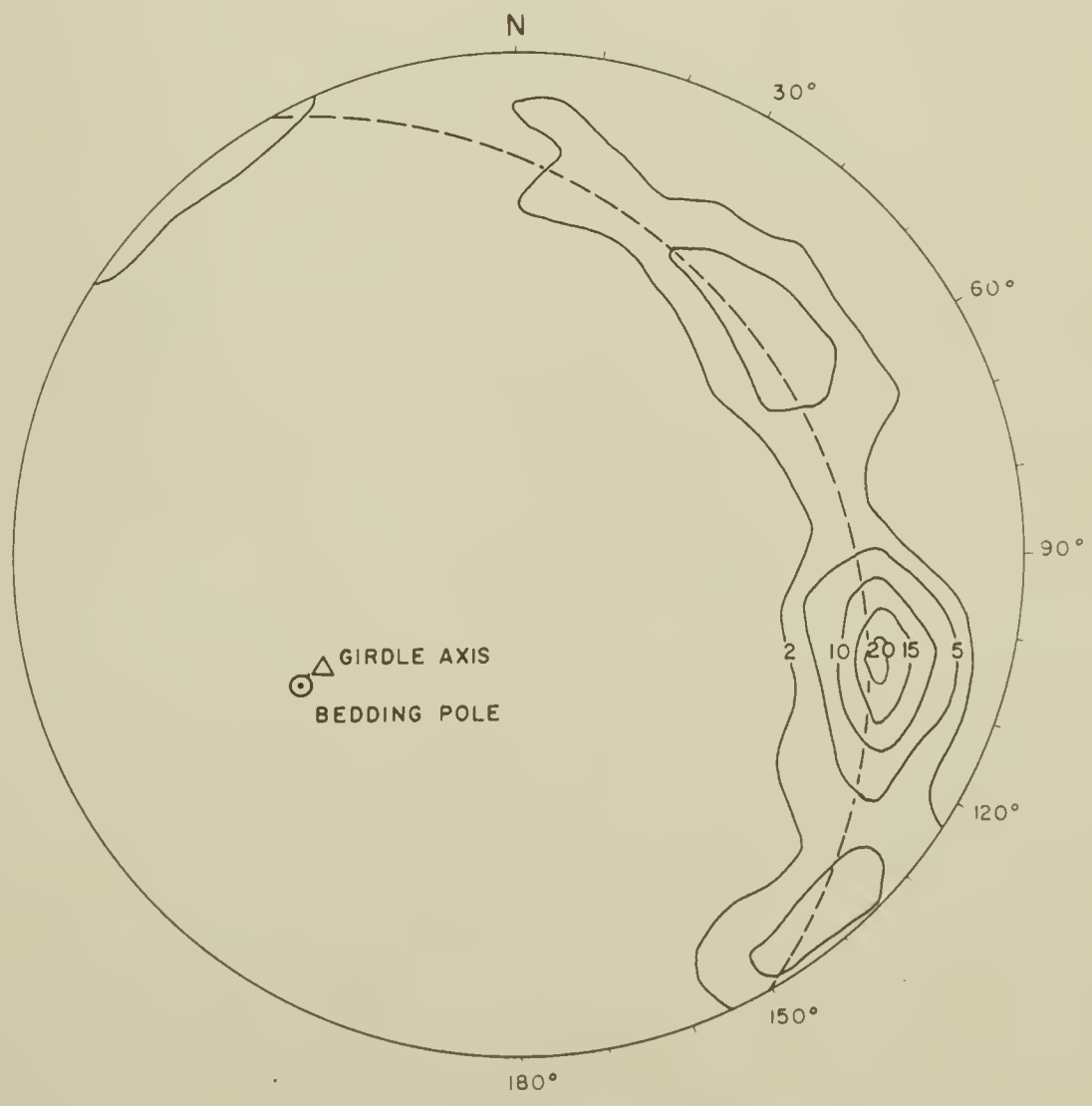
N
30°
60°
90°
120°
150°
180°
2
10
20
15
5
GIRDLE AXIS
BEDDING POLE

FIG.35

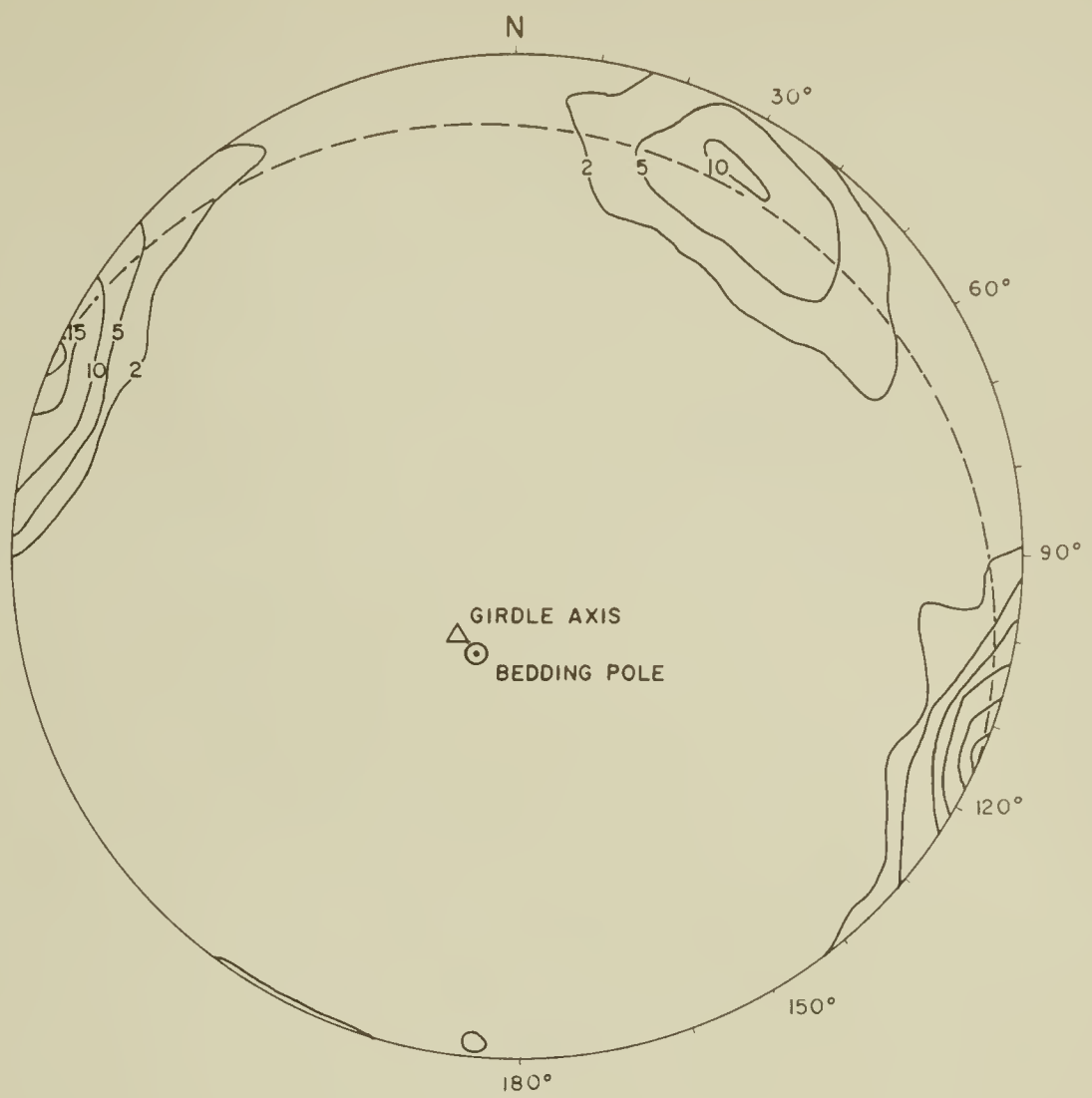
N
30°
60°
90°
120°
150°
180°
2
5
10
15
5
10
2
GIRDLE AXIS
BEDDING POLE

FIG.36

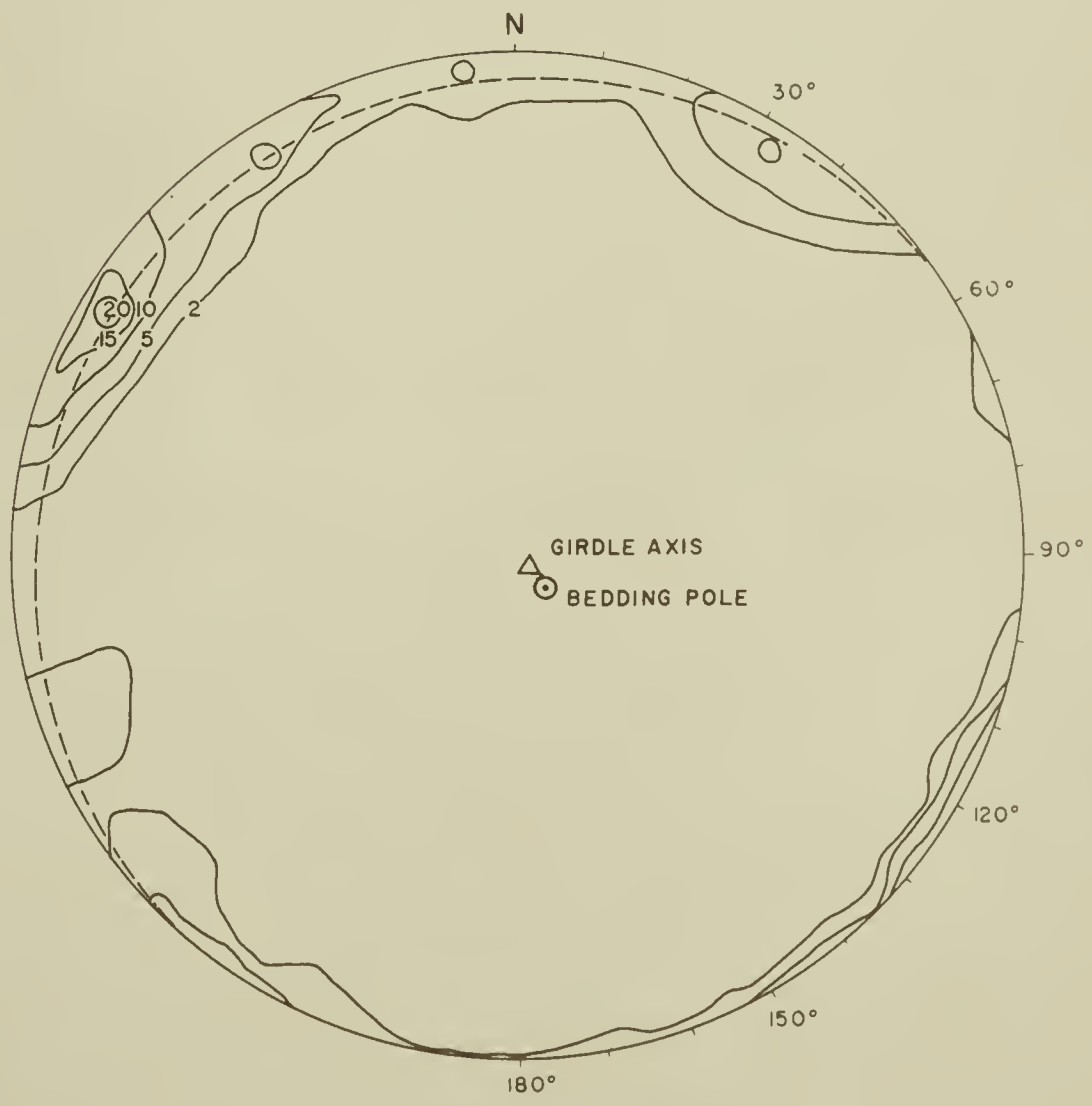
N
30°
60°
90°
120°
150°
180°
20
15
10
5
2
GIRDLE AXIS
BEDDING POLE

FIG.37

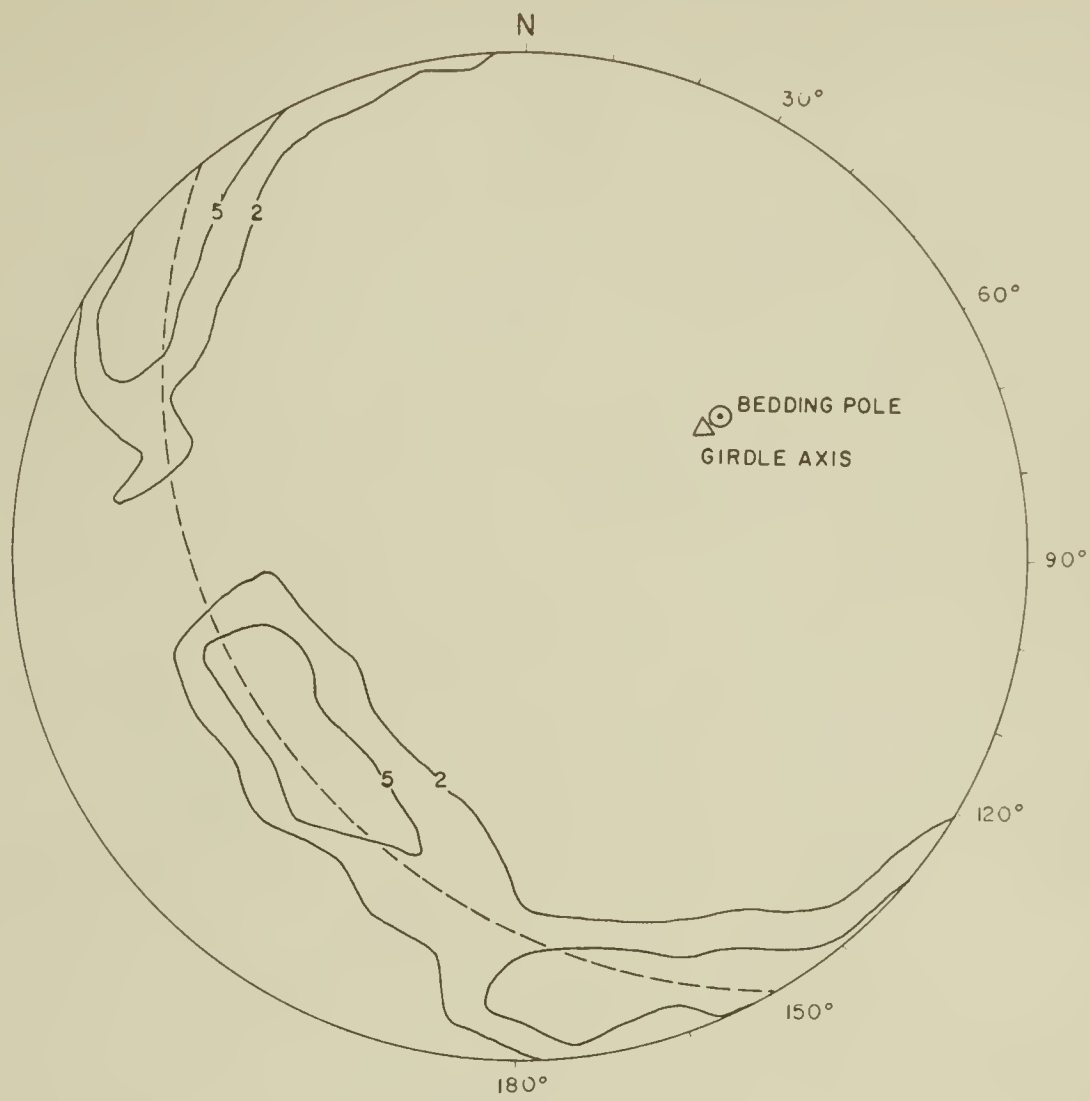
N
30°
60°
90°
120°
150°
180°
5
2
5
2
BEDDING POLE
GIRDLE AXIS

FIG. 38

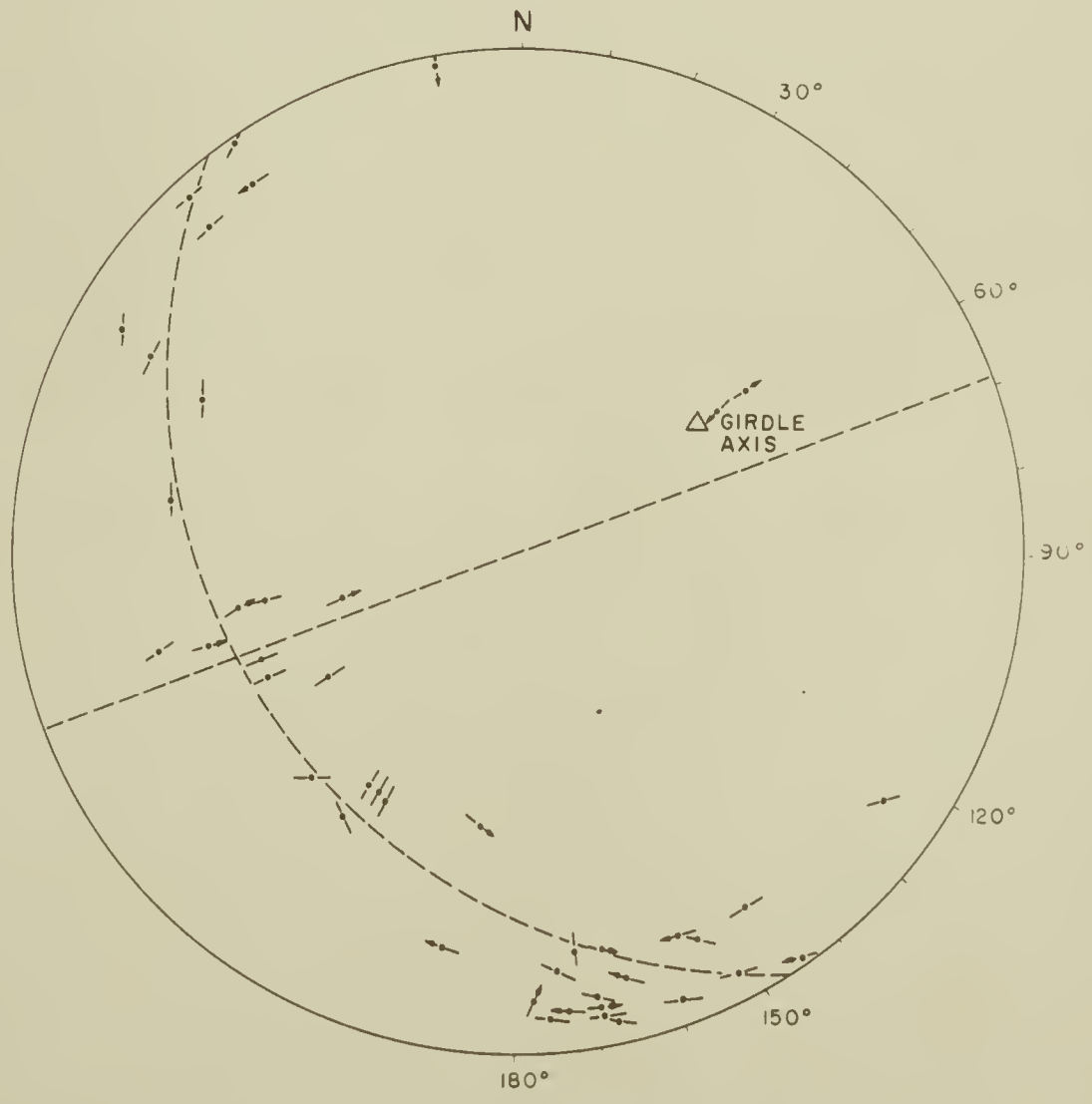
N
30°
60°
90°
120°
150°
180°
GIRDLE
AXIS

FIG. 39

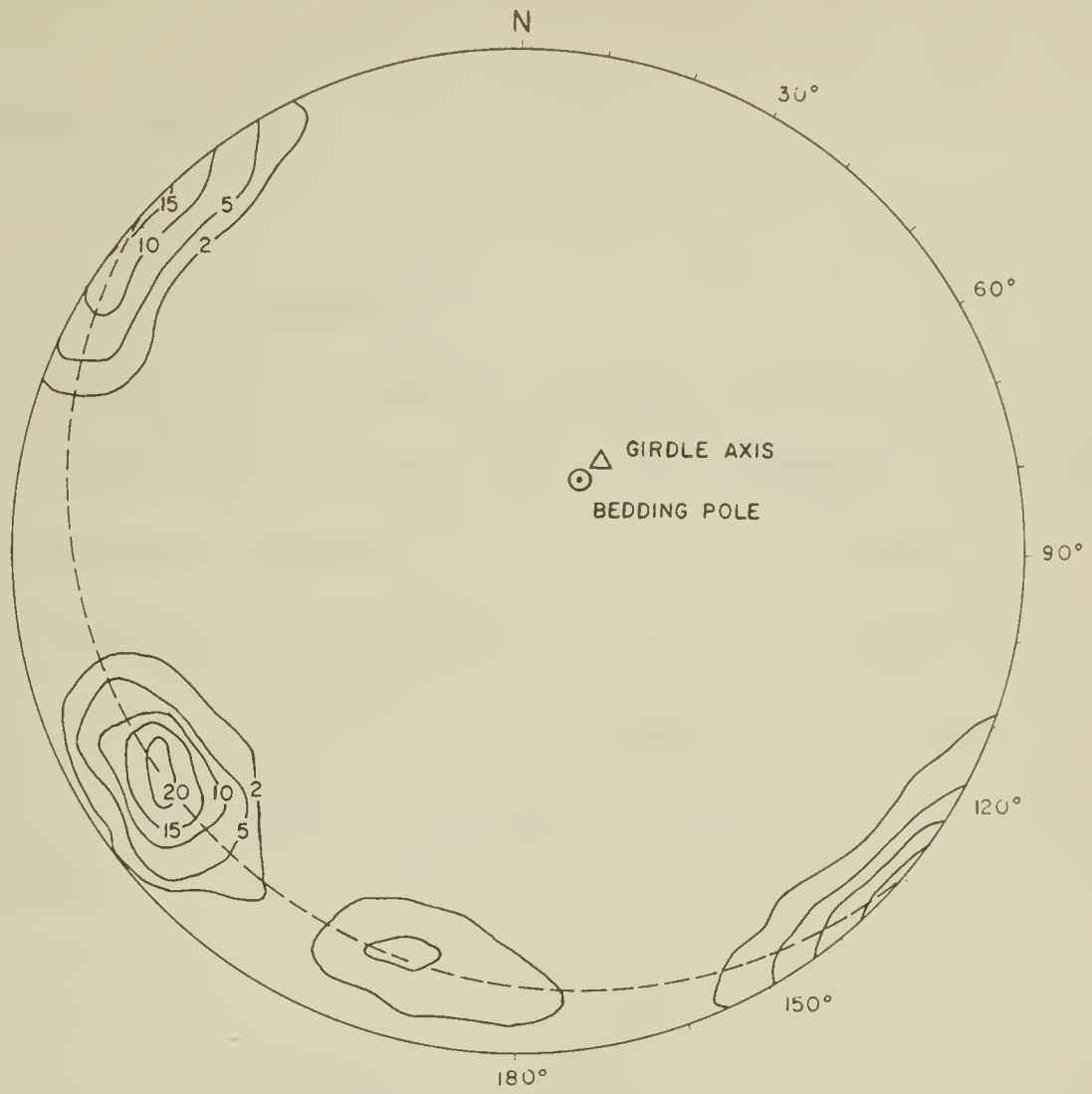
N
30°
60°
90°
120°
150°
180°
15
5
10
2
GIRDLE AXIS
BEDDING POLE
20
10
2
15
5

FIG.40

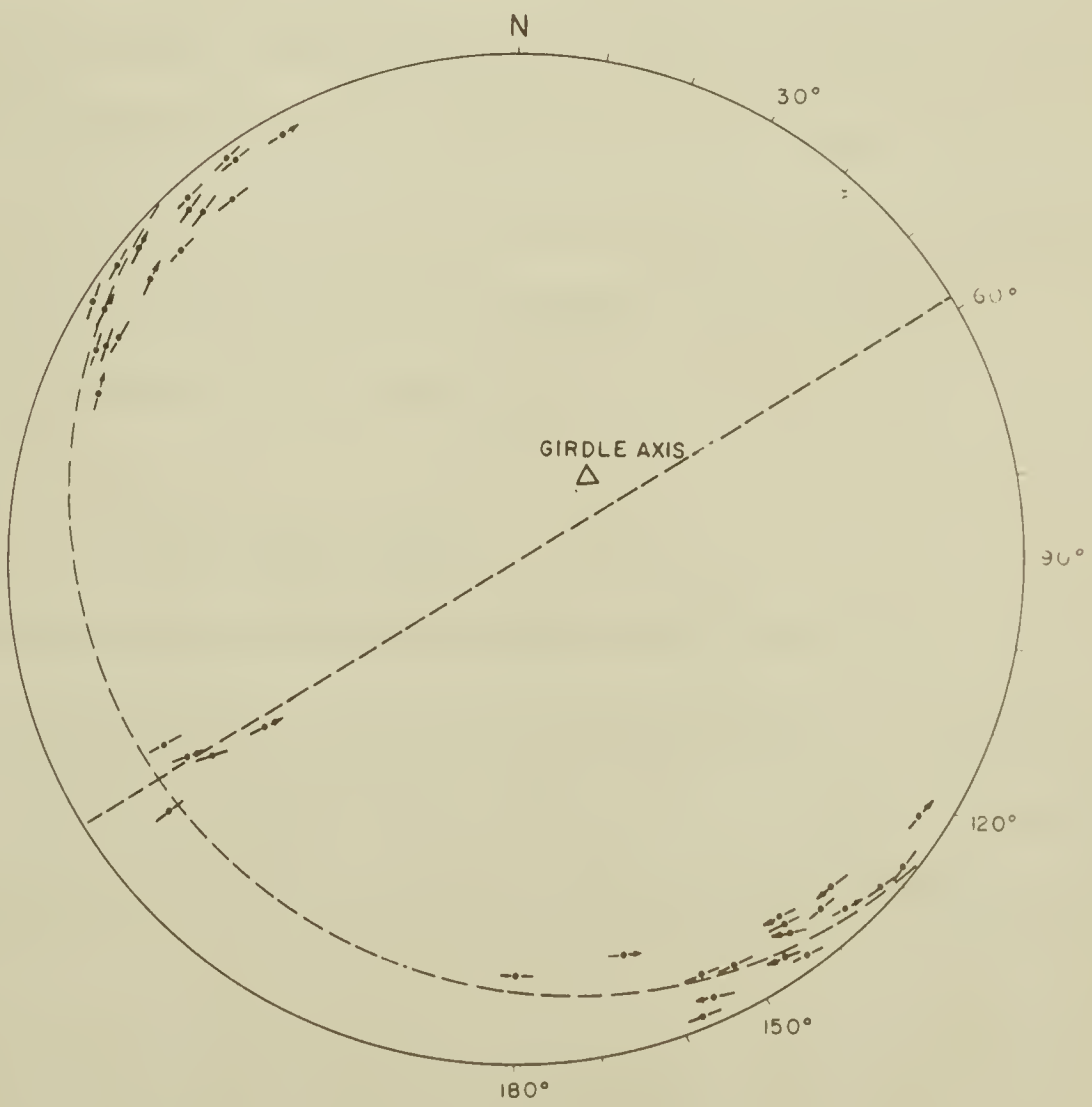
N
30°
60°
GIRDLE AXIS
90°
120°
150°
180°

FIG.41

no relationship to the regional structures.

Exshaw Area

Three very conspicuous joint sets occur in the massive beds of limestones. Two conjugate hkl joint sets (N 37° E/70 SE and N 73° E/81 NW) form very sharply defined maxima and intersect at a dihedral angle of 46 degrees. An h0l joint set (N 43° W/51 NE) with a larger dispersion than the hkl sets is also present (Fig. 42). Notable at this locality is the complete absence of slickensiding and the presence of zones, 1-2 feet thick, in which the fracture frequency is considerably higher than in the surrounding rock body.

The Gap Area

The joints in the limestones of the Banff formation show large dispersions in strike, but two major joint sets can be differentiated (Fig. 43). A 0kl joint set (N 48 E/81 SE) with shear-type slickensiding makes an angle of 60 degrees with a set of joints (N 13 W/ 62 NE) which show no indications of movement. Curved tension gashes filled with crystalline calcite are found to trend parallel to bedding and indicate that shearing has taken place along bedding. Joints cut these structures without being displaced by the bedding slip.

Roche Miette Area

Although fractures in the Palliser limestones at this locality are abundant and regular, they are found to have only poor preferred orientations. A 0kl joint set (N 44 E/ 78 NE) is definitely present, but no other joint sets can be distinguished. The normal to bedding forms the axis to a wide zone into which the remainder of the joints fall.

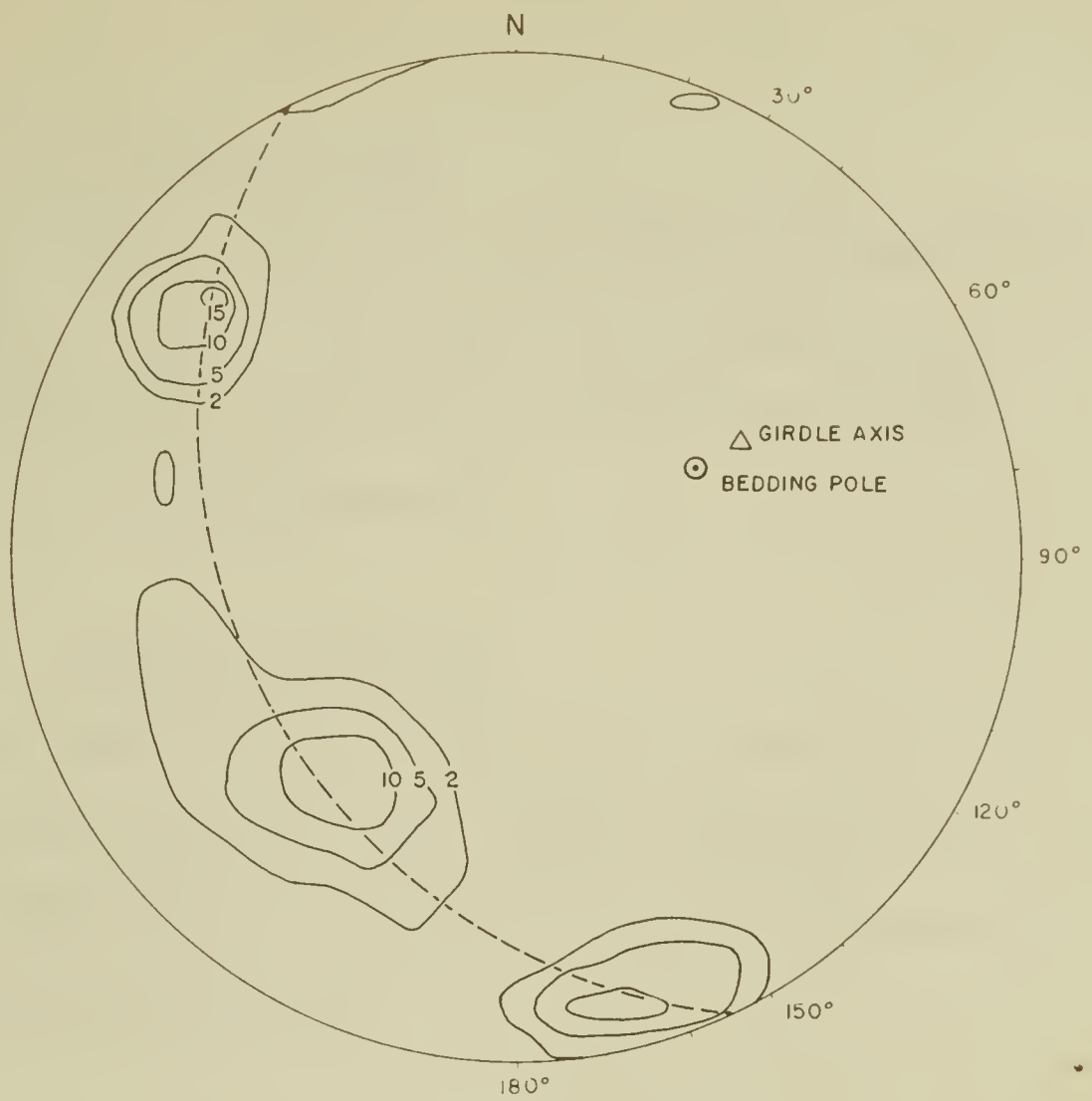
N
30°
60°
90°
120°
150°
180°
15
10
5
2
GIRDLE AXIS
BEDDING POLE
10 5 2

FIG. 42

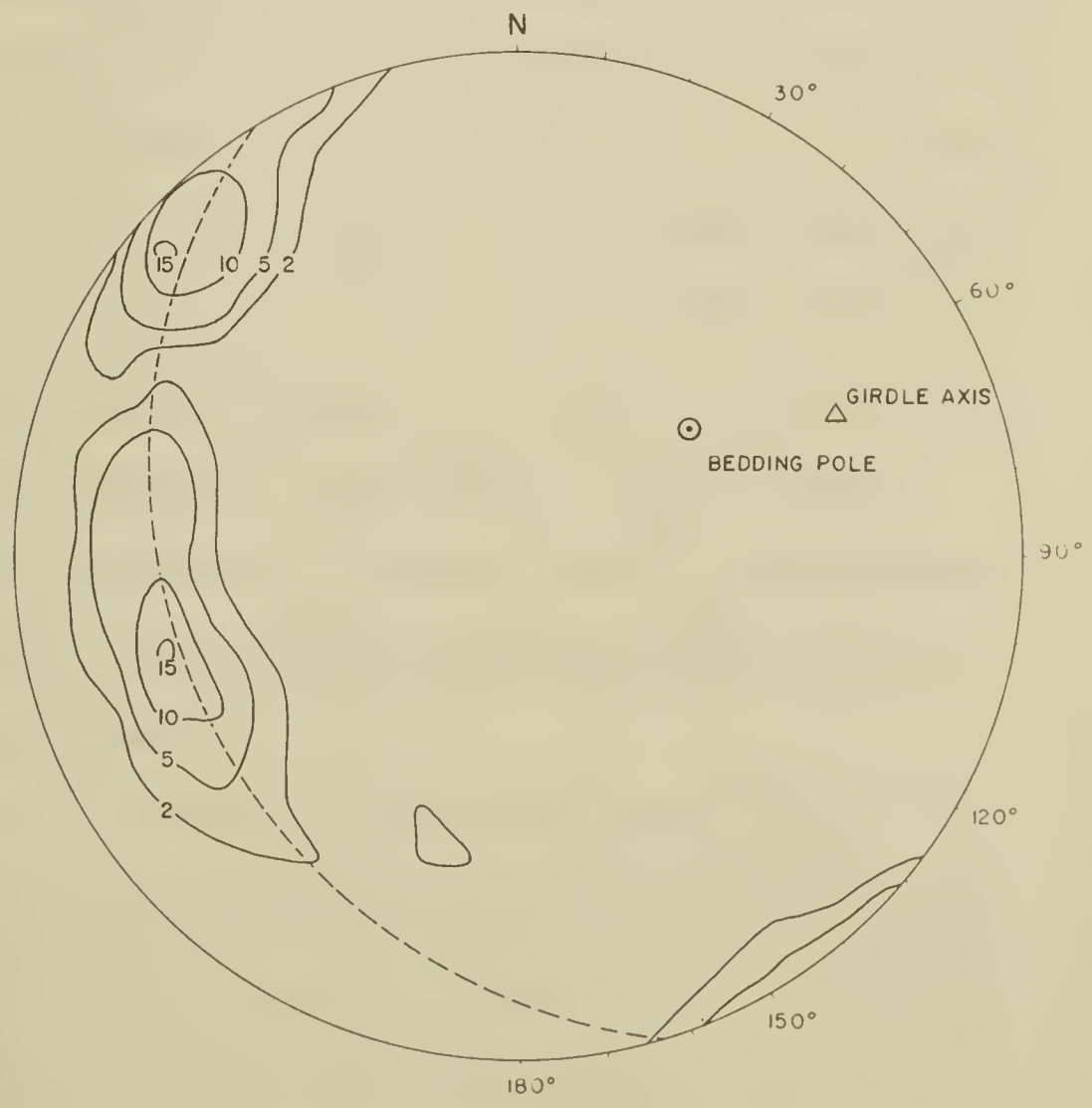
N
30°
60°
90°
120°
150°
180°
15 10 5 2
GIRDLE AXIS
BEDDING POLE
15
10
5
2

FIG. 43

Morro Peak Area

The degree of preferred orientation of joints both in the Palliser and the Alexo formations is low in this area. A 0kl joint set can be defined, but the validity of other concentrations is dubious (Fig. 44 & 45). Fractures in the Palliser formation fall into a well defined girdle.

Mount Murchison Area

Joints in the Eldon dolomites on the east limb of the Bow River anticline fall into two distinct maxima (Fig. 46). The mean fracture planes are orientated N 43° W/ 80°SW and N 60° E/ 89° SE. Shear-type slickensides are present on both joint sets. (Fig. 47).

Summary

The geometry of the fractures in the Foothills of the Canadian Rocky Mountains bears a definite relationship to the geometry of the folds and faults. The observed joints usually belong to an h0l set, okl set, or pair of hkl sets of fracture planes. The 0kl and hkl fractures are found to be generally smooth, planar, and extensive. Slickensiding on their surfaces indicates that shear-type movement has taken place along them. An h0l joint set is found to be present in all domains investigated in the Foothills. The h0l fractures usually are rough and discontinuous in appearance and show large deviations in their strike directions. Slickensiding along the h0l surfaces invariably indicates normal-type movement.

Investigations in the Eastern and Main Ranges show that the relationship between the macroscopic structure and the joints is essentially the same as in the Foothills. An exception are joints in the Eastern Ranges east of Jasper which have unusually large dispersions.

Joints formed at a post-folding stage in the tectonic history of the Rocky Mountains. None of the joints are found to be displaced by bedding plane slip or have been deformed by folding. Attempts to establish the relative ages of different joint sets by their cutting relationships in the outcrop were unsuccessful. Joints of every set are found to cut joints of every other set. Indirectly the age relationships can be inferred from the dispersions shown by the different joint sets. First-formed joints should exhibit lower dispersions than those formed after the contiguity of the rock body was lost due to fracturing. hkl and 0kl joint sets usually show less dispersion than the h0l joint sets. The dispersion of lines of intersection of conjugate hkl sets is also markedly lower than for intersections of 0kl and h0l sets.

The results of a study of the dispersion shown by joint sets were negative. Dispersion is not the direct result of lithology, bedding thickness, structural position, outcrop conditions, or intensity of deformation.

Fracture frequencies are dependent on the bedding thickness and joints show a closer spacing in thin beds. No differences in the fracture frequencies of the limbs and crests of folds could be detected. Fracture frequency does not appear to be a function of the magnitude of the tectonic forces.

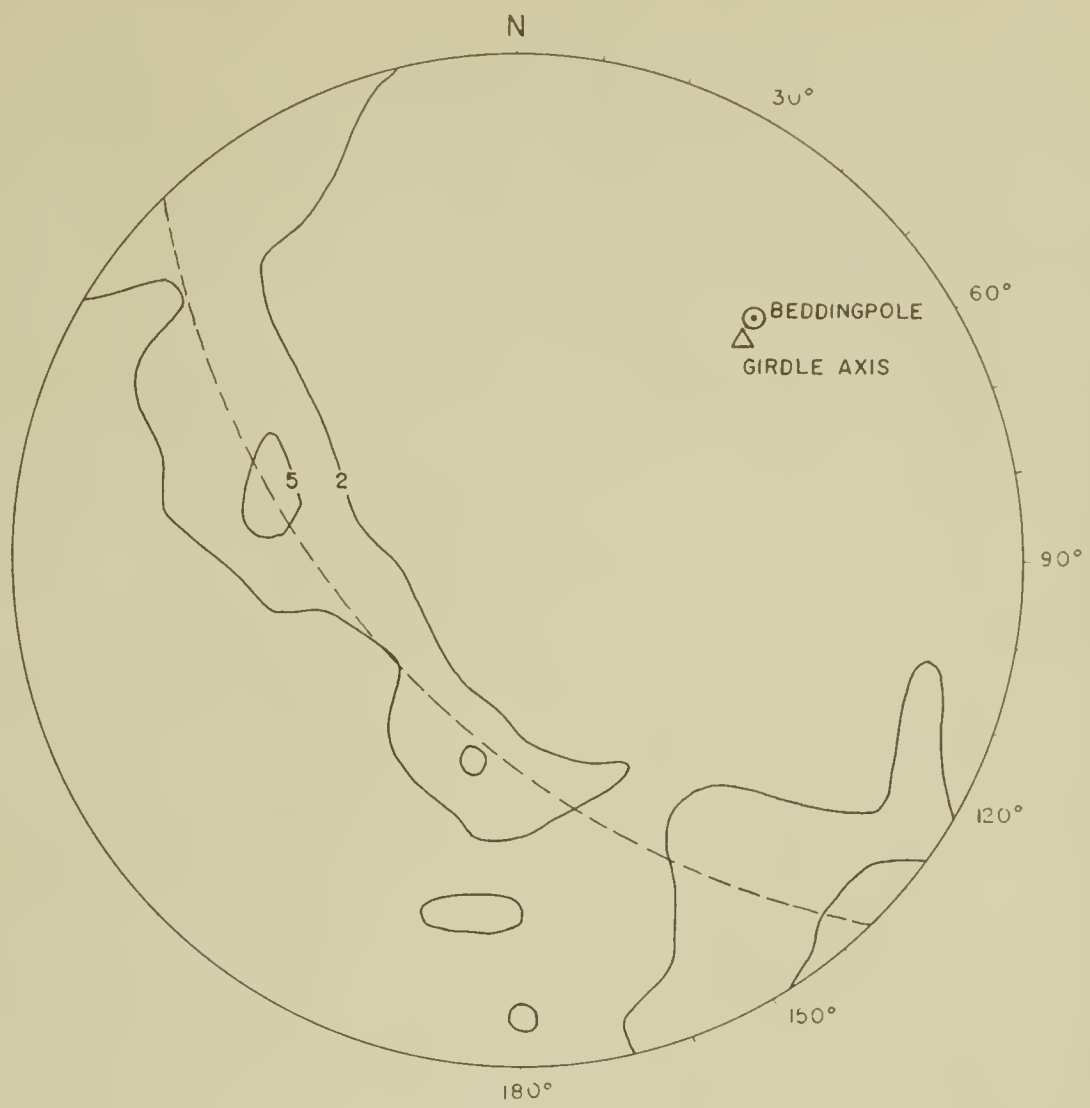
N
30°
60°
90°
120°
150°
180°
BEDDINGPOLE
GIRDLE AXIS
5
2

FIG. 44

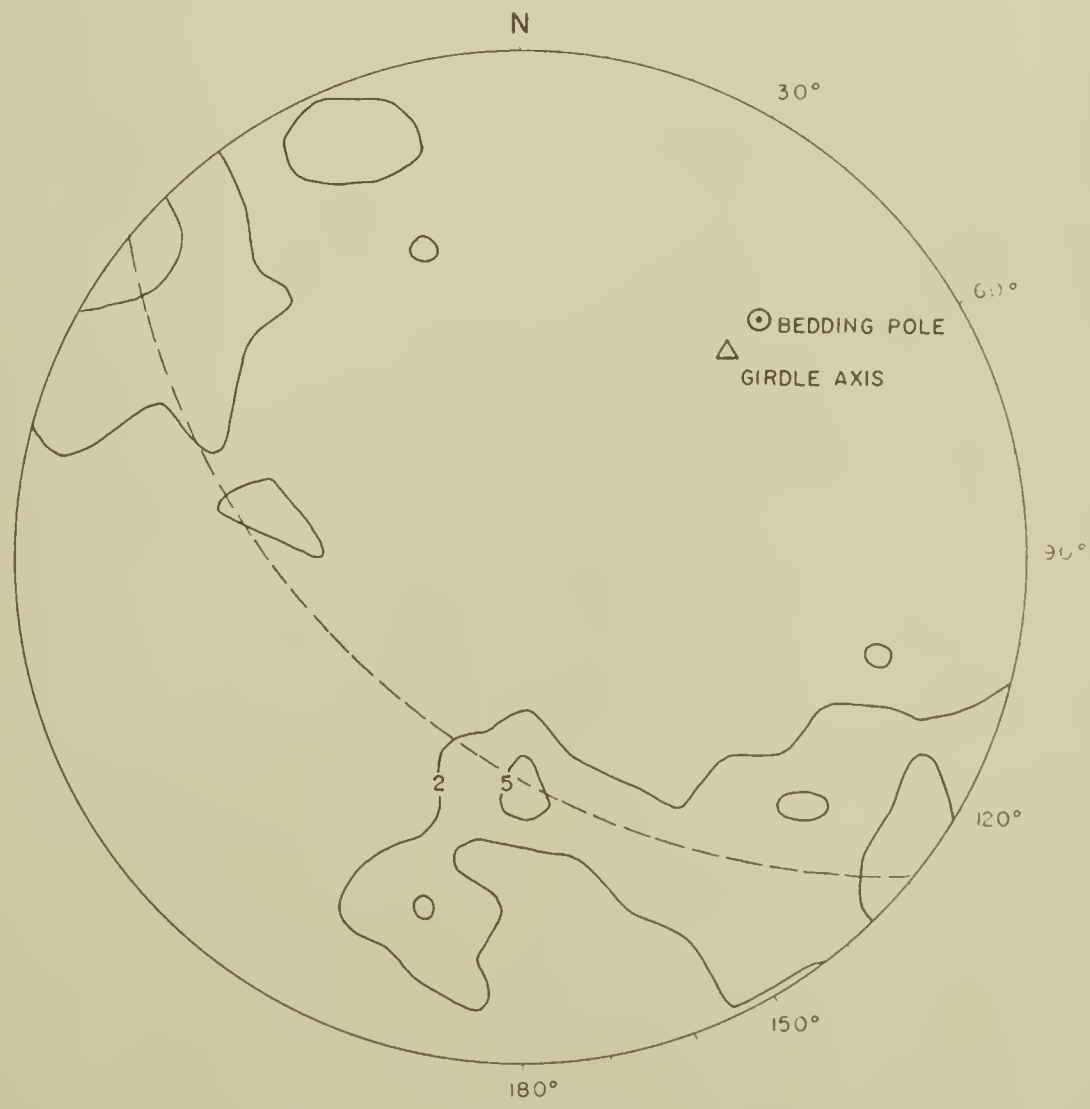
N
30°
BEDDING POLE
GIRDLE AXIS
120°
150°
180°
2
5

FIG. 45

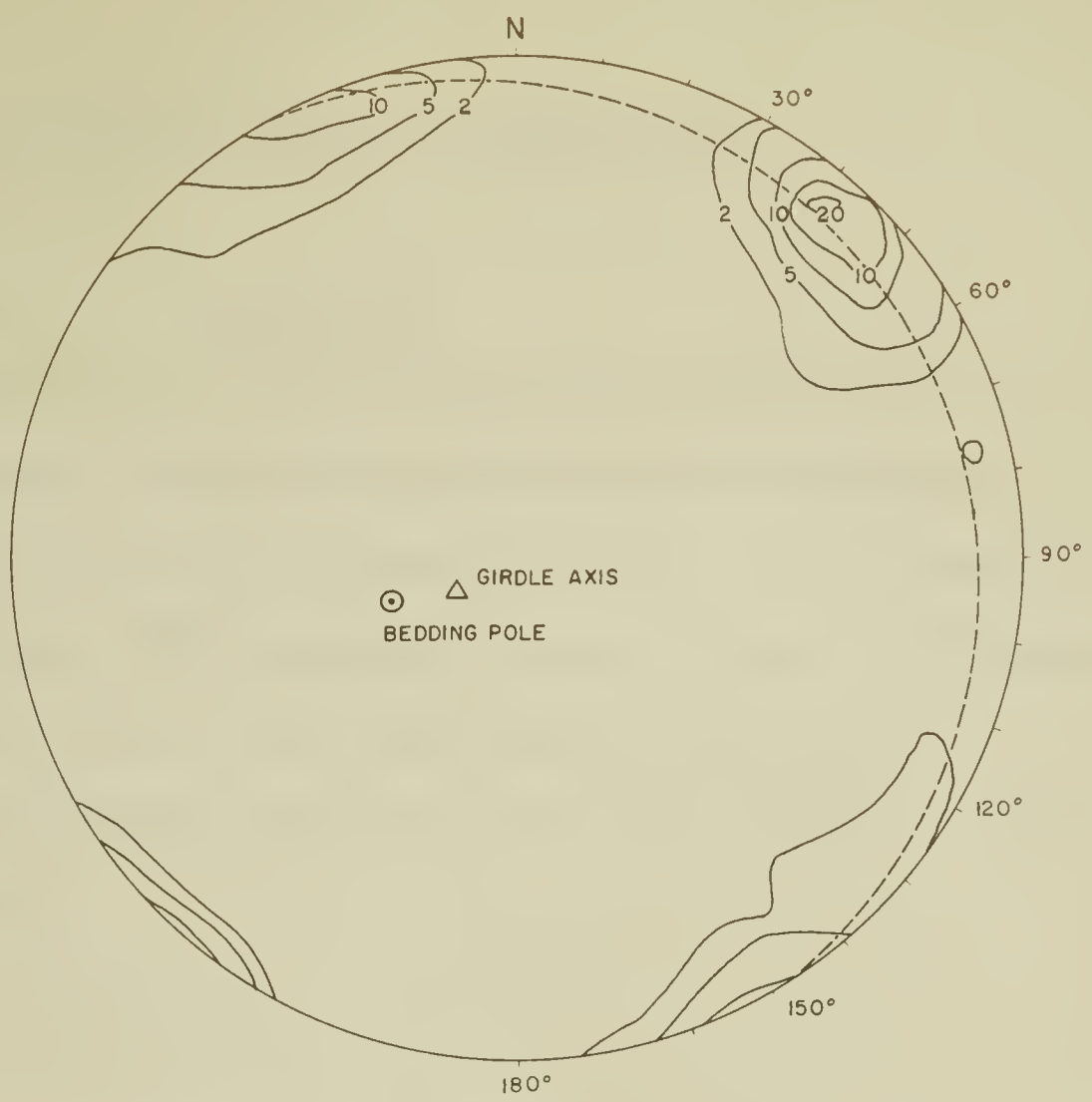
N
30°
60°
90°
120°
150°
180°
10
5
2
2
10
20
5
10
GIRDLE AXIS
BEDDING POLE

FIG. 46

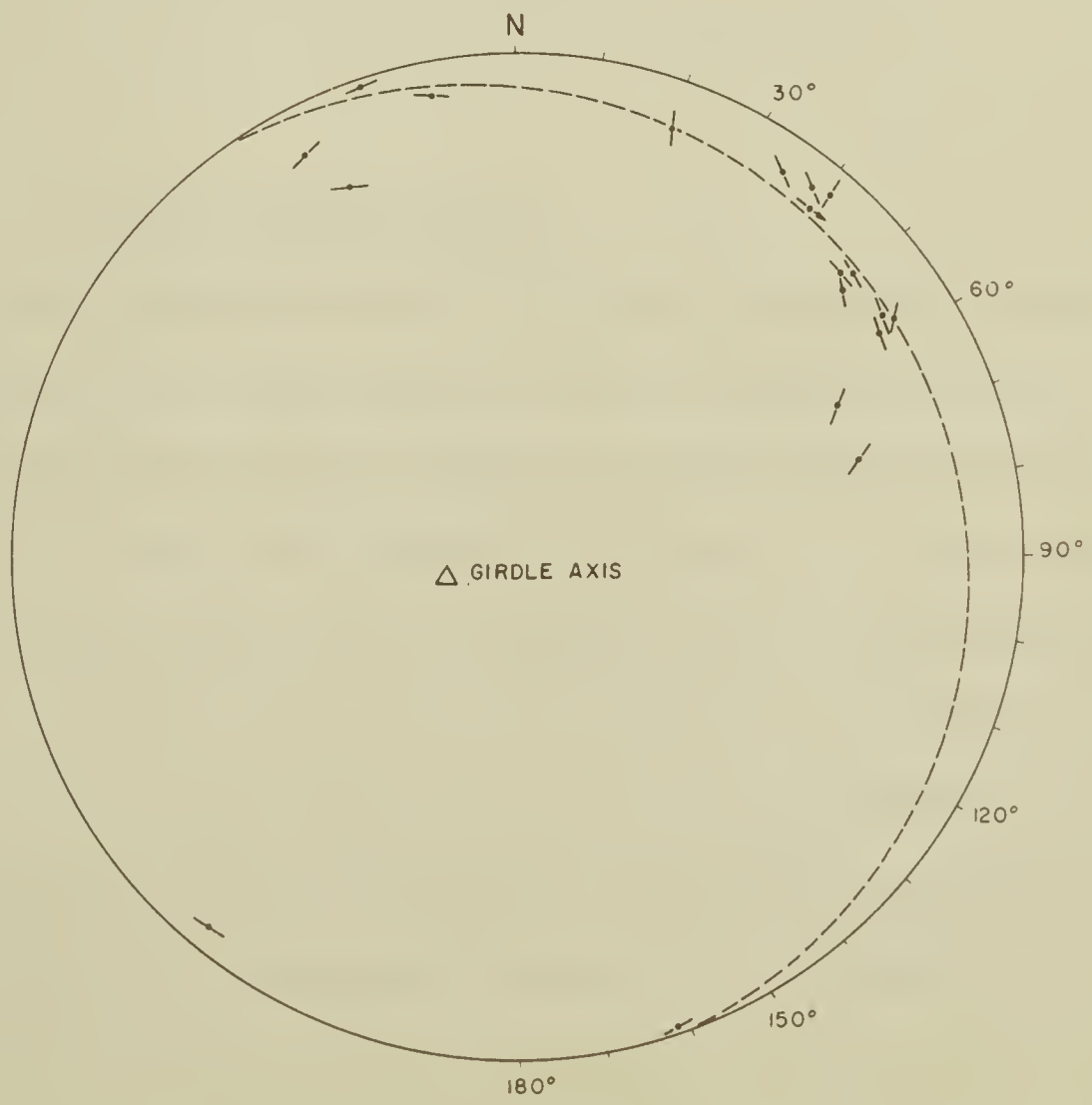
N
30°
60°
90°
120°
150°
180°
GIRDLE AXIS

FIG. 47

KINEMATIC AND DYNAMIC INTERPRETATIONS

Introduction

The geometric analysis of the joints revealed the existence of a very consistent fracture pattern in the Foothills of the Canadian Rocky Mountains. Investigations in the Eastern and Main Ranges indicate that a similar pattern may also exist in those regions. The mechanisms of formation of joints in all the areas investigated, as well as the stress field, must therefore have been similar.

Any theory explaining the formation of the joints has to account for the following observations:

a) the geometry of the joint sets;

b) the movements on the joint surfaces;

c) the changes in dihedral angles between conjugate joint sets;

d) the variability in the number of joint sets present;

e) the development of the joints at a late stage in the tectonic history.

Principal Stress Trajectories

The most persistent geometric property of the joints investigated in each domain is their tendency to fall along a girdle, which can be approximated by a great circle on the stereographic net. The presence of a girdle indicates that the joints are cozonal about an axis, which is given by the girdle axis. In cases where the girdle axis coincides with the normal to the bedding, the joints are perpendicular to the bedding. In the majority of areas investigated the girdle axes are found to plunge approximately 2 - 10 degrees steeper than the normal to the bedding. Two areas in the Eastern Ranges, along the Bow River, are found to be exceptional in having girdle axes inclined at a lower angle than the normal to bedding (Fig. 42 & Fig. 43).

Photoelastic experiments recently carried out by Bell and Currie (1964, pp. 33-51) showed that the maximum principal stress trajectories are subparallel to the upper and lower boundaries of competent units. In one of their experiments a single competent plastic member was surrounded by incompetent gelatine and folded concentrically under uniaxial compression. The maximum principal stress trajectories were found to run within the competent member. In the limbs of the fold the maximum principal stress trajectories were found to be inclined at a slightly lower angle than the bedding (Bell and Currie, 1964, p. 43, Fig. 5b).

The experimental model described above is almost completely analogous to the situation observed in the Cardium formation of the Foothills. Single competent sandstone members enclosed in incompetent shales have been folded concentrically. Principal stress trajectories subparallel to the boundaries of the competent sandstone members explain the formation of fractures virtually perpendicular to the bedding. Furthermore, principal stress trajectories plunging at slightly lower angles than the bedding dip would result in joints cozonal about an axis plunging at a higher angle than the normal to bedding.

Similar conclusions have been reached by other workers. Charlesworth and Evans (1962, pp. 358-359) studied the deviation of slaty cleavage from the mean plane and demonstrated that the maximum principal stress axis acted parallel to the competent members in the stratigraphic succession. Hancock (1964, p. 184) investigated the late-formed joints in the folds of South Pembrokeshire and concluded that the trace of the σ_x axis must have paralleled bedding during the formation of the joints.

The occurrence of girdle axes inclined at a lower angle than the normal to bedding is confined to two localities in the Eastern Ranges (Fig. 42 & Fig. 43). Both stations are located in thick competent units that have been faulted along steeply dipping thrust planes. The deflection of the maximum principal stress

trajectories toward the thrust plane, rather than parallel to the boundaries of the competent unit, would account for the geometry of the joints.

Significance of Variations in Dihedral Angle

Experimental studies have shown that the dihedral angle between conjugate fracture sets will increase with increasing confining pressure (Karman, 1911). Muehlberger (1961, pp. 211-219) suggested a modification to the Mohr envelope of fracture to account for this variability of dihedral angle. Furthermore, he theorized that over a critical stress interval a gradational change from a single extension fracture to two conjugate shear fractures should occur. Duschatko (1953) has been the only author to encounter such a relationship in the field.

In the present study the exact situation postulated by Muehlberger (ibid.) is found to exist, and the change of the dihedral angle is found to vary directly with distance across the structural trend (Fig. 31). Two conjugate joint sets at high dihedral angle in the western portion of the Bow River area are seen to have decreasing dihedral angles to the east. Eventually the two sets are found to be replaced by a single joint set.

Using the Mohr envelope and the modifications suggested by Muehlberger (ibid.), the observations made in the Bow River area can be explained. At the time of joint formation the confining pressures were highest in the western portions of the area and large differential stresses existed. Conjugate shear joint sets with high dihedral angles formed (Fig. 48, point A). The confining pressure, and as a result also the differential stresses, decreased to the east. The radius of curvature of the circle began to approach that of the parabolic vertex of the envelope. Although stress circles were still tangent to the envelope at two points, the dihedral angles progressively decreased with decreasing differential stresses (Fig. 48, point B). Even farther east, the stress circle eventually had the same radius of curvature as

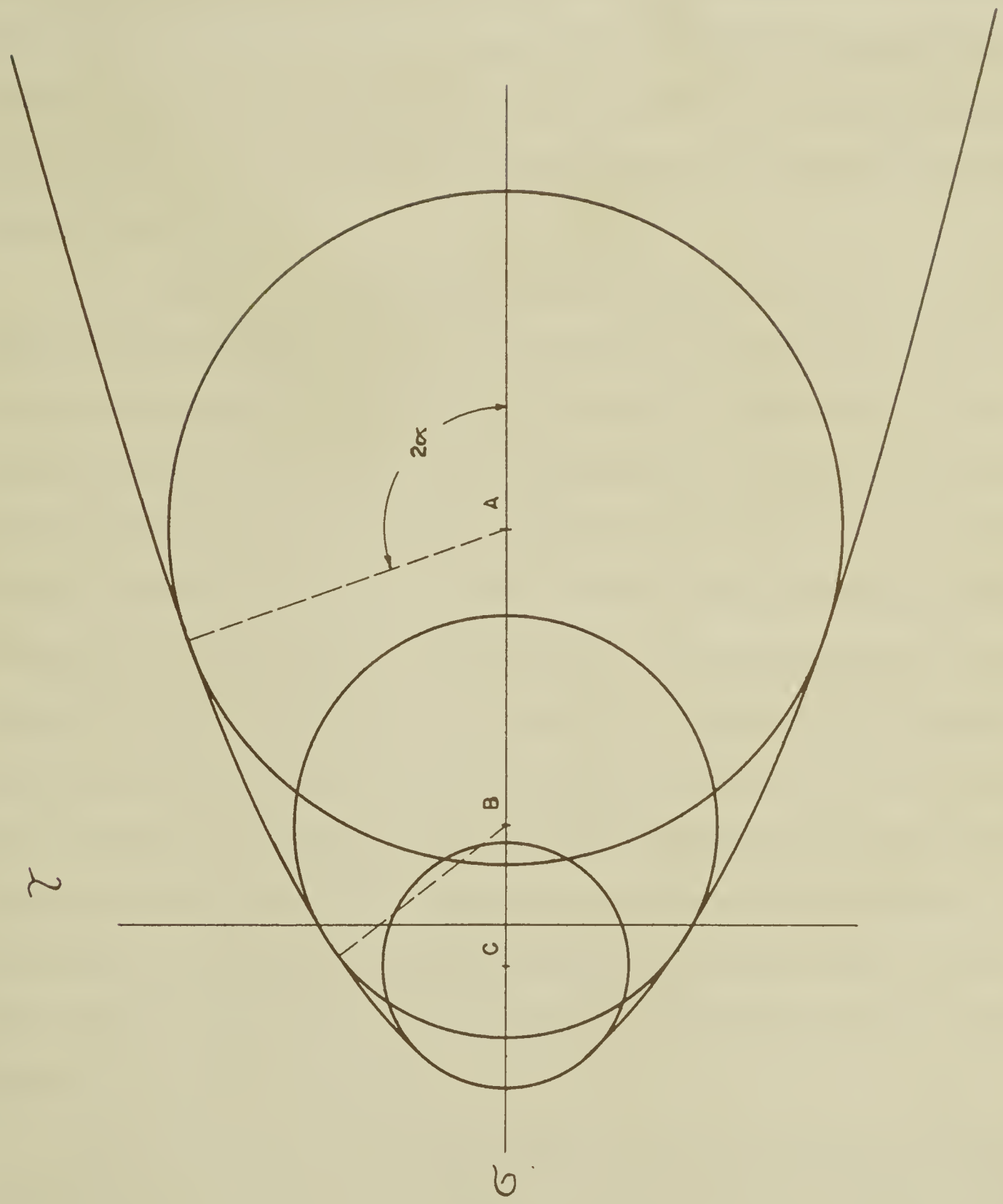

FIG. 48

the parabola forming the vertex of the envelope. Only one set fractures formed at that point (Fig. 48, point C).

The confining pressure is a function of the weight of overburden. The western portion of the Bow River area must at one time have been under a higher overburden than areas to the east. Overburden in the Red Deer River and South Creek areas must have been equivalent to, or less than, that in the eastern portions of the Bow River area. At present, all these locations are at approximately the same topographic elevations.

The trace of the McConnell thrust fault is found to be 3 miles west of the western border of the Bow River area. The attitude of the thrust plane can be seen to change from steeply dipping in the west to nearly flat in the vicinity of Mount Yamnuska, located a few miles north of Kananaskis Falls. At one time the hanging wall of the McConnell thrust must have extended much farther east than it does today. The rocks in the Bow River area formed part of the footwall of the McConnell thrust. Somewhere in the region east of its present trace, the thrust must have cut up in the stratigraphic section in order to die out eventually. In that case, the thrust sheet must have thinned to the east. Rocks of the same structural horizon in the footwall would, therefore, have been overlain by a thcker thrust sheet than those in the east. This model would account for the apparent differences in confining pressure. If the thrust plane had cut up in the stratigraphic section at a constant angle, then the linear relationship observed between the dihedral angles and the distance across the regional strike would be explained.

This hypothesis can be tested by applying the results derived in the Bow River area to some of the other areas investigated. The Red Deer River and South Creek areas are located 12 and 8 miles east of the McConnell thrust respectively. At those distances the angles between conjugate shear sets would be either so low that the sets could not be differentiated, or only one extension set would form. In both areas that

is the observed situation. The Cripple Creek area lies approximately 5 miles east of the McConnell thrust, and two conjugate shear sets with dihedral angle of 47 degrees should form in this area. Two weak shear joint sets are observed at dihedral angle of 49 degrees . An approximate correlation between the confining pressure under which the joints formed and the distance from the present trace of the McConnell thrust seems therefore possible. Only further observations could substantiate this finding.

Origin of Joints

During the main tectonic phase in the Rocky Mountains all principal stresses were compressional, and the formation of extensional joints is inconceivable. The development of shear joints is dependent on two conditions:

a) the intermediate stress axis has to be vertical;

b) the differential stresses have to be large enough to cause shearing in the rock.

Price (1959, pp. 153-155) demonstrated that both of these conditions cannot be satisfied at the same time during the main phase of compression. Geological evidence yields further proof for the late formation of the joints.

At the end of the period of thrusting and folding the following stresses acted in the areas investigated:

σ_1 acting from northeast to southwest = σ_x

σ_2 acting from southeast to northwest = σ_y

σ_3 acting vertical to bedding = σ_z

where σ_1, σ_2, and σ_3 are the maximum, intermediate, and minimum principal stresses respectively. σ_x acts in the ac fabric plane, σ_y in the bc fabric plane, and σ_z is perpendicular to the ab fabric plane

Not all the stresses had been dissipated during the thrusting and folding

because the rocks have a fundamental strength. The residual stresses remained stored in the rocks and acted parallel to the boundaries of the competent units (Fig. 49, point A).

The two lateral stresses σ_x and σ_y consisted of two components:

a) stresses due to gravitational loading equal to

$$\frac{1}{m-1} \quad {}^{*}\sigma_z$$

b) tectonic stresses which are C_a and $\frac{1}{m} * C_a$ in the x and y directions respectively.

m is equal to Poisson's number.

As the area underwent erosion, the amount of gravitational loading σ_z decreased and resulted in a proportional decrease in the gravitational components of the lateral stresses. In addition, the rock body underwent lateral strain in response to uplift. Lateral tensile stresses equal to ahlf the change in load developed (Price, 1959, p. 158). As a result, the lateral stresses decreased at a more rapid rate than σ_z during unloading. At some point (Fig. 49, point B) the vertical stress changed to the intermediate principal stress and σ_y became the minimum principal stress. One of the conditions necessary for the formation of shear joints was now satisfied. With further uplift, the ratio of σ_1/σ_3 increased rapidly. When this ratio reached a critical value, two conjugate hkl shear joint sets developed (Fig. 49, point C). In areas of low confining pressures, conjugate sets of low dihedral angle or only a 0kl extension set formed (Fig. 49, point D).

With the formation of the shear sets, or the single set of extension joints, a large fraction of the residual stresses was dissipated. The maximum principal stress was now σ_z, the intermediate principal stress σ_y, and the minimum principal stress σ_x. Continued erosion and uplift resulted in tensile stresses that eventually decreased σ_x to the point where it became tensile. Shortly thereafter, a set of

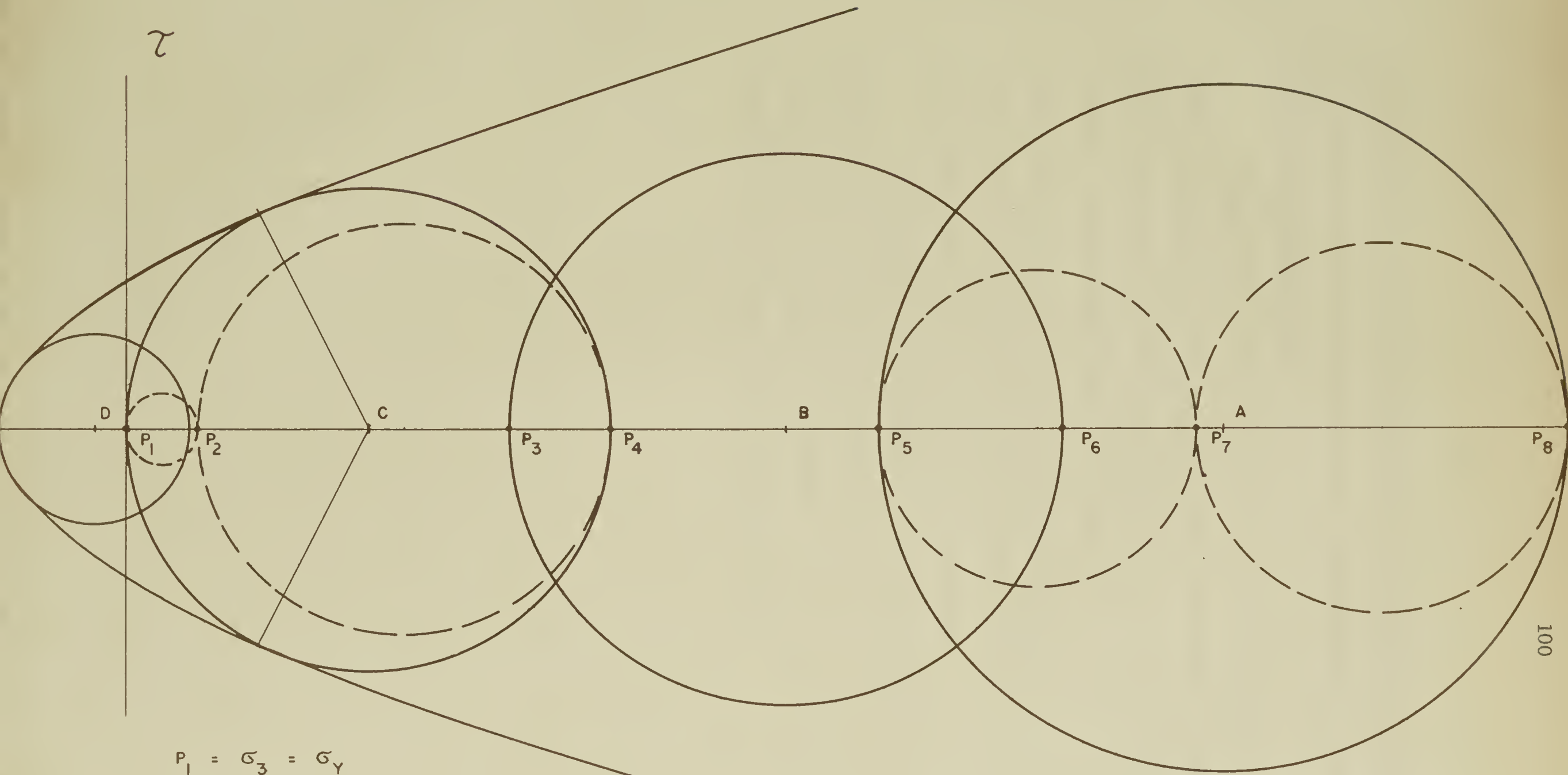

$P_1 = \sigma_3 = \sigma_Y$
$P_2 = \sigma_2 = \sigma_Z$
$P_3 = \sigma_2 = \sigma_3 = \sigma_Y = \sigma_Z$
$P_4 = \sigma_1 = \sigma_X$
$P_5 = \sigma_3 = \sigma_Z$
$P_6 = \sigma_1 = \sigma_X$
$P_7 = \sigma_2 = \sigma_Y$
$P_8 = \sigma_1 = \sigma_X$

FIG.49

h0l extension fractures formed perpendicular to the minimum principal stress axis. The formation of the h0l joints immediately released the tensile stresses; σ_y became the minimum principal stress.

Further uplift resulted in tensile stresses in the a-direction. In areas where a 0kl fracture set or two conjugate joint sets at small dihedral angle had already formed, these stresses resulted in the opening up of the previously formed joints. In regions of large dihedral angles, a 0kl fracture set would form in the absence of a suitable plane along which the tensile stresses could dissipate. This is observed to be the case in the west limb of Kananaskis anticline where two conjugate hkl joint sets, a h0l joint set, as well as a 0kl joint set are present.

The movements observed on the joint surfaces supports this hypothesis. Shear movements are observed on all the 0kl joints and conjugate sets of hkl joints, illustrating their close genetic relationship. Normal-type movement prevades on the h0l joint sets and agrees with an extensional origin.

REFERENCES

Beach, H.H.
1943: Moose Mountain and Morley map-areas, Alberta; Geol. Surv. Canada, Memoir 236.

Bell, R.T. and Currie, J.B.
1964: Photoelastic experiments related to structural geology; Proceed. Geol. Ass. Canada, Vol. 15, pp. 33-51.

Billings, M.P.
1954: Structural geology, 2nd Ed.; Prentice-Hall, Englewood Cliffs, N.J.

Blanchet, P.H.
1957: Development of fracture analysis as exploration method; Bull. Amer. Assoc. Petrol. Geol., Vol. 41, pp. 1748-1759.

Cairnes, D.D.
1914: Moose Mountain district, Southern Alberta; 2nd ed., Geol. Surv. Canada, Memoir 61.

Charlesworth, H.A.K. and Evans, C.R.
1962: Cleavage-boudinage in Precambrian rocks at Jasper, Alberta; Geologie en Mijnbouw, Vol. 41, pp. 356-362.

Clark, L.M.
1954: Geology of Rocky Mountain front ranges near Bow River, Alberta; in Western Canada Sedimentary Basin, ed. L.M. Clark, pp. 29-46.

Cox, A. and Doell, R.
1960: Review of paleomagnetism; Bull. Geol. Soc. Amer., Vol. 71, pp. 645-768.

Dinu, Y.
1912: Geologische Untersuchungen der Beziehung zwischen den Gesteinaspalten, der Tektonik und dem hydrographischen Netz im oestlichen Pfaelzerwalde; Verh. Nat. Met. Ver., Heidelberg, Vol. 11.

Duschatko, R.W.
1953: Fracture studies in the Lucero uplift, New Mexico; Tech. Inf. Bull. RME-3072, Atomic Energy Commission Tech. Inf. Service, Oak Ridge, Tennessee.

1955: Mechanical aid for plotting and counting out pole diagrams; Bull. Geol. Soc. Amer., Vol. 66, pp. 1521-1524.

Fisher, R.A.
1953: Dispersion on a sphere; Proc. Roy. Soc., Ser. A, Vol. 217, pp. 295-305.

Fitzgerald, E.L.
1963: Structural analysis along Torrens River, Alberta Foothills; Bull. Can. Petr. Geol., Vol. 11, pp. 125-137.

Griggs, D. and Handin, J.
1960: Observations on fracture and a hypothesis of earthquakes; in Rock Deformation, G.S.A. Memoir 79, pp. 347-364.

Haman, P.J.
1961: Lineament analysis on aerial photographs; West Canadian Research Publications, Series 2, No. 1.

Hancock, P.L.
1964: The relations between folds and late-formed joints in South Pembrokeshire; Geological Magazine, Vol. 101, pp. 174-184.

Harris, J.F., Taylor, G.L., and Walper, J.L.
1960: Relation of deformational fractures in sedimentary rocks to regional and local structure; Bull. Amer. Assoc. Petrol. Geol., Vol. 44, pp. 1853-1873.

Hills, E.S.
1963: Elements of structural geology; Methuen & Co. Ltd., London.

Hodgson, R.A.
1961: Regional study of jointing in Comb Ridge-Nevajo Mountain area, Arizona and Utah; Bull. Amer. Assoc. Petrol. Geol., Vol. 45, No. 1, pp. 1-38.

1961: Reconnaissance of jointing in Bright Angle area, Grand Canyon, Arizona; Bull. Amer. Assoc. Petrol. Geol., Vol. 45, pp. 95-97.

1961: Classification of structures on joint surfaces; Am. Jour. Sc., Vol. 259, pp. 493-502.

Hoeppener, R.
1953: Faltung und Klueftung in dem Noerdlichen Teil des Rheinischen Schiefergebirges; Geol. Rundschau, Vol. 41, pp. 128-144.

1957: Tektonik und Lagerstaetten im Rheinischen Schiefergebirge; Forschungsberichte des Wirtschafts- und Verkehrsministeriums Nordrhein-Westfalen, No. 337.

Holmes, C.D.
1963: Tidal strain as a possible cause of microseisms and rock jointing; Bull. Geol. Soc. Amer., Vol. 74, pp. 1411-1412.

Howell, J.V. and others
1960: Glossary of Geology and related sciences, 2nd Ed.; American Geological Institute, Washington, D.C.

Karman, Th. von
1911: Festigkeitsversuche unter allseitigem Druck; Zeitschr. Ver. deutsch. Ingenieur, Vol. 4, pp. 1749-1757.

Kendall, P.F. and Briggs, H.
1933: The formation of rock joints and the cleat of coal; Proc. Roy. Soc. Edinburgh, Vol. 53, pp. 164-187.

Knopf, E.B. and Ingerson, E.
1938: Structural petrology; Geol. Soc. Amer., Memoir 6.

Koebel, H.
1940: Ueber Verformung von Klueften bei der Schichtenfaltung am Beispiel des Salzgitter Sattels; Geol. Rundschau, Vol. 31, p. 188.

Lachenbruch, A.H.
1961: Depth and spacing of tension cracks; Journal of Geophysical Research, Vol. 66, pp. 4273-4292.

Metz, K.
1957: Lehrbuch der tektonischen Geologie; Ferdinand Enke Verlag, Stuttgart.

Mollard, J.D.
1959: Photogeophysics its application in petroleum exploration over the glaciated plains of Western Canada; 2nd Int. Williston Basin Conference, pp. 109-117.

Mountjoy, E.W.
1959: Preliminary map, Miette, Alberta; Geol. Surv. Can., Map 40 - 1959.

1961: Mount Robson (southeast) map-area, Rocky Mountains of Alberta and British Columbia; Geol. Surv. Can., Paper 61-31.

Muehlberger, W.R.
1961: Conjugate joint sets of small dihedral angle; Jour. Geology, Vol. 69, pp. 211-219.

Mueller, L.
1933: Untersuchunger ueber statistische Kluftmessung, Geol. u. Bau., Jahrb. 5, pp. 185-255.

Nabholz, W.K.
1956: Untersuchungen ueber Faltung und Klueftung im nordschweizerischen Jura; Ecolgae Geologicae Helvetiae, Vol. 49, pp. 373-406.

Nishimura, E.
1950: On earth tides; Trans. Amer. Geophys. Union, Vol. 31, p. 35 .

Parker, J.M.
1942: Regional systematic jointing in slightly deformed sedimentary rocks; Bull. Geol. Soc. Amer., Vol. 53, pp. 381-408.

Pincus, H.J.
1951: Statistical methods applied to the study of rock fractures: Quantitative comparative analysis of fractures in gneisses and overlying sedimentary rocks in northern New Jersey; Bull. Geol. Soc. Amer., Vol. 62, pp. 81-130.

Price, N.J.
1959: Mechanics of jointing in rocks; Geological Magazine, Vol. 96, pp. 149-167.

Robinson, T.W.
1939: Earth-tides shown by fluctuations of water-levels in wells in New Mexico and Iowa; Amer. Geophys. Union Trans., 20th Ann. Mtg., Pt. 4, pp. 656-666.

Roeder, D.
1960: Der tektonische Stil der Rocky Mountains in Alberta, Canada; Geol. Rundschau, Vol. 50, pp. 577-594.

Salomon, W.
1911: Die Bedeutung der Messung und Kartierung von gemeinen Klueften und Harnischen, mit besonderer Beruecksichtingung des Rheintal-Grabens; Zeitsch. Duetsch. Geol. Ges., Vol. 63, pp. 496-521.

Schmidt, W.
1925: Gefuegestatistik; Tschermaks mineralog. petrog. Mitt., Vol. 38, pp. 395-399.

Seitz, O.
1914/17: Ueber die Tektonik der Luganer Alpen; Verh. Nat. Met. Ver., Heidelberg, N.F., Vol. 13.

de Sitter, L.U.
1956: Structural geology; McGraw-Hill, New York.

Spencer, E.W.
1959: Geologic evolution of the Beartooth Mountains, Montana and Wyoming. Part II: Fracture patterns; Bull. Geol. Soc. Amer., Vol. 70, pp. 467-508.

Stiny, J.
1925: Die Ausfuehrung der Kluftmessung; Der Geologe, No. 38, pp. 873-877.

Strand, T.
1944: A method of counting out petrofabric diagrams; Norsk. Geologisk Tidsskrift, Vol. 24, pp. 112-113.

Turner, F.J.
1948: Mineralogical and structural evolution of the metamorphic rocks; Geol. Soc. Amer., Memoir 30.

Turner, F.J. and Weiss, L.E.
1963: Structural analysis of metamorphic tectonites; McGraw-Hill, New York.

Wager, L.R.
1931: Jointing in the Great Scar limestone and its relation to the tectonics of the area; Geol. Soc. London Quart. Jour., Vol. 87, pp. 392-420.

Wilson, R.L.
1959: Remanent magnetism of late secondary and early tertiary British rocks; Phil. Mag., Vol. 4, 8th Ser., pp. 750-755.

Vorster, W. H.
1956: Generation of electric power from hot water spring; South African Mech. Engineer, Vol. 5, No. 9.

Zwart, H. J.
1951: Breuken en Diaklazen en Robin Hood's Bay; Geologie en Mijnbouw, Vol. 13, pp. 1-4.

APPENDIX I

Direction cosines of counting locations used on Program 913107-001.

..I 913107 COUNTING POINT LOCATIONS

333

0	0	1.00000000	0.00000000	0.00000000	1
336	2	.91298886	-.40648903	.03489949	2
342	6	.94584644	-.30732438	.10452845	3
348	10	.96328729	-.20475323	.17364817	4
354	11	.97624968	-.10260822	.19080898	5
0	12	.97814760	0.00000000	.20791167	6
6	11	.97624971	.10260796	.19080898	7
12	10	.96328733	.20475302	.17364817	8
18	6	.94584652	.30732414	.10452845	9
24	2	.91298894	.40648884	.03489949	10
323	0	.79863539	-.60181516	0.00000000	11
328	6	.84340225	-.52701651	.10452845	12
334	12	.87915314	-.42879185	.20791167	13
340	16	.90329043	-.32877109	.27563734	14
346	20	.91177968	-.22733241	.34202013	15
353	22	.92027274	-.11299551	.37460657	16
0	22	.92718386	0.00000000	.37460657	17
7	22	.92027277	.11299527	.37460657	18
14	20	.91177973	.22733219	.34202013	19
20	16	.90329052	.32877085	.27563734	20
26	12	.87915324	.42879166	.20791167	21
32	6	.84340239	.52701628	.10452845	22
37	0	.79863552	.60181500	0.00000000	23
315	2	.70667584	-.70667619	.03489949	24
319	9	.74541770	-.64798200	.15643445	25
324	16	.77767695	-.56501558	.27563734	26
330	21	.80850425	-.46679039	.35836793	27
337	26	.82734421	-.35118695	.43837113	28
344	28	.84874364	-.24337353	.46947154	29
352	30	.85759727	-.12052766	.49999998	30
0	31	.85716731	0.00000000	.51503805	31
8	30	.85759731	.12052742	.49999998	32
16	28	.84874371	.24337332	.46947154	33
23	26	.82734429	.35118679	.43837113	34
30	21	.80850437	.46679019	.35836793	35
36	16	.77767705	.56501542	.27563734	36
41	9	.74541786	.64798183	.15643445	37
45	2	.70667603	.70667600	.03489949	38
307	0	.60181485	-.79863563	0.00000000	39
311	10	.64609187	-.74324395	.17364817	40
315	16	.67971449	-.67971482	.27563734	41
320	23	.70514751	-.59168925	.39073111	42
326	29	.72509247	-.48908132	.48480959	43
333	34	.73867780	-.37637533	.55919288	44
342	37	.75954745	-.24679212	.60181500	45
350	39	.76533936	-.13495011	.62932036	46
0	40	.76604445	0.00000000	.64278759	47
10	39	.76533938	.13494907	.62932036	48
18	37	.75954751	.24679192	.60181500	49
27	34	.73867789	.37637516	.55919288	50
34	29	.72509261	.48908112	.48480959	51
40	23	.70514763	.59168910	.39073111	52
45	16	.67971467	.67971464	.27563734	53
49	10	.64609203	.74324381	.17364817	54

53	0	.60181505	.79863549	0.00000000	55
302	6	.52701609	-.84340251	.10452845	56
306	16	.56501528	-.77767716	.27563734	57
310	23	.59168898	-.70514774	.39073111	58
315	30	.61237228	-.61237258	.49999998	59
321	36	.62872418	-.50913101	.58778523	60
329	41	.64691228	-.38870432	.65605901	61
338	45	.65561792	-.26488704	.70710676	62
349	48	.65683678	-.12767626	.74314480	63
0	49	.65605905	0.00000000	.75470955	64
11	48	.65683681	.12767613	.74314480	65
22	45	.65561800	.26488684	.70710676	66
31	41	.64691238	.38870415	.65605901	67
39	36	.62872430	.50913086	.58778523	68
45	30	.61237244	.61237242	.49999998	69
50	23	.59168913	.70514761	.39073111	70
54	16	.56501547	.77767702	.27563734	71
58	6	.52701636	.84340235	.10452845	72
294	2	.40648867	-.91298902	.03489949	73
296	12	.42879151	-.87915331	.20791167	74
300	21	.46679008	-.80850444	.35836793	75
304	29	.48908097	-.72509271	.48480959	76
308	37	.49168899	-.62933347	.60181500	77
315	43	.51714504	-.51714529	.68199833	78
323	49	.52395197	-.39482628	.75470955	79
334	54	.52829785	-.25766820	.80901697	80
346	56	.54258247	-.13528112	.82903755	81
0	57	.54463906	0.00000000	.83867054	82
14	56	.54258251	.13528099	.82903755	83
26	54	.52829791	.25766809	.80901697	84
37	49	.52395206	.39482617	.75470955	85
45	43	.51714518	.51714515	.68199823	86
52	37	.49168914	.62933335	.60181500	87
56	29	.48908116	.72509258	.48480959	88
60	21	.46679025	.80850433	.35836793	89
64	12	.42879178	.87915318	.20791167	90
66	2	.40648896	.91298889	.03489949	91
288	6	.30732392	-.94584659	.10452845	92
290	16	.32877064	-.90329060	.27563734	93
293	26	.35118663	-.82734435	.43837113	94
296	33	.36764883	-.75379218	.54463901	95
300	41	.37735468	-.65359773	.65605901	96
307	49	.39482607	-.52395213	.75470955	97
314	55	.39843957	-.41259647	.81915202	98
326	61	.40192534	-.27110221	.87461968	99
342	64	.41691580	-.13546426	.89879399	100
0	66	.40673674	0.00000000	.91354541	101
18	64	.41691583	.13546415	.89879399	102
34	61	.40192541	.27110210	.87461968	103
46	55	.39843970	.41259626	.81915202	104
53	49	.39482620	.52395204	.75470955	105
60	41	.37735482	.65359765	.65605901	106
64	33	.36764907	.75379207	.54463901	107
67	26	.35118689	.82734424	.43837113	108
70	16	.32877092	.90329049	.27563734	109
72	6	.30732422	.94584649	.10452845	110

282	10	.20475285	-.96328737	.17364817	111
284	19	.22874148	-.91743266	.32556813	112
286	28	.24337319	-.84874374	.46947154	113
288	37	.24679175	-.75954757	.60181500	114
291	46	.24894315	-.64851952	.71933978	115
296	54	.25766800	-.52829795	.80901697	116
307	61	.29176564	-.38718626	.87461968	117
315	68	.26488684	-.26488697	.92718382	118
333	72	.27533617	-.14029086	.95105649	119
0	74	.27563740	0.00000000	.96126168	120
27	72	.27533620	.14029079	.95105649	121
45	68	.26488691	.26488690	.92718382	122
57	61	.26404627	.40659557	.87461968	123
64	54	.25766816	.52829787	.80901697	124
69	46	.24894335	.64851945	.71933978	125
72	37	.24679199	.75954749	.60181500	126
74	28	.24337338	.84874369	.46947154	127
76	19	.22874176	.91743260	.32556813	128
78	10	.20475185	.96329190	.17365	129
277	11	.11963003	-.97431030	.19080898	130
278	21	.12992907	-.92449491	.35836793	131
279	30	.13547603	-.85536322	.49999998	132
280	39	.13494982	-.76533940	.62932036	133
281	48	.12767600	-.65683684	.74314480	134
283	56	.12579093	-.54486087	.82903755	135
288	64	.13546405	-.41691586	.89879399	136
297	72	.14029075	-.27533623	.95105649	137
315	78	.14701580	-.14701587	.97814757	138
0	82	.13917318	0.00000000	.99026805	139
45	78	.14701584	.14701583	.97814757	140
63	72	.14029083	.27533618	.95105649	141
72	64	.13546419	.41691582	.89879399	142
77	56	.12579110	.54486083	.82903755	143
79	48	.12767621	.65683679	.74314480	144
80	39	.13495005	.76533936	.62932036	145
81	30	.13547629	.85536318	.49999998	146
82	21	.12992935	.92449487	.35836793	147
83	11	.11963033	.97431026	.19080898	148
270	0	-.00000018	-1.00000000	0.00000000	149
270	12	-.00000017	-.97814760	.20791167	150
270	22	-.00000016	-.92718386	.37460657	151
270	31	-.00000015	-.85716731	.51503805	152
270	40	-.00000013	-.76604445	.64278759	153
270	49	-.00000011	-.65605905	.75470955	154
270	57	-.00000009	-.54463906	.83867054	155
270	66	-.00000007	-.40673674	.91354541	156
270	74	-.00000004	-.27563740	.96126168	157
270	82	-.00000002	-.13917318	.99026805	158
0	90	.00000012	0.00000000	1.00000000	159
90	82	.00000001	.13917318	.99026805	160
90	74	.00000003	.27563740	.96126168	161
90	66	.00000005	.40673674	.91354541	162
90	57	.00000006	.54463906	.83867054	163
90	49	.00000008	.65605905	.75470955	164
90	40	.00000009	.76604445	.64278759	165
90	31	.00000010	.85716731	.51503805	166

90	22	.00000011	.92718386	.37460657	167
90	12	.00000012	.97814760	.20791167	168
90	0	.00000012	1.00000000	0.00000000	169
263	11	-.11963048	-.97431024	.19080898	170
262	21	-.12992940	-.92449487	.35836793	171
261	30	-.13547634	-.85536317	.49999998	172
260	39	-.13495010	-.76533936	.62932036	173
259	48	-.12767624	-.65683679	.74314480	174
257	56	-.12579113	-.54486082	.82903755	175
252	64	-.13546425	-.41691580	.89879399	176
243	72	-.14029085	-.27533618	.95105649	177
225	78	-.14701586	-.14701582	.97814757	178
180	82	-.13917318	.00000002	.99026805	179
135	78	-.14701582	.14701585	.97814757	180
117	72	-.14029076	.27533622	.95105649	181
108	64	-.13546412	.41691584	.89879399	182
103	56	-.12579096	.54486086	.82903755	183
101	48	-.12767604	.65683683	.74314480	184
100	39	-.13494993	.76533939	.62932036	185
99	30	-.13547616	.85536320	.49999998	186
98	21	-.12992921	.92449489	.35836793	187
97	11	-.11963017	.97431028	.19080898	188
258	10	-.20475320	-.96328729	.17364817	189
256	19	-.22874181	-.91743259	.32556813	190
254	28	-.24337350	-.84874365	.46947154	191
252	37	-.24679210	-.75954746	.60181500	192
249	46	-.24894338	-.64851943	.71933978	193
244	54	-.25766819	-.52829786	.80901697	194
237	61	-.26404631	-.40659554	.87461968	195
225	68	-.26488694	-.26488688	.92718382	196
207	72	-.27533622	-.14029076	.95105649	197
180	74	-.27563740	.00000004	.96126168	198
153	72	-.27533618	.14029084	.95105649	199
135	68	-.26488688	.26488693	.92718382	200
123	61	-.26404622	.40659560	.87461968	201
116	54	-.25766803	.52829794	.80901697	202
111	46	-.24894325	.64851949	.71933978	203
108	37	-.24679187	.75954753	.60181500	204
106	28	-.24337324	.84874372	.46947154	205
104	19	-.22874152	.91743265	.32556813	206
102	10	-.20475290	.96328736	.17364817	207
252	6	-.30722435	-.94584645	.10452845	208
250	16	-.32877097	-.90329047	.27563734	209
247	26	-.35118693	-.82734422	.43837113	210
244	33	-.36764911	-.75379206	.54463901	211
240	41	-.37735492	-.65359759	.65605901	212
233	49	-.39482626	-.52395198	.75470955	213
226	55	-.39843977	-.41259628	.81915202	214
214	61	-.40192546	-.27110203	.87461968	215
198	64	-.41691584	-.13546411	.89879399	216
180	66	-.40673674	.00000006	.91354541	217
162	64	-.41691582	.13546419	.89879399	218
146	61	-.40192538	.27110215	.87461968	219
134	55	-.39843964	.41259641	.81915202	220
127	49	-.39482611	.52395211	.75470955	221
120	41	-.37735472	.65359771	.65605901	222

116	33	-.36764887	.75379216	.54463901	223
113	26	-.35118667	.82734433	.43837113	224
110	16	-.32877078	.90329054	.27563734	225
108	6	-.30732407	.94584654	.10452845	226
246	2	-.40648900	-.91298887	.03489949	227
244	12	-.42879183	-.87915316	.20791167	228
240	21	-.46679037	-.80850427	.35836793	229
236	29	-.48908123	-.72509253	.48480959	230
232	37	-.49168922	-.62933329	.60181500	231
225	43	-.51714523	-.51714510	.68199833	232
217	49	-.52395211	-.39482609	.75470955	233
206	54	-.52829794	-.25766802	.80901697	234
194	56	-.54258252	-.13528093	.82903755	235
180	57	-.54463906	.00000008	.83867054	236
166	56	-.54258248	.13528109	.82903755	237
154	54	-.52829787	.25766818	.80901697	238
143	49	-.52395200	.39482625	.75470955	239
135	43	-.51714512	.51714521	.68199833	240
128	37	-.49168903	.62933344	.60181500	241
124	29	-.48908108	.72509264	.48480959	242
120	21	-.46679013	.80850441	.35836793	243
116	12	-.42879156	.87915329	.20791167	244
114	2	-.40648872	.91298899	.03489949	245
238	6	-.52701649	-.84340227	.10452845	246
234	16	-.56501556	-.77767696	.27563734	247
230	23	-.59168923	-.70514751	.39073111	248
225	30	-.61237250	-.61237236	.49999998	249
219	36	-.62872437	-.50913078	.58778523	250
211	41	-.64691242	-.38870409	.65605901	251
202	45	-.65561804	-.26488673	.70710676	252
191	48	-.65683683	-.12767602	.74314480	253
180	49	-.65605905	.00000010	.75470955	254
169	48	-.65683679	.12767622	.74314480	255
158	45	-.65561796	.26488694	.70710676	256
149	41	-.64691234	.38870422	.65605901	257
141	36	-.62872422	.50913098	.58778523	258
135	30	-.61237237	.61237249	.49999998	259
130	23	-.59168902	.70514770	.39073111	260
126	16	-.56501532	.77767713	.27563734	261
122	6	-.52701622	.84340243	.10452845	262
233	0	-.60181514	-.79863541	0.00000000	263
229	10	-.64609215	-.74324371	.17364817	264
225	16	-.67971474	-.67971457	.27563734	265
220	23	-.70514772	-.59168900	.39073111	266
214	29	-.72509270	-.48908099	.48480959	267
207	34	-.73867794	-.37637506	.55919288	268
198	37	-.75954754	-.24679185	.60181500	269
190	39	-.76533940	-.13494984	.62932036	270
180	40	-.76604445	.00000011	.64278759	271
170	39	-.76533936	.13495007	.62932036	272
162	37	-.75954749	.24679200	.60181500	273
153	34	-.73867783	.37637529	.55919288	274
146	29	-.72509255	.48908121	.48480959	275
140	23	-.70514753	.59168922	.39073111	276
135	16	-.67971459	.67971472	.27563734	277
131	10	-.64609191	.74324392	.17364817	278

127	0	-.60181490	.79863560	0.00000000	279
225	2	-.70667610	-.70667593	.03489949	280
221	9	-.74541794	-.64798173	.15643445	281
216	16	-.77767715	-.56501530	.27563734	282
210	21	-.80850442	-.46679010	.35836793	283
203	26	-.82734434	-.35118666	.43837113	284
196	28	-.84874373	-.24337322	.46947154	285
188	30	-.85759732	-.12052726	.49999998	286
180	31	-.85716731	.00000013	.51503805	287
172	30	-.85759729	.12052753	.49999998	288
164	28	-.84874365	.24337348	.46947154	289
157	26	-.82734423	.35118691	.43837113	290
150	21	-.80850432	.46679027	.35836793	291
144	16	-.77767697	.56501554	.27563734	292
139	9	-.74541774	.64798197	.15643445	293
135	2	-.70667595	.70667608	.03489949	294
217	0	-.79863561	-.60181488	0.00000000	295
212	6	-.84340244	-.52701620	.10452845	296
206	12	-.87915330	-.42879154	.20791167	297
200	16	-.90329055	-.32877076	.27563734	298
194	20	-.91177976	-.22733208	.34202013	299
187	22	-.92027277	-.11299519	.37460657	300
180	22	-.92718386	.00000014	.37460657	301
173	22	-.92027275	.11299537	.37460657	302
166	20	-.91177968	.22733235	.34202013	303
160	16	-.90329048	.32877095	.27563734	304
154	12	-.87915317	.42879181	.20791167	305
148	6	-.84340233	.52701638	.10452845	306
143	0	-.79863543	.60181512	0.00000000	307
204	2	-.91298900	-.40648870	.03489949	308
198	6	-.94584655	-.30732405	.10452845	309
192	10	-.96328736	-.20475288	.17364817	310
186	11	-.97624972	-.10260786	.19080898	311
180	12	-.97814760	.00000015	.20791167	312
174	11	-.97624970	.10260807	.19080898	313
168	10	-.96328730	.20475319	.17364817	314
162	6	-.94584649	.30732424	.10452845	315
156	2	-.91298888	.40648898	.03489949	316
180	0	-1.00000000	.00000015	0.00000000	317
348	1	.97799857	-.20788021	.01745240	318
354	4	.99209925	-.10427408	.06975646	319
6	4	.99209928	.10427382	.06975646	320
12	1	.97799861	.20788000	.01745240	321
279	1	.15641042	-.98753793	.01745240	322
81	1	.15641072	.98753788	.01745240	323
273	2	.05230391	-.99802119	.03489949	324
87	2	.05230412	.99802118	.03489949	325
267	2	-.05230427	-.99802117	.03489949	326
93	2	-.05230396	.99802119	.03489949	327
261	1	-.15641078	-.98753787	.01745240	328
99	1	-.15641057	.98753791	.01745240	329
192	1	-.97799864	-.20787986	.01745240	330
186	4	-.99209929	-.10427372	.06975646	331
174	4	-.99209927	.10427393	.06975646	332
168	1	-.97799858	.20788016	.01745240	333

1

APPENDIX II

Domains of the Bow River (B1-20), Red Deer River (RD1-7), Cripple Creek (C1), and South Creek (S1-2) areas. The structural position of each domain is described where possible with reference to folds, and the stratigraphic position in terms of the lower (L), middle (M) and upper (U) sandstone units (ss) of the Cardium Formation. The number of measurements (N), mean strike (S), mean dip (D), radius of the 95 percent confidence circle about the mean (CR), and precision parameter (K) for each joint set in each domain are given; for bedding only the mean strike, mean dip and number of measurements are shown.

Domain	Location	Structure	N	S	D	C.R.	K
B1	West limb	bedding	29	175	14 SW		
	Kananaski's Anticline	hol	79	150	82 NE	2.7	36
		okl	68	66	88 SE	2.0	71
	L M U ss	hkl	66	32	81 SE	1.9	89
		hkl	80	104	82 NE	4.4	14
B2	East limb	bedding	13	107	11 NE		
	Kananaski's Anticline	hol	52	153	87 SW	3.9	26
		hkl	100	41	87 SE	1.8	61
	L M ss	hkl	85	101	86 SW	1.4	122
B3	West limb	bedding	24	4	16 NW		
	Horseshoe Anticline	hol	87	160	79 NE	3.0	27
		hkl	98	50	83 SE	2.9	26
	L M U ss	hkl	54	97	87 NE	3.9	16
B4	West limb	bedding	43	7	17 NW		
	Horseshoe Anticline	hol	92	174	79 NE	3.6	17
		hkl	30	35	75 SE	7.9	12
	L M ss	hkl	126	100	85 NE	1.7	67
B5	Crest	bedding	45	51	11 NW		
	Horseshoe Anticline	hol	55	165	89 NE	2.8	47
		hkl	75	52	80 SE	3.0	31
	L ss	hkl	101	91	86 SW	1.7	66
B6	East limb	bedding	37	96	15 NE		
	Horseshoe Anticline	hol	103	163	85 SW	2.1	46
		hkl	70	63	80 SE	2.3	54
	L M ss	hkl	65	99	78 SW	1.6	122
B7	East limb	bedding	18	110	14 NE		
	Horseshoe Anticline	hol	93	162	86 SW	2.6	33
		hkl	39	51	82 SE	3.1	14
	L M U ss	hkl	113	88	81 SE	1.8	53
B8	East limb	bedding	25	95	15 NE		
	Horseshoe Anticline	hol	80	165	87 SW	2.3	48
		hkl	64	56	84 SE	2.4	57
	L M U ss	hkl	92	92	79 SW	1.7	73
B9	West limb	bedding	20	36	12 NW		
	Oldfort Anticline	hol	102	163	86 NE	2.4	35
		hkl	82	59	83 SE	2.2	52
	U ss	hkl	45	91	85 SW	2.5	74
B10	West limb	bedding	40	166	38 SW		
	Oldfort Anticline	hol	104	153	60 NE	3.3	18
	M ss	okl	122	62	82 SE	2.4	18

B11	West limb	bedding	22	33	14 NW		
	Cutoff Anticline	hol	120	155	83 NE	2.0	44
	M ss	okl	113	67	83 SE	2.5	28
B12	West limb	bedding	11	41	13 NW		
	Cutoff Anticline	hol	68	152	88 NE	2.2	61
	M ss	okl	117	68	84 SE	1.4	92
B13	West limb	bedding	20	32	14 NW		
	Cutoff Anticline	hol	58	147	81 NE	4.1	22
		hkl	46	20	77 SE	5.8	14
	L ss	hkl	140	83	87 SE	2.3	27
B14	West limb	bedding	11	173	22 SW		
	Flattop Anticline	hol	90	160	70 NE	2.3	42
	U ss	okl	127	61	80 SE	2.7	22
B15	West limb	bedding	14	8	20 NW		
	Flattop Anticline	hol	88	169	76 NE	3.0	26
	L M ss	okl	133	68	83 SE	3.0	18
B16	Crest	bedding	10	40	10 NW		
	Flattop Anticline	hol	71	153	86 NE	2.5	45
	L ss	okl	168	60	81 SE	2.9	16
B17	East limb	bedding	8	71	19 NW		
	Flattop Anticline	hol	102	144	88 SW	2.6	30
	L ss	okl	131	55	80 SE	3.3	15
B18	East limb	bedding	7	76	16 NW		
	Flattop Anticline	hol	122	150	89 NE	2.7	24
	L ss	okl	120	57	77 SE	3.2	17
B19	West limb	bedding	10	32	22 NW		
	Tight Anticline	hol	74	153	80 NE	2.0	72
	L ss	okl	92	57	78 SE	1.5	99
B20	West limb	bedding	9	163	48 SW		
	Tight Anticline	hol	75	154	59 NE	5.7	9
	L ss	okl	111	52	80 SE	3.3	17
RD1	Crest	bedding	19	50	6 NW		
		hol	70	125	87 SW	2.8	38
	L ss	okl	137	38	85 SE	2.3	29
RD2	Crest	bedding	24	34	7 NW		
		hol	116	128	89 SW	2.0	44
	U ss	okl	171	35	85 SE	1.4	59
RD3	East limb	bedding	39	118	14 NE		
		hol	115	124	73 SW	3.8	13
	L ss	okl	155	22	89 SE	1.5	54

RD4	East limb	bedding	47	143	34 NE		
		hol	119	131	56 SW	3.2	17
	L ss	okl	151	26	74 NW	2.5	30
RD5	East limb	bedding	57	138	29 NE		
		hol	102	127	63 SW	2.0	48
	U ss	okl	176	30	82 NW	1.6	44
RD6	East limb	bedding	15	149	41 NE	2.3	
		hol	89	136	55 SW	3.7	17
	L ss	hkl	139	19	63 NW	2.5	35
		hkl	43	52	79 NW	10.1	5
RD7	East limb	bedding	32	151	38 NE	2.1	
		hol	70	117	63 SW	4.5	15
	U ss	okl	154	20	61 NW	2.3	24
C1	L U ss	bedding	12	147	38 SW		
		hol	103	136	48 NE	3.1	21
		okl	148	59	88 NW	3.7	11
S1	L ss	bedding	13	134	16 SW		
		hol	117	147	72 NE	1.3	101
		hkl	127	40	88 SE	1.8	48
		hkl	33	103	72 NE	2.8	81